

**THE PREPARATION AND PROPERTIES OF SOME COMPLEX FLUORIDES**

by

**David Robin Russell**

A Thesis submitted to the University of Glasgow  
in fulfilment of the requirements for the Degree  
of Doctor of Philosophy.

**August 1965**

ProQuest Number: 13849359

All rights reserved

INFORMATION TO ALL USERS

The quality of this reproduction is dependent upon the quality of the copy submitted.

In the unlikely event that the author did not send a complete manuscript and there are missing pages, these will be noted. Also, if material had to be removed, a note will indicate the deletion.



ProQuest 13849359

Published by ProQuest LLC (2019). Copyright of the Dissertation is held by the Author.

All rights reserved.

This work is protected against unauthorized copying under Title 17, United States Code  
Microform Edition © ProQuest LLC.

ProQuest LLC.  
789 East Eisenhower Parkway  
P.O. Box 1346  
Ann Arbor, MI 48106 – 1346

## ACKNOWLEDGEMENTS

The work described in this thesis was carried out in the Inorganic Chemistry Laboratories of Imperial College of Science and Technology, London and the Royal College of Science and Technology, Glasgow.

The author wishes to express sincere thanks to his supervisor Dr. D. W. A. Sharp for his continued encouragement and advice. The author would also like to thank Dr. A. J. E. Welch and Mr. T. S. Wylie for the use of X-ray equipment, Mr. F. S. Warner for much help in programming the Ferranti Sirius computer, and staff and fellow students at both colleges for useful discussion.

The award of a D. S. I. R. Research Studentship for the period 1960 - 1963 is gratefully acknowledged.

August 1963

Royal College of Science,  
Glasgow.

## ABSTRACT

### The Preparation and Properties of Some Complex Fluorides

A wide range of complex fluorides with the general formula  $ABF_6$ , A being a univalent cation and B a quinquevalent element, has been prepared in an attempt to discover the chief factors influencing their solid state structures. New preparations have been used for some complexes of this type and some previously unreported compounds have been obtained; non-aqueous solvents such as sulphur dioxide and anhydrous hydrogen fluoride have been found to be useful reaction media. The types of unit cell found amongst these complexes were examined using X-ray powder photography. With the structures of over eighty complex fluorides now available it has been possible to draw a clearly defined relationship between the size of the A and B ions and the structure which is adopted.

To assist in the interpretation and calculation of lattice constants from X-ray powder photographs, a series of programmes has been written for the Ferranti Sirius computer. Included in the series are programmes to calculate  $\sin^2 \theta$  values and lattice spacings, least squares refinement of unit cell parameters with corrections for systematic errors, and an analytical routine to interpret the photograph of a substance with an unknown unit cell.

The vibrational spectra of octahedral  $MF_6^{n-}$  anions have been studied for a series of complex fluorides with known crystal structures, using far infra-red ( $1100-200 \text{ cm}^{-1}$ ) spectroscopy. The splittings of the fundamental vibration frequencies have been correlated with the

type of octahedral distortion known to occur in these compounds. The visible and ultra-violet reflectance spectra of a similar series of octahedral  $MF_6^{2-}$  anions containing transition elements have been recorded. It has been possible to assign the absorptions observed to electronic transitions occurring between the partly filled d-levels of the metal according to the predictions of ligand field theory. Conclusions have been drawn on the nature of the fluoride ion as a ligand.

Attempts have been made to extend the very limited number of known metal carbonyl fluorides by reacting metal fluorides with carbon monoxide at high pressures. Evidence was obtained for the possible existence of a ruthenium carbonyl fluoride, but the compound could not be obtained in sufficient quantity for characterisation. Reactions of the previously known carbonyl fluorides of platinum and rhodium were investigated and a phosphine adduct of the former prepared.

## CONTENTS

	<u>Page</u>
<u>Introduction</u>	1
<u>Chapter 1</u>	
The Structural Chemistry of Complex Fluorides $ABF_6$	4
Experimental	17
X-ray Results	25
<u>Chapter 2</u>	
The Vibrational Spectra of Complex Fluorides	47
Experimental	60
<u>Chapter 3</u>	
The Electronic Spectra of Transition Metal Complex Fluorides	65
Diagrams of Spectra	75
Experimental	78
<u>Chapter 4</u>	
Metal Carbonyl Fluorides	80
Experimental	90
<u>Chapter 5</u>	
Computer Programmes for X-ray Powder Photography	99
Description of Programmes	106
Appendix	131
<u>References</u>	135

## INTRODUCTION

Fluorine occupies a unique position in the Periodic Table, being the most electronegative element. This arises from the fact that it is the smallest atom of the halogen series of elements, which have one electron less than required for an inert gas configuration. The small size of the fluorine atom, coupled with the absence of suitable outer orbitals for additional interactions, causes certain simplifications in the chemistry of fluorine. Since for a given cation the greatest lattice energy is available for the smallest anion, of all simple halides the fluorides are the most likely to be ionic. The extreme electronegativity of fluorine often induces high oxidation states in many elements; in such cases the ionisation energy of the element is too large to permit complete ionic bonding, the higher valency fluorides are therefore covalent. In these molecules the low polarisability of fluorine atoms reduces intermolecular interactions to a minimum and they are usually low boiling liquids or gases. Within the molecule the covalent bonds must still have considerable ionic character however, which would result in the central atom having a considerable positive charge. Where there are suitable empty orbitals available, it is not unreasonable to expect that multiple bonding will occur through overlap of these orbitals with filled p-orbitals on the fluorine atoms. This may be an explanation of the "abnormal" strength and shortness of bonds in simple fluorides such as  $\text{SiF}_4$  and  $\text{SF}_6$ .

Many binary fluorides will readily accept fluoride ions to complete the central atom coordination sphere, to form a complex fluoroanion.

Thus,  $\text{BF}_3$  reacts with alkali metal fluorides to form tetrafluoroborates  $\text{BF}_4^-$ ,  $\text{PF}_3$  forms hexafluorophosphates  $\text{PF}_6^-$ .

The six-coordinated ion  $\text{BF}_6^{n-}$  is particularly common, and occurs over a wide range of elements. In the few examples of such complexes where a full structure determination has been carried out, it appears that bond shortening through multiple bond formation is still present. It is also apparent that the  $\text{BF}_6^{n-}$  entity persists in the solid state in the majority of complexes. In view of the great variety of elements forming hexafluoride molecules and ions, measurement of the physical properties of these complexes could provide useful comparative information in several fields of theoretical chemistry.

Two major practical difficulties arise in the chemistry of fluorine. One is the general instability of fluorides to moisture. Although fluorine bonds are usually strong, many fluorides are hydrolysed violently by water. The driving force for a hydrolysis reaction comes principally from the greater lattice energy of oxides, and the stability of HF. The oxide ion  $\text{O}^{2-}$  is almost as small as the fluoride ion [  $\text{O}^{2-}$  1.40;  $\text{F}^-$  1.36 Å ] and consequently the increased charge favours higher lattice energies for oxides. Glass is attacked by many fluorine compounds particularly at elevated temperatures. However attack can be kept to a minimum if the precaution is first taken of removing adsorbed water by baking the glass above  $250^\circ\text{C}$  under high vacuum. Hydrolysis of a fluoride gives hydrogen fluoride, which rapidly attacks glass to give silicon tetrafluoride and more water, so that the presence of even a trace of water acts as a catalyst for the hydrolysis. Where handling operations are to be performed that would be inconvenient on a



vacuum line, use can be made of a glove box, the interior of which is kept dry with a desiccating agent.

One sharp difference between metal fluorides as compared with metal chlorides, bromides and iodides is the rarity of complexes of the former with  $\pi$ -bonding ligands. Carbonyl halide complexes of many metals have a decreasing order of stability  $\text{Cl} > \text{Br} > \text{I}$ , and a natural extrapolation would predict that carbonyl fluorides would be most stable of all. However only carbonyl fluorides of two metals are known to date, and their formulae do not resemble those of the corresponding metal carbonyl chlorides, bromides and iodides. Whether this anomaly is to be connected with the absence of suitable vacant orbitals for back bonding, or with the extreme electronegativity and small size of the fluorine atom, has not yet been decided.

In spite of the straightforward nature of much of fluorine chemistry, binary fluorides are still being prepared. As experimental techniques for the handling of fluorine compounds are gradually developed, and more resistant materials are discovered it is likely that still more compounds will be prepared. Continued studies of the properties of fluorine compounds should give further valuable information for the advancement of chemical theory.

## Chapter 1

### The Structural Chemistry of Complex Fluorides of General Formula $ABF_6$

The work described in this chapter has been accepted  
for publication in the Journal of the Chemical Society.

#### 1.1 Introduction

The structures of complex fluorides  $ABF_6$  have been surveyed by COX (1956), who was unable with the data then available to explain the distribution of compounds among the various known structural types solely on the ratio of ionic sizes. With the increased volume of data that is now available, of which part is the writer's work to be described here, a clearly defined relationship between the ion sizes and the structures adopted has become apparent.

There are two ways of describing the types of structure found occurring among complex halides  $A_m BX_n$  depending upon the strength of the internal binding forces of the individual complex ions. If these are weak, then the structure is best discussed in relation to a close-packed array of X ions, with A and/or B either incorporated into the close-packing or filling some of the interstices. If however there is a strongly bound complex ion  $BX_n$  present, it is simpler to regard the structure as being derived from simple ionic structures  $AX_m$  by replacing A or X with the  $BX_n$  ion.

For complex fluorides  $ABF_6$ , the  $BF_6$  octahedron is usually quite firmly bound and close analogies can be drawn between the  $ABF_6$  structures and the well-known NaCl and CsCl lattices. The structures found will therefore be discussed from this viewpoint, the discussion is also

restricted to  $A^I B^V F_6$  compounds since the much wider range of  $A^{II} B^{IV} F_6$  fluorides contains several examples of compounds where discrete  $BF_6$  octahedra apparently do not exist.

The structures found to occur amongst  $A^I B^V F_6$  complexes are summarised in Table 1.1. It can be seen that for over 80 different compounds only five distinct structural types occur. The cations A are arranged across the table in order of increasing ionic radius. The order of elements B forming the rows has been chosen to show the simplest pattern of structure types combined with observed trends in unit cell volume, but in fact this order corresponds closely with the order of increasing ionic radius. Ionic radii are listed for the elements B, but although it is most unlikely these anions contain ionic bonding, in the absence of detailed covalent radii it is expected that the same trends will be observed.

It is immediately apparent that the cation A has the greatest influence over which structure is adopted. Thus all lithium salts have the rhombohedral  $NaOsF_6$  structure, all caesium salts (except  $CsPF_6$ ) have the  $KOsF_6$  structure. Second order effects (possibly size of B, orbital occupation in A and B) control the intermediate region of the table. The main anomalies in the table occur with the fluorophosphates, which may be connected with the very small size of the phosphorus atom.

A detailed description of each structure, with comments on the discrepancies between some of the results presented here and previous work, now follows.

Table 1.1

Structures occurring among complex fluorides  $A^I B^V F_6$

	A	Li	Na	Ag	K	Tl	NH <sub>4</sub>	Rb	Cs
	$r_A +$	0.60	0.95	1.26	1.33	1.40	1.48	1.48	1.69
B	$r_B^{5+}$								
P	0.54	R <sub>4</sub>	C <sub>2</sub>	C <sub>2</sub>	$\begin{cases} C_2 \\ R_2 \end{cases}$	C <sub>2</sub>	C <sub>2</sub>	C <sub>2</sub>	C <sub>2</sub>
As	0.47	R <sub>4</sub>	R <sub>4</sub>	C <sub>2</sub>	R <sub>2</sub>	R <sub>2</sub>		R <sub>2</sub>	R <sub>2</sub>
V	0.59	R <sub>4</sub>	R <sub>4</sub>	T	R <sub>2</sub>	R <sub>2</sub>		R <sub>2</sub>	R <sub>2</sub>
Ru	0.6	R <sub>4</sub>	R <sub>4</sub>	T	R <sub>2</sub>	R <sub>2</sub>		R <sub>2</sub>	R <sub>2</sub>
Ir	0.6	R <sub>4</sub>	R <sub>4</sub>	T	R <sub>2</sub>			R <sub>2</sub>	R <sub>2</sub>
Os	0.6	R <sub>4</sub>	R <sub>4</sub>	T	R <sub>2</sub>			R <sub>2</sub>	R <sub>2</sub>
Re	0.6	R <sub>4</sub>	C <sub>2</sub>		T			R <sub>2</sub>	R <sub>2</sub>
Mo	0.62	R <sub>4</sub>	C <sub>2</sub>		T	R <sub>2</sub>		R <sub>2</sub>	R <sub>2</sub>
W	0.62	R <sub>4</sub>	C <sub>2</sub>		T			R <sub>2</sub>	R <sub>2</sub>
Sb	0.65	R <sub>4</sub>	C <sub>2</sub>	T	T	R <sub>2</sub>	R <sub>2</sub>	R <sub>2</sub>	R <sub>2</sub>
Nb	0.70	R <sub>4</sub>	C <sub>2</sub>	T	T	R <sub>2</sub>	R <sub>2</sub>	R <sub>2</sub>	R <sub>2</sub>
Ta	0.70	R <sub>4</sub>	C <sub>2</sub>	T	T	R <sub>2</sub>	R <sub>2</sub>	R <sub>2</sub>	R <sub>2</sub>

R<sub>4</sub> Rhombohedral, NaOsF<sub>6</sub>

C<sub>1</sub> Cubic, NaSbF<sub>6</sub>

R<sub>2</sub> Rhombohedral, KO<sub>2</sub>F<sub>6</sub>

C<sub>2</sub> Cubic, CsPF<sub>6</sub>

T Tetragonal, KNbF<sub>6</sub>

### 1.2 The Rhombohedral, NaOsF<sub>6</sub>, Structure: R<sub>3</sub>

This structure is found exclusively among the salts of the smallest cations Li<sup>+</sup> and Na<sup>+</sup>. The type was first recognised by JACK (1959) in NaOsF<sub>6</sub>, and a recent single crystal determination on LiSbF<sub>6</sub> by BURNS (1962) has shown that Li<sup>+</sup> and SbF<sub>6</sub><sup>-</sup> ions are disposed in a slightly distorted sodium chloride lattice. Although the true unit cell has parameters shown in Table 1.3, those of the tetramolecular rhombohedron best representing the lattice structure ( $a = 7.50$ ,  $\alpha = 92.6^\circ$ ) show the small extent of the angular distortion from cubic symmetry. The SbF<sub>6</sub><sup>-</sup> octahedron is regular within experimental error, but oriented in such a way that the Sb - F bond is at an angle of  $16.9^\circ$  to the Sb....Li line.

The LiSbF<sub>6</sub> structure closely resembles that found for VF<sub>3</sub> by GUTMANN and JACK (1951), with the Li and Sb atoms occupying the V atom positions in the bimolecular VF<sub>3</sub> unit cell. (Table 1.2).

Table 1.2

Atom Coordinates in the VF<sub>3</sub> and LiSbF<sub>6</sub> Structures

Compound	Space group	Positions			Bond lengths	
		B	A	6F	A-F	B-F
VF <sub>3</sub>	R $\bar{3}o$	(0,0,0)	( $\frac{1}{2}, \frac{1}{2}, \frac{1}{2}$ )	(0.645, -0.145, 0.250)	1.94	1.94
LiSbF <sub>6</sub>	R $\bar{3}$	(0,0,0)	( $\frac{1}{2}, \frac{1}{2}, \frac{1}{2}$ )	(0.656, -0.134, 0.259) <sup>x</sup>	2.032	1.877

<sup>x</sup> transformed from parameters for trimolecular hexagonal cell given by BURNS (1962).

From this relationship between the two structures, it might be expected that the R<sub>3</sub> structure will only occur for ABF<sub>6</sub> complexes where both A and B are small and comparable in size. It is surprising

therefore that of the sodium salts, only those with the smaller B atoms, (As, V, Ru, Ir, Os,) have this structure. Possibly the lattice can accommodate an increase in size of either A or B but not both.

Table 1.3

Lattice constants of compounds with the  $\text{NaOsF}_6$  structure ( $R_4$ ).

	Li		Na		Reference
	a(A)	$\alpha^\circ$	a(A)	$\alpha^\circ$	
P	5.077	57.98	-	-	Present work
As	5.233	57.42	5.586	57.06	Present work
V	5.30	56.5	5.629	56.55	Present work
Ru	5.39	56.0	5.80	55.2	BOSTON and SHARP (1960)
Ir	5.41	56.0	5.80	55.2	"
Os	5.45	55.5	5.80	55.2	"
Re	5.45	55.5	-	-	Present work
Mo	5.45	57.1	-	-	KEMMITT and SHARP (1961)
W	5.45	57.4	-	-	Present work
Sb	5.458	57.01	-	-	Present work
	5.45	56.88	-	-	BURNS (1962)
Nb	5.473	58.09	-	-	KEMMITT and SHARP (1961)
Ta	5.479	58.05	-	-	"

### 1.3 The Cubic Structures $\text{NaSbF}_6$ ( $C_1$ ) and $\text{CsPF}_6$ ( $C_2$ )

These structures are both related to the NaCl lattice, differing in the symmetry of their unit cells.  $\text{NaSbF}_6$  is reported by SCHREWELIUS (1958) to have a face-centred unit cell containing  $\text{Na}^+$  and  $\text{SbF}_6^-$  ions oriented in a manner similar to that found in  $\text{LiSbF}_6$  by BURNS (1962). However TEUFER (1956) disagrees with the positions of the F atoms,

placing them on the cell edges and quoting a reliability index of 0.095 for an unstated number of reflexions. In view of the unusually short Sb-F bond length (1.78Å) obtained by Teufer (1.88 in  $\text{LiSbF}_6$ ), the structure of  $\text{NaSbF}_6$  cannot be considered as settled. EDWARDS and PEACOCK (1961) report that the structure of  $\text{NaMoF}_6$  is similar to the  $\text{NaSbF}_6$  structure proposed by TEUFER (1956). The  $C_2$ ,  $\text{CsPF}_6$  structure has been studied by BODE and CLAUSEN (1951). Although a primitive cubic unit cell is assigned to the structure, the departure from a face-centred unit cell is said to be slight and consequently no face-centred forbidden lines were observed. In the case of  $\text{KPF}_6$ , two crystalline forms were found, one stable below  $40^\circ$  belonging to the  $C_2$  type, and the other being  $R_0$  type. In the cubic form ( $\alpha\text{-KPF}_6$ ) seven faint lines could be indexed as non-face-centred reflexions. In both  $\alpha\text{-KPF}_6$  and  $\text{CsPF}_6$  the poor agreement between observed and calculated intensities for F-only reflexions is explained by postulating a statistical distribution of  $\text{PF}_6$  octahedra over all the configurations obtained by rotating through an angle of  $\pm 20^\circ$ , with a consequent reduction in intensity of the F reflexions.

The chief difference between  $C_1$  and  $C_2$  seems to be the coordination number of the cation, which is said to reach 12 in  $\alpha\text{-KPF}_6$  (BODE and CLAUSEN, 1951). COX (1956) reports  $\text{AgPF}_6$  and  $\text{AgAsF}_6$  as belonging to the cubic NaCl type but does not distinguish between  $C_1$  and  $C_2$ . However the anomalous fact that  $\text{NaPF}_6$  has a unit cell smaller than  $\text{AgPF}_6$ , pointed out by Cox, can be explained if  $\text{AgPF}_6$  and  $\text{AgAsF}_6$  have the  $C_2$ -type structure whereas  $\text{NaPF}_6$  has the  $C_1$ -type structure. This is consistent with the frequently observed fact that the larger cations have higher coordination numbers.

Table 1.4Lattice constants of compounds with  $C_1$  and  $C_2$  structures

	$C_1$ a(A)	$C_2$ a(A)	Reference
$NaPF_6$	7.61		BODE and TEUFER (1952,a)
$NaReF_6$	8.18		PEACOCK (1957 a)
$NaMoF_6$	8.194		EDWARDS and PEACOCK (1961)
$NaWF_6$	8.18		HARGREAVES and PEACOCK (1957)
$NaSbF_6$	8.18		SCHREWELIUS (1938); TEUFER (1956)
$NaNbF_6$	8.26		COX (1956); KEMMITT and SHARP (1961)
$NaTaF_6$	8.28		" ; "
$AgPF_6$		7.52	COX (1956)
$AgAsF_6$		7.74	"
$\alpha$ - $KPF_6$		7.76	BODE and CLAUSEN (1951)
$NH_4PF_6$		7.90 7.920	" " Present work
$TlPF_6$		7.94	BODE and TEUFER (1952,b)
$RbPF_6$		7.92	COX (1956)
$CaPF_6$		8.19	BODE and CLAUSEN (1951)

1.4 The Tetragonal,  $KNbF_6$ , Structure: T

Complex fluoroacid salts of the medium-sized cations  $Ag^+$  and  $K^+$  are found to have this structure, the tetragonal unit cell of which has a  $c$ -parameter close to twice the  $a$  dimension. A full structure determination on potassium hexafluoronioate by BODE and DOHREN (1958) shows that the lattice is based on a  $CsCl$ -type arrangement of  $K^+$  and



$\text{NbF}_6^-$  ions. The  $\text{NbF}_6$  octahedron is slightly distorted to a bisphenoid and the full unit cell contains one each of the left-hand and right-hand orientations. Each potassium atom has eight fluorine atoms as nearest neighbours at 2.50Å and four further fluorines as next nearest neighbours at 2.94Å.

Because of the relation between the  $a$  and  $c$  parameters of this unit cell, the X-ray powder photographs of compounds with the  $\text{KNbF}_6$  structure often appear to be characteristic of cubic phases unless lines corresponding to a Bragg angle greater than about  $30^\circ$  are present, when the splitting of lines is then clearly seen. A further difficulty arises in that lines  $h,k,l$  with  $l$  odd are very weak and in a few photographs were not seen at all. In such cases it would be possible to index all lines on a pseudo cubic cell with  $a$  approximately equal to  $c$ , but to be consistent with closely related compounds where these lines were seen, all  $c$ -parameters are listed as approximately  $2a$ .

All disagreements with previous work occur among the compounds in Table 1.5.  $\text{AgVF}_6$  is reported by COX (1956) to have a primitive cubic unit cell. It was difficult to prepare a sufficiently crystalline sample of  $\text{AgVF}_6$  to obtain a good powder photograph, but the best photograph could be indexed quite well on a tetragonal cell. As this compound is on the boundary between cubic and tetragonal cells it may well exist in two phases. SHARP and SHARPE (1956) give cubic unit cells for silver hexafluoro-niobate and -tantalate, but the present work gave photographs of tetragonal phases only.

Tetragonal phases reported for  $\text{KMnF}_6$ ,  $\text{KWF}_6$  (HARGREAVES and PEACOCK, 1957) and for  $\text{KReF}_6$  (PEACOCK, 1957) appear to be similar to the  $\text{KNbF}_6$

Table 1.5Lattice constants of compounds with the  $\text{KNbF}_6$  structure (T)

	Ag		K		References
	a	c	a	c	
V	4.90	9.42			Present work
Ru	4.85	9.54			"
Ir	4.85	9.70			"
Os	4.92	9.58			"
Re			5.044	10.09	" ; PEACOCK (1957)
Mo			5.88	9.98	" ; HARGREAVES and PEACOCK (1957)
W			5.85	10.08	" ; "
Sb	4.96	9.61	5.151	10.04	Present work
Nb	4.968	9.551	5.18	10.05	{ Ag salts: Present work K salts: BODE and DOHREN (1958)
Ta	4.993	9.634	5.20	10.05	

structure but have  $\underline{a}$  doubled. No extra lines corresponding to this larger unit cell could be found on a photograph of  $\text{KReF}_6$ , and  $\sin^2\theta$  data kindly supplied by Dr. R. D. Peacock for  $\text{KMoF}_6$  and  $\text{KWF}_6$  could be indexed satisfactorily with the values shown in Table 1.5.

BODE and VOSS (1951), and BODE (1951) have examined potassium and silver hexafluoroantimonates by the powder method and have given them cubic unit cells ( $\underline{a} = 10.15$  and  $9.85$  resp.) containing eight molecules. They were also able to assign positions to all atoms in the unit cell on the basis of visually estimated intensities. However powder photographs of samples prepared here, which contain many of the lines listed by Bode and Voss, have been successfully interpreted by assuming a tetragonal

cell similar to that found for  $\text{KNbF}_6$  and containing only two molecules.

The most probable cause for these disagreements lies in the special relationship between  $a$  and  $c$  discussed earlier.

### 1.5 The Rhombohedral, $\text{KOsF}_6$ , Structure; $R_3$

This is the most widely occurring structure amongst the  $\text{ABF}_6$  complexes, and is characteristic of the largest cations  $\text{Cs}^+$ ,  $\text{Rb}^+$ ,  $\text{Tl}^+$ . The representative compound  $\text{KOsF}_6$  has been described by HEFWORTH, JACK and WESTLAND (1956) and is closely related to the  $\text{BaSiF}_6$  structure reported by HOARD and VINCENT (1940). The space group of  $\text{KOsF}_6$ ,  $\overline{R3}$ , has lower symmetry than  $\text{BaSiF}_6$ ,  $\overline{R3m}$ , and the  $\text{OsF}_6$  octahedron is found to be distorted by a contraction along a 3-fold axis. All six fluorine atoms remain equidistant from the central osmium atom however, which means that the  $\text{OsF}_6$  octahedron has point group symmetry of  $\overline{3}$  ( $D_{3d}$ ). This point will be taken up in Chapter 2. A possible distortion of the  $\text{SiF}_6$  octahedron in  $\text{BaSiF}_6$  was not ruled out by Hoard and Vincent, although it was expected to be small. The potassium ions in  $\text{KOsF}_6$  are surrounded by twelve fluorine atoms, six arranged in a puckered ring around the potassium at 2.84 Å to form an approximately close-packed two-dimensional sheet, and two sets of three F atoms arranged above and below at a slightly greater distance (3.17 Å). In this structure therefore the large cation has almost achieved the maximum coordination number of twelve.

### 1.6 Discussion

As has been pointed out above, the dominant factor influencing the structures of  $\text{ABF}_6$  complexes is the cation  $\text{A}^+$ . This is not surprising when considering the relative sizes of the A and B ions. The sequence

Table 1.6Lattice constants of compounds having the  $KOsF_6$  structure  $R_6$ 

		K	K	NH <sub>4</sub>	Tl	Rb	Cs
P	a	4.85	<sup>2</sup>				
	$\alpha$	94°					
As	a	4.92	<sup>2</sup>		5.04 <sup>4</sup>	5.00 <sup>5</sup>	5.20 <sup>5</sup>
	$\alpha$	97.2°			97.0°	96.1°	96.0°
V	a	4.92	<sup>6</sup>		5.10 <sup>1</sup>	5.01 <sup>5</sup>	5.24 <sup>5</sup>
	$\alpha$	97.2°			95.2°	97.0°	96.2°
Ru	a	4.97	<sup>7,8</sup>		5.09 <sup>1</sup>	5.07 <sup>7,8</sup>	5.25 <sup>7,8</sup>
	$\alpha$	97.4°			96.6°	96.9°	96.3°
Ir	a	4.98	<sup>8</sup>			5.105 <sup>1</sup>	5.27 <sup>8</sup>
	$\alpha$	97.4°				97.00°	96.2°
Os	a	4.991	<sup>8</sup>			5.106 <sup>1</sup>	5.28 <sup>8</sup>
	$\alpha$	97.18°				96.74°	96.1°
Re	a					5.11 <sup>9</sup>	5.28 <sup>9</sup>
	$\alpha$					96.7°	95.9°
Mo	a				5.135 <sup>11</sup>	5.11 <sup>10</sup>	5.29 <sup>10</sup>
	$\alpha$				96.13°	96.5°	96.0°
W	a					5.14 <sup>10</sup>	5.31 <sup>10</sup>
	$\alpha$					97.6°	95.5°
Sb	a			5.10 <sup>12</sup>	5.16 <sup>12</sup>	5.11 <sup>12</sup>	5.32 <sup>12</sup>
	$\alpha$			96.0°	96.0°	96.5°	96.9°
Nb	a			5.19 <sup>13</sup>	5.142 <sup>11</sup>	5.14 <sup>8</sup>	5.32 <sup>8</sup>
	$\alpha$			96.1°	96.37°	96.4°	95.8°
Ta	a			5.18 <sup>13</sup>	5.148 <sup>11</sup>	5.14 <sup>8</sup>	5.32 <sup>8</sup>
	$\alpha$			96.1°	96.34°	96.4°	95.8°

<sup>1</sup> Present work. <sup>2</sup> BODE and CLAUSEN (1951). <sup>3</sup> ROOF (1955). <sup>4</sup> SHARP, Ph.D Thesis, Cambridge, 1957. <sup>5</sup> COX (1956). <sup>6</sup> KLEMM (1954). <sup>7</sup> WEISE and KLEMM (1955). <sup>8</sup> HEPWORTH et al. (1956). <sup>9</sup> PEACOCK (1957). <sup>10</sup> HARGREAVES and PEACOCK (1957). <sup>11</sup> KEMMERT and SHARP (1961). <sup>12</sup> SCHREWELIUS (1942). <sup>13</sup> BODE and DOHREN (1957).

obtained for the structures when they are listed in increasing order of cation coordination number  $N_c$  follows closely that sequence of structures observed in Table 1.1 as the cation increases in size.

Structure	$R_4$	$C_1$	T	$R_2$	$C_2$
Coord. No.	6	6	8 + 4	6 + 6	12

This correspondence is observed quite generally among the structures of many series of compounds (WELLS, 1962). The prediction of HOARD and VINCENT (1940) that the  $BaSiF_6$  structure (similar to  $R_2$ ) will be possible for compounds  $ABX_6$  only when the ratio B:X is equal to or greater than unity is completely vindicated in the fluorides  $ABF_6$  (F radius 1.33). It appears that the tendency for a cation to increase its coordination number will occur even at the expense of distorting the  $BF_6$  octahedron, as found by ROOF (1955) for  $KAsF_6$ .

The central B atom in the  $BF_6^-$  anions is generally small and cannot have much influence on the structure as a whole. However the presence of partly filled d-orbitals in several of the B atoms might be expected to produce some distortion in the surrounding octahedron of F atoms. Unfortunately X-ray powder photography is not a sufficiently precise technique for the detection of such distortions, and a full single crystal analysis would be necessary, or alternatively other methods sensitive to such distortions (see Chapters 2 and 3). In any case these distortions are expected to be smaller than those caused by the cation  $A^+$ . It is interesting to note however that the change over from  $R_4$  to  $C_1$  for the sodium salts occurs between the same pair of elements (Os and Re) as the change from  $R_2$  to T in the potassium salts.

Whether this is an effect of the size of B may be revealed if the corresponding complex fluorides of technetium(V) could be prepared and examined since in the author's view this is just the position that Tc(V) would appear in the B(V) series. The recently prepared compound  $KPtF_6$  has the  $R_3$ -type structure (BARTLETT and LOHMANN, 1962). The other salts are expected to follow the corresponding complexes of iridium(V).

The missing compounds of Table 1.1, which would be difficult to prepare, are expected to fit in with existing sequences. Thus the thallium salts  $TlIrF_6$ ,  $TlOsF_6$ ,  $TlWF_6$  should have the  $R_3$  structure and  $AgReF_6$ ,  $AgMoF_6$ , and  $AgWF_6$  the tetragonal T structure. The missing ammonium salts are expected to follow the corresponding rubidium compounds provided there is no hydrogen-bonding in the structure (WADDINGTON, 1958).

Hexafluorobismuthates(V) have been reported (FISCHER and RUDZITIS, 1959) but no lattice constants were given, it was stated that a powder photograph of  $KBiF_6$  was similar to that of  $KSbF_6$ . Attempts to prepare fluorobismuthates(V) here were not successful except for the potassium salt which seemed to give two phases, one isomorphous with  $KSbF_6$ . In view of the large size of the Bi(V) ion, (estimated 0.75 Å), anomalous behaviour to that predicted from Table 1.1 may be found.

## Experimental

### Fluorinating Agents

Fluorine was obtained by electrolysis of the molten adduct  $KF \cdot 2HF$  in a 60 amp. cell kindly loaned by Imperial Chemical Industries Ltd. Provided the first few ampere-hours of gas were vented it could be assumed that the gas from the cell consisted of fluorine contaminated only with hydrogen fluoride and various carbon fluorides from attack of the carbon anode. These were removed by passing the gas through a column of sodium fluoride pellets, and traps cooled in liquid oxygen. The fluorine was often used diluted with nitrogen, obtained from cylinders and dried by passing through phosphorus pentoxide towers. Reactions were carried out in a nickel reactor, collecting the products in vacuum-baked all-glass apparatus as has previously been described (e.g. PEACOCK, 1960).

Anhydrous Hydrogen Fluoride was obtained from Imperial Chemical Industries. When used as solvent it was condensed into a stainless steel, 25ml capacity bomb fitted with a valve. The bomb was designed by Baskerville and Lindsay Ltd, and obtained with a grant from the Research Fund of the Chemical Society.

Bromine Trifluoride was prepared by passing chlorine trifluoride through liquid bromine in a steel bottle at  $10^{\circ}C$ . The chlorine trifluoride was used direct from a cylinder generously supplied by Imperial Chemical Industries Ltd.

Fluorinations were carried out in silica bottles by adding bromine trifluoride in small quantities to a suspension of the reactants in liquid bromine which acted as a moderator. When reaction was complete,

the excess bromine trifluoride and bromine were removed under vacuum.

#### Preparation of Lithium Hexafluorophosphate

Hexafluorophosphates have been prepared by the action of bromine trifluoride on a mixture of metal halide and excess phosphorus pentoxide (COX, 1956). Samples prepared in this way in the present work always contained lithium fluoride, detected by X-ray powder photography and a high Li analysis.

Phosphorus pentafluoride was prepared by heating a diazonium fluorophosphate Phosfluorogen A (from the Ozark-Mahoning Co.) and purified by distillation at  $-78^{\circ}$  under vacuum. An excess was distilled onto 0.5 gm lithium fluoride in a steel bomb. Five to ten millilitres of anhydrous hydrogen fluoride were then distilled into the bomb and the reaction left overnight at  $50^{\circ}\text{C}$ . All volatile material was removed under vacuum at room temperature, and the solid handled in the dry-box. Li was analysed by evaporation to  $\text{Li}_2\text{SO}_4$  with concentrated sulphuric acid. (Found: Li, 4.7%. Calc. for  $\text{LiPF}_6$ : Li, 4.54%).

Lithium hexafluorophosphate is a white, extremely hygroscopic solid, which decomposes under vacuum above  $60^{\circ}\text{C}$ , losing  $\text{PF}_5$ .

#### Preparation of Ammonium Hexafluorophosphate

Ammonium hexafluorophosphate was prepared from excess phosphorus pentafluoride and Analar ammonium fluoride as above.

#### Preparation of Li and Na Hexafluoroarsenates

Lithium and sodium hexafluoroarsenates were prepared as previously described (EMBLEUS and WOOLF, 1950) by the action of bromine trifluoride on a mixture of alkali metal chloride and arsenic trioxide.



### Attempted Preparation of Ammonium Hexafluoroarsenate

Arsenic pentafluoride was prepared by the action of fluorine on arsenic metal at 100°, and purified by distillation first in a stream of fluorine and then in vacuo. An excess was then distilled into a steel bomb containing 0.5gm Analar ammonium fluoride and 10ml of anhydrous hydrogen fluoride. The reaction was left at room temperature overnight, and after removing the excess volatile material under vacuum at 50°C the solid was removed in a dry-box. The composition of the solid, determined from a Kjeldahl ammonium analysis corresponded to the formula  $\text{NH}_4\text{As}_2\text{F}_{11}$  (found:  $\text{NH}_4$  3.75, 3.84%; calc. for  $\text{NH}_4\text{F} \cdot 2\text{AsF}_5$ :  $\text{NH}_4$  3.76%).

The product fumed strongly in moist air, gave infra-red absorptions at 3640(w), 3560(sh), 3330(m) ( $\text{NH}_4^+$  and possibly HF); 1626(W) ( $\text{NH}_4^+$ ) and a broad band with maxima at 767, 722 and  $703\text{cm}^{-1}$  (PEACOCK and SHARP, 1959 give  $700\text{cm}^{-1}$  for As-F). An X-ray powder photograph gave the lines listed below.

### Preparation of Li, Na, Ag and Tl Hexafluorovanadates

Lithium, sodium and silver hexafluorovanadates have been prepared by the action of bromine trifluoride on a mixture of the alkali halide or silver powder and vanadium trichloride (EMELEUS and GUTMANN, 1949). The X-ray powder photographs of samples prepared in this way in the present work were found to vary from one preparation to another, and the silver compound appeared to be amorphous.

Vanadium pentafluoride was prepared by the action of fluorine on vanadium metal at 350°C (CLARK and EMELEUS, 1957) and distilled under vacuum into a steel bomb containing either LiF, NaF, AgF or TlF and anhydrous hydrogen fluoride. Silver fluoride was prepared by the

method of ANDERSON, BAK and HILLEBERT (1953); and thallous fluoride by evaporating a solution of thallous carbonate in hydrofluoric acid to dryness and drying at 200°. The reaction was allowed to occur overnight at 50°C. After removing excess volatile products under vacuum at 50°C. the white products (silver salt was orange-red) were removed in the dry-box.

Analyses were carried out by reduction with sulphur dioxide followed by titration with permanganate. Found (Li): V, 28.9. Calc. for  $\text{LiVF}_6$ : V, 29.6% Found (Na): V 26.6 Calc. for  $\text{NaVF}_6$ : V 27.1% Found (Ag): V, 19.0 Calc. for  $\text{AgVF}_6$ : V, 18.7% Found (Tl): equiv., 124. Calc. for  $\text{TlVF}_6$ : equiv., 123.

#### Preparation of Thallium (1) Hexafluororuthenate

This compound has been obtained by the reaction of  $\text{RuF}_5$  with TlF in  $\text{SeF}_4$  (HEPWORTH, PEACOCK and ROBINSON, 1954). The preparation was carried out here in anhydrous hydrogen fluoride.

Ruthenium pentafluoride was prepared by the action of fluorine on Ru metal at 350° (HOLLOWAY and PEACOCK, 1963) and purified by vacuum sublimation at 80°. Approximately equimolar amounts of  $\text{RuF}_5$  and TlF were weighed out from the dry-box (slight excess TlF) and reacted together in a steel bomb with hydrogen fluoride as solvent. After removing the solvent in vacuo, a brown product was obtained. This was analysed for Tl as chromate, after first removing ruthenium by alkaline hydrolysis. Found: Tl, 49.8. Calc. for  $\text{TlRuF}_6$ : Tl 48.6%. Some faint lines in the powder photograph could not be indexed. These are possibly due to a decomposition product.

Preparation of  $\text{AgRuF}_6$ ,  $\text{AgIrF}_6$ ,  $\text{AgOsF}_6$ ,  $\text{RbIrF}_6$ ,  $\text{RbOsF}_6$

These were prepared as previously described by the reaction of bromine trifluoride on mixtures of silver powder or rubidium chloride, and either Ru metal powder, iridium or osmium bromides. (Ru: HEFWORTH, PEACOCK and ROBINSON, 1954; Os, Ir: HEFWORTH, ROBINSON and WESTLAND, 1954).

Preparation of  $\text{Li}$  and  $\text{K}$  Hexafluororhenates

These complexes were prepared by PEACOCK's method (1957).

Anhydrous lithium iodide was prepared by dehydrating  $\text{LiI} \cdot 4\text{H}_2\text{O}$ .

Lithium carbonate was dissolved in hydriodic acid (55%) and evaporated to crystals of  $\text{LiI} \cdot 4\text{H}_2\text{O}$ . The hydrate was heated to  $450^\circ$  in a stream of hydrogen and hydrogen iodide obtained by passing hydrogen and iodine vapour through a platinised asbestos catalyst at  $300^\circ$ . When cool the white lithium iodide was ground and stored in the dry-box. Rhenium hexafluoride was prepared by the action of fluorine on rhenium metal at  $350^\circ\text{C}$  and purified by vacuum distillation. It was then distilled into a solution of iodide in liquid sulphur dioxide, controlling the subsequent reaction by cooling. After the reaction was complete, the sulphur dioxide, iodine and excess rhenium fluoride were removed under vacuum leaving a grey-blue solid. Even before the last traces of iodine could be removed a blue sublimate began to form above the solid at less than  $50^\circ\text{C}$ . The product was instantly hydrolysed by water but dissolved completely to give an almost clear solution. An unpleasant odour resembling that of some sulphur compounds was noticed, possibly some reaction with the  $\text{SO}_2$  solvent had occurred.

Although the majority of lines on the X-ray powder photograph could be indexed on a rhombohedral unit cell, a few would not fit in and were considered to be due to decomposition products. Found:

Re, 56.3%. Calc. for  $\text{LiReF}_6$ : Re, 60.7% ( as per-rhenate).

$\text{KReF}_6$  was prepared in a similar manner using potassium iodide and gave a pale blue material.

#### Preparation of Lithium Hexafluorotungstate

Lithium hexafluorotungstate was prepared from lithium iodide and tungsten hexafluoride as described above for  $\text{LiReF}_6$ . Tungsten hexafluoride was obtained by reacting tungsten metal with fluorine at  $300^\circ$  and purified by vacuum distillation. The product was brown in colour and small quantities of a brown solid sublimed above about  $60^\circ\text{C}$ . Again, a few faint lines in the X-ray powder photograph could not be indexed and were attributed to decomposition products.

Tungsten was weighed as  $\text{WO}_3$  after fluorine had been removed by evaporation to dryness with hydrochloric acid. Found: W, 58.7%. Calc. for  $\text{LiWF}_6$ : W, 60.3%.

A sulphurous odour similar to that obtained from hydrolysis of the  $\text{LiReF}_6$  sample was noticed on hydrolysis.

#### Preparation of Li, Ag and K Hexafluoroantimonates

These were prepared as previously described (WOOLF and EMELEUS, 1949) by fluorinating equivalent mixtures of antimony trioxide and the alkali halide or silver powder with bromine trifluoride.

#### Silver Hexafluoroniobate and Hexafluorotantalate

These were prepared as previously described (SHARP and SHARPE, 1956) by fluorinating equivalent mixtures of silver powder and either niobium or tantalum pentoxide.

#### Attempted Preparation of Hexafluorobismuthates(V)

Hexafluorobismuthates (V) have been reported to be formed by the

inter-action of bismuth pentafluoride and a metal fluoride (FISCHER and RUDZITIS, 1959). Although X-ray powder photographs were taken no details were given other than the photograph of the potassium salt was similar to that of  $\text{KSbF}_6$ .

Mixtures of sodium, potassium, rubidium or caesium chlorides and an excess of bismuth trichloride or trifluoride were heated to  $500^\circ\text{C}$  in a stream of fluorine for two hours. The products were handled in the dry-box and X-ray powder photographs taken. It was found that of the four alkali metals all gave different photographs, which in turn were different from any other  $\text{ABF}_6$  photographs. The best photograph was that of the potassium compound in which two phases seemed to be present, one of them isomorphous with  $\text{KSbF}_6$ . Analysis for Bi in the potassium compound was carried out by evaporation of the solid with nitric acid followed by precipitation of bismuth hydroxide and ignition to  $\text{Bi}_2\text{O}_3$ . Found: Bi, 59.2%. Calc. for  $\text{KBiF}_6$ : Bi, 57.7%.

All the solids reacted violently with water giving orange precipitates of bismuth pentoxide.

X-ray Powder Photography.  $\text{CuK}_\alpha$  and  $\text{CoK}_\alpha$  X - radiations, filtered by nickel and iron foil respectively, were used from Metropolitan-Vickers (Imperial College), Solus-Schall or Raymax (Royal College, Glasgow) sets. The values of  $\sin^2\theta$  listed were obtained using a Unicam 9cm powder camera, except  $\text{NaAsF}_6$  for which a 19cm camera was used. Photographs were taken on Ilford G Industrial film and were developed and fixed in standard Ilford solutions. The photographs were measured to 0.005cm using a Hilger and Watts Film measuring rule.

Two methods were used to calibrate the camera. Several photographs

of NaF, LiF,  $\alpha$ -quartz and tungsten, the d-spacings of which are known with considerable accuracy, were taken and a camera constant from each film calculated. The diameter and knife-edge spacings were also measured to 0.0002cm by the Metrology Department, R.C.S.T., Glasgow, and a constant calculated from this. As the photographic determinations seemed to approach the physically-measured constant, but with much less precision, this latter was finally adopted. The constant used, one quarter of the angular separation of the knife-edges was  $86.006^\circ$ , or 1.5012 radians.

Samples for X-ray examination were handled in the dry-box and sealed in Lindemann glass capillary tubes with warm picein wax. The capillary tubes, 0.5mm diameter were obtained from Pantak Ltd.

Calculations. Derivation of the lattice constants from powder photograph measurements was carried out on the R.C.S.T. Ferranti Sirius computer, using the programmes described in Chapter 5.

1	1.0000	0.0000	0, 1, 0	0.0000
2	1.0018	0.0036	0, 2, 0	0.0072
3	1.0036	0.0072	0, 3, 0	0.0144
4	1.0054	0.0108	0, 4, 0	0.0216
5	1.0072	0.0144	0, 5, 0	0.0288
6	1.0090	0.0180	0, 6, 0	0.0360
7	1.0108	0.0216	0, 7, 0	0.0432
8	1.0126	0.0252	0, 8, 0	0.0504
9	1.0144	0.0288	0, 9, 0	0.0576
10	1.0162	0.0324	0, 10, 0	0.0648
11	1.0180	0.0360	0, 11, 0	0.0720
12	1.0198	0.0396	0, 12, 0	0.0792
13	1.0216	0.0432	0, 13, 0	0.0864
14	1.0234	0.0468	0, 14, 0	0.0936
15	1.0252	0.0504	0, 15, 0	0.1008
16	1.0270	0.0540	0, 16, 0	0.1080
17	1.0288	0.0576	0, 17, 0	0.1152
18	1.0306	0.0612	0, 18, 0	0.1224
19	1.0324	0.0648	0, 19, 0	0.1296
20	1.0342	0.0684	0, 20, 0	0.1368
21	1.0360	0.0720	0, 21, 0	0.1440
22	1.0378	0.0756	0, 22, 0	0.1512
23	1.0396	0.0792	0, 23, 0	0.1584
24	1.0414	0.0828	0, 24, 0	0.1656
25	1.0432	0.0864	0, 25, 0	0.1728
26	1.0450	0.0900	0, 26, 0	0.1800
27	1.0468	0.0936	0, 27, 0	0.1872
28	1.0486	0.0972	0, 28, 0	0.1944
29	1.0504	0.1008	0, 29, 0	0.2016
30	1.0522	0.1044	0, 30, 0	0.2088
31	1.0540	0.1080	0, 31, 0	0.2160
32	1.0558	0.1116	0, 32, 0	0.2232
33	1.0576	0.1152	0, 33, 0	0.2304
34	1.0594	0.1188	0, 34, 0	0.2376
35	1.0612	0.1224	0, 35, 0	0.2448
36	1.0630	0.1260	0, 36, 0	0.2520
37	1.0648	0.1296	0, 37, 0	0.2592
38	1.0666	0.1332	0, 38, 0	0.2664
39	1.0684	0.1368	0, 39, 0	0.2736
40	1.0702	0.1404	0, 40, 0	0.2808
41	1.0720	0.1440	0, 41, 0	0.2880
42	1.0738	0.1476	0, 42, 0	0.2952
43	1.0756	0.1512	0, 43, 0	0.3024
44	1.0774	0.1548	0, 44, 0	0.3096
45	1.0792	0.1584	0, 45, 0	0.3168
46	1.0810	0.1620	0, 46, 0	0.3240
47	1.0828	0.1656	0, 47, 0	0.3312
48	1.0846	0.1692	0, 48, 0	0.3384
49	1.0864	0.1728	0, 49, 0	0.3456
50	1.0882	0.1764	0, 50, 0	0.3528
51	1.0900	0.1800	0, 51, 0	0.3600
52	1.0918	0.1836	0, 52, 0	0.3672
53	1.0936	0.1872	0, 53, 0	0.3744
54	1.0954	0.1908	0, 54, 0	0.3816
55	1.0972	0.1944	0, 55, 0	0.3888
56	1.0990	0.1980	0, 56, 0	0.3960
57	1.1008	0.2016	0, 57, 0	0.4032
58	1.1026	0.2052	0, 58, 0	0.4104
59	1.1044	0.2088	0, 59, 0	0.4176
60	1.1062	0.2124	0, 60, 0	0.4248
61	1.1080	0.2160	0, 61, 0	0.4320
62	1.1098	0.2196	0, 62, 0	0.4392
63	1.1116	0.2232	0, 63, 0	0.4464
64	1.1134	0.2268	0, 64, 0	0.4536
65	1.1152	0.2304	0, 65, 0	0.4608
66	1.1170	0.2340	0, 66, 0	0.4680
67	1.1188	0.2376	0, 67, 0	0.4752
68	1.1206	0.2412	0, 68, 0	0.4824
69	1.1224	0.2448	0, 69, 0	0.4896
70	1.1242	0.2484	0, 70, 0	0.4968
71	1.1260	0.2520	0, 71, 0	0.5040
72	1.1278	0.2556	0, 72, 0	0.5112
73	1.1296	0.2592	0, 73, 0	0.5184
74	1.1314	0.2628	0, 74, 0	0.5256
75	1.1332	0.2664	0, 75, 0	0.5328
76	1.1350	0.2700	0, 76, 0	0.5400
77	1.1368	0.2736	0, 77, 0	0.5472
78	1.1386	0.2772	0, 78, 0	0.5544
79	1.1404	0.2808	0, 79, 0	0.5616
80	1.1422	0.2844	0, 80, 0	0.5688
81	1.1440	0.2880	0, 81, 0	0.5760
82	1.1458	0.2916	0, 82, 0	0.5832
83	1.1476	0.2952	0, 83, 0	0.5904
84	1.1494	0.2988	0, 84, 0	0.5976
85	1.1512	0.3024	0, 85, 0	0.6048
86	1.1530	0.3060	0, 86, 0	0.6120
87	1.1548	0.3096	0, 87, 0	0.6192
88	1.1566	0.3132	0, 88, 0	0.6264
89	1.1584	0.3168	0, 89, 0	0.6336
90	1.1602	0.3204	0, 90, 0	0.6408
91	1.1620	0.3240	0, 91, 0	0.6480
92	1.1638	0.3276	0, 92, 0	0.6552
93	1.1656	0.3312	0, 93, 0	0.6624
94	1.1674	0.3348	0, 94, 0	0.6696
95	1.1692	0.3384	0, 95, 0	0.6768
96	1.1710	0.3420	0, 96, 0	0.6840
97	1.1728	0.3456	0, 97, 0	0.6912
98	1.1746	0.3492	0, 98, 0	0.6984
99	1.1764	0.3528	0, 99, 0	0.7056
100	1.1782	0.3564	0, 100, 0	0.7128

X-ray Powder Data.Lithium Hexafluorophosphate

Int.	d(A)	$\sin^2 \theta_{\text{obs}}$	h, k, l	$\sin^2 \theta_{\text{calc}}$
4	4.23	0.0352	0, 0, 3	0.0352
10	4.03	0.0365	1, 0, 1	0.0361
10	3.54	0.0474	0, 1, 2	0.0472
3	2.551	0.0913	1, 0, 4	0.0919
2	2.418	0.1016		
1	2.186	0.1244	0, 1, 5	0.1254
10	2.124	0.1318	1, 1, 3	0.1311
2	2.019	0.1458	2, 0, 2	0.1452
2	1.853	0.1731		
8	1.768	0.1902	0, 2, 4	0.1899
1	1.629	0.2241	2, 0, 5	0.2234
8	1.600	0.2322	1, 1, 6	0.2318
			2, 1, 1	0.2320
5	1.562	0.2435	1, 2, 2	0.2432
1	1.528	0.2545		
1	1.502	0.2635		
3	1.435	0.2885	2, 1, 4	0.2880
3	1.421	0.2943	3, 0, 0	0.2937
3	1.378	0.3129	0, 2, 7	0.3129
4	1.360	0.3214	1, 2, 5	0.3215
2	1.346	0.3279	3, 0, 3	0.3275
3	1.269	0.3688	2, 0, 8	0.3689
3	1.220	0.3990	1, 1, 9	0.3996
2	1.202	0.4115	2, 1, 7	0.4111
4	1.178	0.4284	3, 0, 6	0.4280
			1, 3, 1	0.4283
4	1.163	0.4397	3, 1, 2	0.4395
2	1.128	0.4667	1, 2, 8	0.4671
1	1.109	0.4835	0, 1, 11	0.4835
			1, 3, 4	0.4845
2	1.0721	0.5171	3, 1, 5	0.5179
3	1.0619	0.5270	2, 2, 6	0.5262
			4, 0, 1	0.5265
3	1.0517	0.5373	0, 0, 12	0.5366
			0, 4, 2	0.5377
2	1.0112	0.5812	2, 0, 11	0.5817
3	0.9945	0.6008	2, 1, 10	0.6015
1	0.9754	0.6246	3, 2, 1	0.6247
2	0.9670	0.6356	2, 3, 2	0.6359
2	0.9480	0.6612	1, 0, 13	0.6627
3	0.9344	0.6807	3, 2, 4	0.6807
2	0.9090	0.7993	4, 1, 3	0.7200
2	0.8827	0.7627	0, 1, 14	0.7635

Lithium Hexafluorophosphate (cont.)

Int.	d(A)	$\sin^2\theta_{\text{obs}}$	h, k, l	$\sin^2\theta_{\text{calc}}$	
2	0.8635	0.7969	1, 3, 10	0.7972	} resolved into $\alpha_1$ and $\alpha_2$ lines.
1	0.8609	0.8019	3, 2, 7	0.8024	
2	0.8514	0.8199	0, 5, 1	0.8195	
			4, 1, 6	0.8195	
2	0.8317	0.8590	2, 1, 13	0.8586	
			2, 3, 8	0.8587	
2	0.7996	0.9296	2, 2, 12	0.9295	
			4, 2, 2	0.9295	
1	0.7816	0.9727	0, 4, 11	0.9730	
			2, 4, 4	0.9731	
1	0.7757	0.9877	1, 0, 16	0.9875	
			4, 1, 9	0.9876	

Reliability factor = 0.0006

Hexagonal cell constants     $a = 4.922$      $c = 12.622 \text{ \AA}$

Rhombohedral    "     $a = 5.077$      $\alpha = 57.98^\circ$



Ammonium Hexafluorophosphate

Int.	d(A)	$\sin^2 \theta_{\text{obs}}$	h, k, l	$\sin^2 \theta_{\text{calc}}$
10	4.58	0.0284	1, 1, 1	0.0289
8	3.97	0.0377	2, 0, 0	0.0382
7	2.800	0.0758	2, 2, 0	0.0762
2	2.388	0.1042	3, 1, 1	0.1047
5	2.286	0.1137	2, 2, 2	0.1142
1	1.982	0.1513	4, 0, 0	0.1521
4	1.814	0.1806	5, 3, 1	0.1806
4	1.768	0.1902	4, 2, 0	0.1901
6	1.614	0.2283	4, 2, 2	0.2280
2	1.522	0.2565	3, 3, 3	0.2564
4	1.398	0.3039	4, 4, 0	0.3038
3	1.337	0.3326	5, 3, 1	0.3322
4	1.318	0.3422	4, 4, 2	0.3417
3	1.250	0.3803	6, 2, 0	0.3796
1	1.206	0.4087	5, 3, 3	0.4080
2	1.193	0.4177	6, 2, 2	0.4175
1	1.143	0.4547	4, 4, 4	0.4554
2	1.108	0.4837	5, 5, 1	0.4838
1	1.0978	0.4931	6, 4, 0	0.4932
1	1.0576	0.5313	6, 4, 2	0.5311
1	1.0312	0.55888	5, 5, 3	0.5595
1	0.9895	0.60691	8, 0, 0	0.60685
1	0.9601	0.64467	6, 4, 4	0.64471
1	0.9551	0.68259	8, 2, 2	0.68258

Reliability factor = 0.0004

Cubic cell constant  $a = 7.920 \text{ \AA}$

Lithium Hexafluoroarsenate (Co  $K_{\alpha}$  radiation)

Int.	d(A)	$\sin^2 \theta_{\text{obs}}$	h, k, l	$\sin^2 \theta_{\text{calc}}$	
6	4.34	0.0425	0, 0, 3	0.0426	
10	4.11	0.0472	1, 0, 1	0.0474	
10	3.63	0.0613	0, 1, 2	0.0615	
3	2.606	0.1179	1, 0, 4	0.1180	
1	2.514	0.1265	1, 1, 0	0.1274	
2	2.237	0.1599	0, 1, 5	0.1603	
8	2.170	0.1697	0, 0, 6	0.1697	
			1, 1, 3	0.1697	
1	2.141	0.1744	0, 2, 1	0.1744	
1	2.010	0.1980			
6	1.805	0.2454	0, 2, 4	0.2449	
1	1.709	0.2735	1, 0, 7	0.2731	
1	1.669	0.2868	2, 0, 5	0.2872	
7	1.641	0.2966	1, 1, 6	0.2966	
3	1.629	0.3011	2, 1, 1	0.3013	
3	1.591	0.3158	1, 2, 2	0.3154	
1	1.526	0.3434	0, 1, 8	0.3435	
3	1.468	0.3714	2, 1, 4	0.3717	
4	1.448	0.3816	0, 0, 9	0.3811	
			3, 0, 0	0.3811	
3	1.412	0.4005	0, 2, 7	0.3999	
4	1.389	0.4144	1, 2, 5	0.4140	
3	1.375	0.4237	3, 0, 3	0.4234	
3	1.305	0.4698	2, 0, 8	0.4703	
4	1.255	0.5077	1, 1, 9	0.5078	
			2, 2, 0	0.5078	
2	1.233	0.5266	2, 1, 7	0.5266	
3	1.207	0.5498	2, 2, 3	0.5501	
			3, 0, 6	0.5501	
3	1.202	0.5545	1, 3, 1	0.5548	
3	1.186	0.5691	3, 1, 2	0.5688	
2	1.158	0.5969	1, 2, 8	0.5970	
1	1.145	0.6108	0, 1, 11	0.6110	} resolved into $\alpha_1$ and $\alpha_2$ lines.
2	1.095	0.6668	3, 1, 5	0.6667	
2	1.023	0.7650	2, 1, 10	0.7651	
2	0.9555	0.8772	3, 2, 4	0.8772	
2	0.9287	0.9290	4, 1, 3	0.9290	
2	0.9125	0.9623	0, 1, 14	0.9623	

Reliability factor = 0.0004

Hexagonal cell constants    a = 5.028    c = 13.063 A

Rhombohedral    "    a = 5.233     $\alpha$  = 57.42°

Sodium Hexafluoroarsenate

Int.	d(A)	$\sin^2 \theta_{\text{obs}}$	h, k, l	$\sin^2 \theta_{\text{calc}}$
22	4.67	0.0272	0, 0, 3	0.0274
53	4.39	0.0308	1, 0, 1	0.0309
100	3.86	0.0398	0, 1, 2	0.0400
13	2.789	0.0764	1, 0, 4	0.0765
6	2.669	0.0833	1, 1, 0	0.0835
2	2.389	0.1039	0, 1, 5	0.1038
16	2.315	0.1106	0, 0, 6	0.1094
			1, 1, 3	0.1108
2	2.283	0.1137	0, 2, 1	0.1143
3	2.192	0.1234	2, 0, 2	0.1234
11	1.926	0.1599	0, 2, 4	0.1599
1	1.831	0.1768	1, 0, 7	0.1768
1	1.779	0.1874	2, 0, 5	0.1875
14	1.753	0.1930	1, 1, 6	0.1929
3	1.733	0.1976	2, 1, 1	0.1978
6	1.693	0.2068	1, 2, 2	0.2069
2	1.632	0.2223	0, 1, 8	0.2223
4	1.561	0.2433	2, 1, 4	0.2434
4	1.538	0.2506	3, 0, 0	0.2504
2	1.508	0.2603	0, 2, 7	0.2602
5	1.480	0.2707	1, 2, 5	0.2707
2	1.461	0.2777	3, 0, 3	0.2777
4	1.392	0.3059	2, 0, 8	0.3057
1	1.342	0.3292	1, 1, 9	0.3296
2	1.337	0.3314	1, 0, 10	0.3317
1	1.332	0.3339	2, 2, 0	0.3338
2	1.313	0.3437	2, 1, 7	0.3436
2	1.282	0.3603	3, 0, 6	0.3597
			2, 2, 3	0.3611
2	1.274	0.3651	1, 3, 1	0.3646
2	1.259	0.3742	3, 1, 2	0.3737
1	1.235	0.3890	1, 2, 8	0.3892
1	1.224	0.3957	0, 1, 11	0.3955
1	1.203	0.4095	1, 3, 4	0.4102
1	1.195	0.4149	0, 2, 10	0.4151
1	1.164	0.4375	3, 1, 5	0.4375
			0, 0, 12	0.4375
1	1.156	0.4430	2, 2, 6	0.4431
1	1.138	0.4576	0, 4, 2	0.4572
1	1.091	0.4995	2, 1, 10	0.4992
1	1.067	0.5223	1, 1, 12	0.5218
			0, 4, 5	0.5220
1	1.047	0.5417	2, 3, 2	0.5413
			1, 0, 13	0.5421
1	1.033	0.5559	3, 1, 8	0.5559
1	1.015	0.5767	3, 2, 4	0.5770

Sodium Hexafluoroarsenate (cont.)

Int.	d(A)	$\sin^2 \theta_{\text{obs}}$	h, k, l	$\sin^2 \theta_{\text{calc}}$
1	1.008	0.5845	4, 1, 0	0.5849
1	0.9752	0.6249	0, 1, 14	0.6244
			0, 2, 15	0.6258
1	0.9441	0.6666	1, 3, 10	0.6665
1	0.9286	0.6881	3, 0, 12	0.6880
1	0.9253	0.6943	4, 1, 6	0.6947
1	0.9156	0.7077	2, 0, 14	0.7070
			5, 0, 2	0.7076
			2, 1, 13	0.7084
1	0.9058	0.7241	2, 3, 8	0.7242
1	0.8768	0.7730	2, 2, 12	0.7729
			5, 0, 5	0.7729
1	0.8662	0.7920	1, 2, 14	0.7920
			4, 2, 2	0.7926
1	0.8232	0.8768	1, 5, 2	0.8224
			1, 3, 13	0.8768

Lines with  $\sin^2 \theta > 0.5$  were resolved into  $\alpha'$  and  $\alpha''$  components

Reliability factor = 0.0004

Hexagonal cell constants    a = 5.335    c = 13.976 Å

Rhombohedral    "    a = 5.586     $\alpha = 57.06^\circ$

Lithium Hexafluorovanadate

Int.	d(A)	$\sin^2 \theta_{\text{obs}}$	h, k, l	$\sin^2 \theta_{\text{calc}}$
2	5.00	0.0238		
9	4.57	0.0285	0, 0, 3	0.0293
4	4.20	0.0337	1, 0, 1	0.0341
10	3.87	0.0441	0, 1, 2	0.0440
4	3.15	0.0598		
2	2.822	0.0746		
3	2.645	0.0850	1, 0, 4	0.0838
2	2.269	0.1155	0, 1, 5	0.1137
8	2.197	0.1232	1, 1, 3	0.1255
4	2.078	0.1379	2, 0, 2	0.1384
4	1.833	0.1770	0, 2, 4	0.1784
1	1.781	0.1916	1, 0, 7	0.1936
2	1.684	0.2095	2, 0, 5	0.2084
6	1.663	0.2149	1, 1, 6	0.2135

Reliability factor = 0.0012

Hexagonal cell constants a = 5.004 c = 13.34 A

Rhombohedral " a = 5.30  $\alpha$  = 56.5°Sodium Hexafluorovanadate

Int.	d(A)	$\sin^2 \theta_{\text{obs}}$	h, k, l	$\sin^2 \theta_{\text{calc}}$
4	4.76	0.0282	0, 0, 3	0.0284
6	4.41	0.0305	1, 0, 1	0.0305
10	3.90	0.0391	0, 1, 2	0.0393
4	2.828	0.0743	1, 0, 4	0.0749
4	2.745	0.0789		
8	2.319	0.1106	1, 1, 3	0.1097
5	1.940	0.1579	0, 2, 4	0.1583
7	1.771	0.1894	1, 1, 6	0.1899
5	1.734	0.1977	2, 1, 1	0.1972
4	1.696	0.2066	1, 2, 2	0.2061
5	1.635	0.2223		
2	1.568	0.2416	2, 1, 4	0.2418
1	1.521	0.2567	0, 2, 7	0.2563
1	1.493	0.2667	1, 2, 5	0.2685
2	1.407	0.3004	2, 0, 8	0.3009
2	1.355	0.3235	1, 1, 9	0.3236
4	1.335	0.3336	2, 2, 0	0.3335

Reliability factor = 0.0008

Hexagonal cell constants a = 5.333 c = 14.14 A

Rhombohedral " a = 5.629  $\alpha$  = 56.55°

Silver Hexafluorovanadate

Int.	d(A)	$\sin^2 \theta_{\text{obs}}$	h, k, l	$\sin^2 \theta_{\text{calc}}$
3	3.86	0.0399		
2	3.51	0.0483	1, 1, 0	0.0496
2	3.43	0.0505		
10	3.35	0.0528	1, 0, 2	0.0516
1	3.16	0.0597	0, 0, 3	0.0604
2	3.04	0.0643		
2	2.568	0.1060	2, 0, 1	0.1058
4	2.122	0.1320	1, 0, 4	0.1321
3	2.052	0.1411		
3	2.006	0.1477		
6	1.938	0.1583	2, 0, 3	0.1594
3	1.876	0.1689	0, 0, 5	0.1678
3	1.795	0.1844	2, 1, 3	0.1841
2	1.734	0.1976	2, 2, 0	0.1981
2	1.703	0.2050	2, 2, 1	0.2048
4	1.677	0.2113		

Reliability factor = 0.0010

Tetragonal cell constants  $a = 4.90$   $c = 9.42$  A

Thallium Hexafluorovanadate

Int.	d(A)	$\sin^2 \theta_{\text{obs}}$	h, k, l	$\sin^2 \theta_{\text{calc}}$
5	4.71	0.0268		
10	3.80	0.0412	1, 1, 0	0.0411
7	3.46	0.0496	0, 1, 2	0.0504
5	2.670	0.0834	0, 0, 3	0.0827
1	2.181	0.1249	1, 1, 3	0.1244
2	2.119	0.1323	1, 2, 2	0.1337
5	1.889	0.1666	2, 2, 0	0.1661
4	1.851	0.1735		
4	1.731	0.1982		
2	1.689	0.2082	3, 0, 5	0.2079
3	1.657	0.2164	3, 1, 2	0.2172
5	1.454	0.2811		
1	1.259	0.3752	4, 1, 3	0.3752

Reliability factor = 0.0006

Hexagonal cell constants  $a = 7.54$   $c = 7.99$  A

Rhombohedral "  $a = 5.10$   $\alpha = 95.2^\circ$

Silver Hexafluororuthenate

Int.	d(A)	$\sin^2 \theta_{\text{obs}}$	h, k, l	$\sin^2 \theta_{\text{calc}}$
10	3.41	0.0512	1, 1, 0	0.0503
			1, 0, 2	0.0512
2	2.452	0.1002	2, 0, 0	0.1007
2	2.574	0.1051	0, 0, 4	0.1044
2	2.535	0.1088	2, 0, 1	0.1072
			1, 1, 3	0.1091
8	1.966	0.1533	2, 1, 2	0.1521
			1, 1, 4	0.1548
3	1.716	0.2013	2, 2, 0	0.2016
2	1.697	0.2058	2, 0, 4	0.2053
2	1.551	0.2530	3, 1, 0	0.2521
			3, 0, 2	0.2530
3	1.508	0.2609	1, 0, 6	0.2603
			2, 2, 3	0.2604
1	1.463	0.2769	3, 1, 2	0.2782
2	1.393	0.3054	2, 2, 4	0.3062
2	1.293	0.3545	3, 2, 2	0.3539
2	1.286	0.3582	3, 1, 4	0.3567

Reliability factor = 0.0008

Tetragonal cell constants  $a = 4.85$   $c = 9.54$  AThallium Hexafluororuthenate

Int.	d(A)	$\sin^2 \theta_{\text{obs}}$	h, k, l	$\sin^2 \theta_{\text{calc}}$
10	3.79	0.0414	1, 1, 0	0.0419
6	3.50	0.484		
9	3.31	0.0541	0, 1, 2	0.0543
10	2.986	0.0667	0, 2, 1	0.0657
7	2.499	0.951	2, 0, 2	0.0957
3	2.357	0.1070	2, 1, 1	0.1071
6	2.275	0.1148		
5	2.184	0.1246	3, 0, 3	0.1247
10	2.085	0.1367	1, 2, 2	0.1371
2	1.891	0.1663	2, 2, 0	0.1660
2	1.848	0.1740	1, 0, 4	0.1743
4	1.812	0.1810		
3	1.767	0.1902	1, 3, 1	0.1897
4	1.723	0.2001		
2	1.663	0.2150	3, 0, 3	0.2145
6	1.520	0.2571	2, 1, 4	0.2568

Reliability factor = 0.0006

Hexagonal cell constants  $a = 7.60$   $c = 7.72$  ARhombohedral ,,  $a = 5.08$   $\alpha = 96.6^\circ$

Silver Hexafluoroiridate

Int.	d(A)	$\sin^2 \theta_{\text{obs}}$	h, k, l	$\sin^2 \theta_{\text{calc}}$
1	4.79	0.0259	0, 0, 2	0.0257
			1, 0, 0	0.0257
10	3.40	0.0515	1, 0, 2	0.0511
			1, 1, 0	0.0511
1	2.748	0.0786	1, 1, 2	0.0762
1	2.430	0.1004	0, 0, 4	0.1018
			2, 0, 0	0.1018
8	1.973	0.1523	1, 1, 4	0.1525
			2, 1, 2	0.1525
3	1.707	0.2036	2, 0, 4	0.2031
			2, 2, 0	0.2031
1	1.607	0.2292		
3	1.528	0.2536	1, 0, 6	0.2536
			3, 0, 2	0.2536
			3, 1, 0	0.2536
1	1.395	0.3048	2, 2, 4	0.3042
4	1.292	0.3548	2, 1, 6	0.3547
			3, 1, 4	0.3547
			3, 2, 2	0.3547
1	1.141	0.4557	1, 1, 8	0.4557
			3, 0, 6	0.4557
			3, 3, 0	0.4557
			4, 1, 2	0.4557
1	1.083	0.4562	2, 0, 8	0.5062
			4, 0, 4	0.5062
			4, 2, 0	0.5062
1	1.032	0.5571	3, 2, 6	0.5566
			3, 3, 4	0.5567
1	0.9501	0.6574	3, 1, 8	0.6576
			4, 1, 6	0.6576
			4, 3, 2	0.6576
			5, 0, 2	0.6576

Reliability factor = 0.0004

Tetragonal cell constants a = 4.85 c = 9.70 A



Rubidium Hexafluoroiridate

Int.	d(A)	$\sin^2 \theta_{\text{obs}}$	h, k, l	$\sin^2 \theta_{\text{calc}}$
5	5.05	0.0233	1, 0, 1	0.0238
10	3.81	0.0408	1, 1, 0	0.0408
9	3.32	0.0538	0, 1, 2	0.0540
3	3.03	0.0646	0, 2, 1	0.0645
5	2.43	0.1012	2, 0, 2	0.1038
5	2.198	0.1227	3, 0, 0	0.1233
10	2.092	0.1355	1, 2, 2	0.1354
4	1.903	0.1636	2, 2, 0	0.1630
2	1.850	0.1733	1, 0, 4	0.1748
2	1.781	0.1869	1, 3, 1	0.1866
8	1.656	0.2160	0, 2, 4	0.2154
			3, 1, 2	0.2168
10	1.521	0.2563	2, 1, 4	0.2561
			0, 4, 2	0.2574
3	1.486	0.2685	3, 2, 1	0.2680
7	1.439	0.2858	4, 1, 0	0.2850
6	1.410	0.2984	2, 3, 2	0.2987
5	1.325	0.3379	1, 3, 4	0.3374
4	1.251	0.3783	4, 0, 4	0.3781
			5, 0, 2	0.3794
2	1.214	0.4027	1, 1, 6	0.4030
2	1.188	0.4198	3, 2, 4	0.4187
			4, 2, 2	0.4201
2	1.047	0.5411	2, 4, 4	0.5406
			3, 4, 2	0.5420

Reliability factor = 0.0007

Hexagonal cell constants    a = 7.647    c = 7.689 A

Rhombohedral                "            a = 5.105     $\alpha$  = 97.00°

Silver Hexafluoro-osmate

Int.	d(A)	$\sin^2 \theta_{\text{obs}}$	h, k, l	$\sin^2 \theta_{\text{calc}}$
1	4.84	0.0253	1, 0, 0	0.0250
			0, 0, 2	0.0263
10	3.45	0.0499	1, 1, 0	0.0497
10	3.40	0.0513	1, 0, 2	0.0510
1	2.802	0.0756	1, 1, 2	0.0757
2	2.452	0.0987	2, 0, 0	0.0991
1	2.386	0.1041	0, 0, 4	0.1045
9	1.992	0.1493	2, 1, 2	0.1497
3	1.961	0.1540	1, 1, 4	0.1536
3	1.731	0.1978	2, 2, 0	0.1977
4	1.707	0.2036	2, 0, 4	0.2028
			2, 2, 1	0.2041
5	1.550	0.2469	3, 1, 0	0.2469
			3, 0, 2	0.2482
3	1.515	0.2581	1, 0, 6	0.2585
1	1.473	0.2729	3, 1, 2	0.2728
2	1.402	0.3016	2, 2, 4	0.3013
4	1.308	0.3468	3, 2, 2	0.3466
3	1.289	0.3568	2, 1, 6	0.3569
1	1.226	0.3943	4, 0, 0	0.3945
2	1.160	0.4403	1, 0, 8	0.4397
			2, 1, 7	0.4410
1	1.076	0.4939	4, 2, 0	0.4928
1	0.9625	0.6407	5, 1, 0	0.6402
			4, 3, 2	0.6414
			5, 0, 2	0.6414

Reliability factor = 0.0008

Tetragonal cell constants    a = 4.92    c = 9.58 A

Rubidium Hexafluoro-osmate

Int.	d(A)	$\sin^2 \theta_{\text{obs}}$	h, k, l	$\sin^2 \theta_{\text{calc}}$
5	4.97	0.0240	1, 0, 1	0.0242
10	3.78	0.0416	1, 1, 0	0.0416
8	3.31	0.0543	0, 1, 2	0.0543
2	3.02	0.0652	0, 2, 1	0.0653
4	2.495	0.0953	2, 0, 2	0.0953
4	2.190	0.1236	3, 0, 0	0.1237
1	2.124	0.1314	1, 1, 3	0.1315
10	2.084	0.1366	1, 2, 2	0.1363
5	1.897	0.1647	2, 2, 0	0.1648
4	1.847	0.1738	1, 0, 4	0.1739
3	1.776	0.1881	1, 3, 1	0.1882
6	1.664	0.2139	3, 0, 3	0.2133
			0, 2, 4	0.2148
6	1.647	0.2185	3, 1, 2	0.2180
8	1.523	0.2554	2, 1, 4	0.2556
2	1.513	0.2588	0, 4, 2	0.2589
1	1.483	0.2696	3, 2, 1	0.2699
6	1.437	0.2873	4, 1, 0	0.2872
5	1.406	0.2998	2, 3, 2	0.2997
4	1.326	0.3369	1, 3, 4	0.3372
2	1.284	0.3593	0, 0, 6	0.3591
3	1.268	0.3685	3, 3, 0	0.3688
3	1.253	0.3772	4, 1, 3	0.3765
			4, 0, 4	0.3780
3	1.249	0.3802	5, 0, 2	0.3813
3	1.217	0.4002	1, 1, 6	0.3998
5	1.189	0.4192	3, 2, 4	0.4188
5	1.186	0.4221	4, 2, 2	0.4220
4	1.133	0.4626	1, 5, 2	0.4628
3	1.110	0.4813	3, 0, 6	0.4813
3	1.099	0.4911	6, 0, 0	0.4910
3	1.090	0.4992	0, 5, 4	0.5003
3	1.066	0.5218	2, 2, 6	0.5220
4	1.056	0.5323	5, 2, 0	0.5317
5	1.045	0.5427	0, 2, 7	0.5423
5	1.010	0.5811	6, 0, 3	0.5802
			5, 1, 4	0.5817
6	0.9606	0.6435	4, 1, 6	0.6435
3	0.9460	0.6638	1, 3, 7	0.6639
6	0.9171	0.7069	0, 7, 2	0.7069
			5, 3, 2	0.7069
4	0.9047	0.7262	3, 3, 6	0.7258
4	0.8752	0.7756	7, 1, 0	0.7758

Rubidium Hexafluoro-osmate (cont.)

Int.	d(A)	$\sin^2 \theta_{obs}$	h, k, l	$\sin^2 \theta_{calc}$
5	0.8485	0.8257	3, 5, 4	0.8257
			7, 0, 4	0.8257
3	0.8372	0.8480	6, 0, 6	0.8476
5	0.8281	0.8661	6, 2, 4	0.8664
6	0.8179	0.8886	5, 2, 6	0.8880
3	0.8081	0.9100	8, 0, 2	0.9102
4	0.8060	0.9153	0, 7, 5	0.9149
			5, 3, 5	0.9149
5	0.7925	0.9464	6, 3, 3	0.9464
2	0.7905	0.9510	7, 2, 2	0.9510

Lines with  $\sin^2 \theta$  0.6 were resolved into and components

Reliability factor = 0.0005

Hexagonal cell constants a = 7.633 c = 7.736 A

Rhombohedral " a = 5.106  $\alpha$  = 96.74°

Int.	d(A)	$\sin^2 \theta_{obs}$	h, k, l	$\sin^2 \theta_{calc}$
8	4.40	0.0289	0, 0, 8	0.0289
2	4.81	0.0219	1, 0, 1	0.0219
10	3.89	0.0402	0, 1, 8	0.0416
2	3.87	0.0402		
4	2.76	0.0570	1, 0, 4	0.0706
2	2.73	0.0593	3, 1, 8	0.0596
6	2.24	0.0843	2, 1, 8	0.1159
5	1.81	0.1240		
6	1.74	0.1341	1, 0, 7	0.1363
7	1.72	0.1367		
5	1.62	0.1507	4, 1, 8	0.0796

Lithium Hexafluororhenate

Int.	d(A)	$\sin^2 \theta_{\text{obs}}$	h, k, l	$\sin^2 \theta_{\text{calc}}$
10	4.19	0.0338	1, 0, 1	0.0340
4	3.72	0.0428	0, 1, 2	0.0434
6	3.35	0.0530		
5	3.10	0.0618		
5	2.668	0.0835	1, 0, 4	0.0812
4	2.499	0.0952	1, 1, 0	0.0927
4	2.219	0.1207	1, 1, 3	0.1211
2	2.161	0.1272	0, 2, 1	0.1268
5	2.056	0.1406		
4	1.850	0.1736	0, 2, 4	0.1741
6	1.720	0.2010	2, 0, 5	0.2025
5	1.668	0.2136		
3	1.615	0.2278	1, 2, 2	0.2292
5	1.558	0.2447		
2	1.523	0.2562	0, 0, 9	0.2551
2	1.493	0.2666	2, 1, 4	0.2670
5	1.418	0.2957	1, 2, 5	0.2954
5	1.392	0.3069	3, 0, 3	0.3069
5	1.357	0.3226	2, 0, 8	0.3255
5	1.143	0.4545	0, 0, 12	0.4539

Reliability factor = 0.0014

Hexagonal cell constants a = 5.06 c = 13.73 A

Rhombohedral " a = 5.43  $\alpha$  = 55.5°Lithium Hexafluorotungstate

Int.	d(A)	$\sin^2 \theta_{\text{obs}}$	h, k, l	$\sin^2 \theta_{\text{calc}}$
9	4.46	0.0299	0, 0, 3	0.0286
1	4.32	0.0318	1, 0, 1	0.0318
10	3.82	0.0408	0, 1, 2	0.0414
2	3.09	0.0622		
4	2.726	0.0800	1, 0, 4	0.0798
6	2.328	0.1096	0, 1, 5	0.1086
3	2.278	0.1145	1, 1, 3	0.1150
3	1.931	0.1593		
3	1.776	0.1884	1, 0, 7	0.1856
7	1.725	0.1997	1, 1, 6	0.2016
3	1.484	0.2697	0, 2, 7	0.2722
2	1.453	0.2816	1, 2, 5	0.2817
2	1.362	0.3203	2, 0, 8	0.3203
4	1.307	0.3481	1, 0, 10	0.3492

Reliability factor = 0.0014

Hexagonal cell constants a = 5.24 c = 13.61 A

Rhombohedral " a = 5.45  $\alpha$  = 57.4°

Potassium Hexafluororhenate

Int.	d(A)	$\sin^2 \theta_{\text{obs}}$	h, k, l	$\sin^2 \theta_{\text{calc}}$
9	5.05	0.0233	0, 0, 2	0.0231
			1, 0, 0	0.0231
6	4.51	0.0292	1, 0, 1	0.0289
10	3.56	0.0468	1, 0, 2	0.0464
			1, 1, 0	0.0464
5	3.37	0.0523	0, 0, 3	0.0522
			1, 1, 1	0.0522
4	2.906	0.0702	1, 1, 2	0.0696
2	2.804	0.0755	1, 0, 3	0.0755
3	2.527	0.0928	0, 0, 4	0.0929
2	2.443	0.0994	1, 1, 3	0.0988
			2, 0, 1	0.0988
3	2.262	0.1159	1, 0, 4	0.1162
4	2.202	0.1223	2, 1, 1	0.1221
8	2.059	0.1398	1, 1, 4	0.1396
			2, 1, 2	0.1396
4	2.018	0.1456	0, 0, 5	0.1454
			2, 0, 3	0.1454
5	1.874	0.1687	1, 0, 5	0.1687
			2, 1, 3	0.1688
3	1.787	0.1857	2, 0, 4	0.1862
2	1.766	0.1899	1, 1, 5	0.1921
4	1.685	0.2089	0, 0, 6	0.2096
			2, 1, 4	0.2096
3	1.653	0.2168	3, 0, 1	0.2154
3	1.596	0.2327	1, 0, 6	0.2329
3	1.576	0.2386	2, 0, 5	0.2388
			2, 2, 3	0.2388
			3, 1, 1	0.2388
2	1.524	0.2553	1, 1, 6	0.2563
			3, 1, 2	0.2563
4	1.504	0.2621	2, 1, 5	0.2621
			3, 0, 3	0.2621
2	1.451	0.2817	2, 2, 4	0.2796
3	1.438	0.2864	3, 1, 3	0.2855
1	1.395	0.3043	3, 2, 0	0.3030
1	1.383	0.3098	3, 2, 1	0.3089
5	1.345	0.3279	3, 1, 4	0.3264
			3, 2, 2	0.3264
3	1.290	0.3562	3, 2, 3	0.3556
3	1.251	0.3786	2, 0, 7	0.3789
5	1.224	0.3953	1, 0, 8	0.3964
			2, 2, 6	0.3964

Reliability factor = 0.0009

Tetragonal cell constants a = 5.044 c = 10.09 A

Lithium Hexafluoroantimonate

Int.	d(A)	$\sin^2 \theta_{\text{obs}}$	h, k, l	$\sin^2 \theta_{\text{calc}}$
6	4.52	0.0291	0, 0, 3	0.0291
10	4.27	0.0326	1, 0, 1	0.0328
10	3.74	0.0423	0, 1, 2	0.0425
4	2.707	0.0810	1, 0, 4	0.0810
2	2.583	0.0889	1, 1, 0	0.0888
8	2.321	0.1101	0, 1, 5	0.1100
9	2.251	0.1171	0, 0, 6	0.1158
			1, 1, 3	0.1175
1	2.216	0.1207	0, 2, 1	0.1212
7	1.873	0.1689	0, 2, 4	0.1694
1	1.782	0.1867	1, 0, 7	0.1870
1	1.733	0.1976	2, 0, 5	0.1982
3	1.704	0.2043	1, 1, 6	0.2041
1	1.682	0.2096	2, 1, 1	0.2095
2	1.646	0.2186	1, 2, 2	0.2191
1	1.587	0.2353	0, 1, 8	0.2351
2	1.517	0.2576	2, 1, 4	0.2576
2	1.498	0.2640	3, 0, 0	0.2651
1	1.466	0.2758	0, 2, 7	0.2752
3	1.437	0.2866	1, 2, 5	0.2865
4	1.419	0.2943	3, 0, 3	0.2940
2	1.354	0.3232	2, 0, 8	0.3234
4	1.302	0.3496	1, 1, 9	0.3484
			1, 0, 10	0.3506
3	1.278	0.3629	2, 1, 7	0.3634
2	1.244	0.3829	2, 2, 3	0.3822
2	1.224	0.3955	3, 1, 2	0.3956
2	1.062	0.5266	3, 0, 9	0.5248
			2, 1, 10	0.5270
1	0.9849	0.6117	3, 2, 4	0.6104
			2, 2, 9	0.6130
3	0.8226	0.8769	4, 1, 9	0.8775

Reliability factor = 0.0007

Hexagonal cell constants    a = 5.191    c = 13.613 Å

Rhombohedral                "                a = 5.438     $\alpha$  = 57.01°

Silver Hexafluoroantimonate

Int.	d(A)	$\sin^2 \theta_{\text{obs}}$	h, k, l	$\sin^2 \theta_{\text{calc}}$
10	3.46	0.0496	1, 1, 0	0.0488
			1, 0, 2	0.0504
1	2.48	0.097	2, 0, 0	0.0972
1	2.392	0.1040	0, 0, 4	0.1036
			2, 0, 1	0.1036
10	2.010	0.1470	2, 1, 2	0.1471
10	1.980	0.1526	2, 0, 3	0.1542
2	1.751	0.1939	2, 2, 0	0.1939
5	1.726	0.1994	2, 0, 4	0.2003
			2, 2, 1	0.2003
4	1.565	0.2425	3, 1, 0	0.2422
			3, 0, 2	0.2438
4	1.544	0.2492	3, 1, 1	0.2486
3	1.523	0.2561	1, 0, 6	0.2566
4	1.413	0.2977	2, 2, 4	0.2968
1	1.318	0.3420	1, 0, 7	0.3402
			3, 2, 2	0.3403
7	1.308	0.3473	3, 1, 4	0.3445
1	1.297	0.3530	2, 1, 6	0.3531
3	1.167	0.4364	1, 0, 8	0.4367
			2, 1, 7	0.4367
			4, 1, 2	0.4368
1	1.136	0.4604	1, 1, 8	0.4608
			3, 3, 2	0.4609
2	1.043	0.5465	3, 2, 6	0.5460
2	0.961	0.6432	4, 1, 6	0.6424
			0, 0, 10	0.6439
			4, 2, 5	0.6440

Reliability factor = 0.0008

Tetragonal cell constants  $a = 4.96$   $c = 9.61 \text{ \AA}$



Potassium Hexafluoroantimonate

Int.	d(A)	$\sin^2 \theta_{obs}$	h, k, l	$\sin^2 \theta_{calc}$
6	5.10	0.0228	1, 0, 0	0.0228
10	3.60	0.0458	1, 1, 0	0.0450
			1, 0, 2	0.0462
3	2.943	0.0686	1, 1, 2	0.0686
2	2.572	0.0899	2, 0, 0	0.0899
1	2.508	0.0945	0, 0, 4	0.0946
2	2.459	0.0983	1, 1, 3	0.0981
2	2.298	0.1126	2, 1, 0	0.1125
1	2.245	0.1179	2, 1, 1	0.1182
8	2.091	0.1360	2, 1, 2	0.1359
4	2.063	0.1396	1, 1, 4	0.1394
1	1.900	0.1647	2, 1, 3	0.1654
3	1.818	0.1798	2, 2, 0	0.1796
4	1.795	0.1845	2, 0, 4	0.1845
1	1.758	0.1923	1, 1, 5	0.1925
1	1.709	0.2035	2, 2, 2	0.2032
2	1.695	0.2069	2, 1, 4	0.2067
6	1.625	0.2252	3, 0, 2	0.2252
3	1.590	0.2352	1, 0, 6	0.2350
3	1.548	0.2480	3, 1, 2	0.2480
1	1.517	0.2581	1, 1, 6	0.2574
4	1.472	0.2743	2, 2, 4	0.2739
1	1.427	0.2920	3, 2, 0	0.2916
1	1.416	0.2963	3, 0, 4	0.2963
3	1.372	0.3155	3, 2, 2	0.3152
3	1.365	0.3188	3, 1, 4	0.3187
3	1.352	0.3251	2, 1, 6	0.3246
1	1.286	0.3593	4, 0, 0	0.3588
1	1.246	0.3828	4, 0, 2	0.3824
2	1.212	0.4045	4, 1, 2	0.4048
1	1.198	0.4143	3, 0, 6	0.4142
1	1.187	0.4217	1, 1, 8	0.4224
1	1.166	0.4371	3, 1, 6	0.4366
2	1.151	0.4489	4, 2, 0	0.4483
2	1.145	0.4536	4, 0, 4	0.4531
			4, 2, 1	0.4543
2	1.086	0.5035	3, 2, 6	0.5037
2	1.046	0.5428	4, 2, 4	0.5426
3	1.009	0.5843	4, 3, 2	0.5839
			5, 0, 2	0.5839
2	0.938	0.6752	5, 2, 2	0.6735
			5, 1, 4	0.6770
1	0.921	0.7011	2, 1, 10	0.7016
			3, 1, 9	0.7017

Reliability factor = 0.0008

Tetragonal cell constants a = 5.151 c = 10.04 A

Silver Hexafluoroniobate

Int.	d(A)	$\sin^2 \theta_{\text{obs}}$	h, k, l	$\sin^2 \theta_{\text{calc}}$
10	3.49	0.0487	1, 1, 0	0.0486
9	3.41	0.0512	1, 0, 2	0.0506
8	2.003	0.1477	2, 1, 2	0.1472
6	1.966	0.1533	1, 1, 4	0.1531
4	1.747	0.1942	2, 2, 0	0.1934
3	1.715	0.2018	2, 0, 4	0.2013
6	1.560	0.2437	3, 0, 2	0.2436
4	1.509	0.2600	1, 0, 6	0.2594
			2, 0, 5	0.2600
2	1.410	0.2984	2, 2, 4	0.2977
2	1.322	0.3389	3, 2, 2	0.3400
2	1.308	0.3468	3, 1, 4	0.3459
3	1.293	0.3541	2, 1, 6	0.3557
1	1.191	0.4175	4, 1, 1	0.4167
			0, 0, 8	0.4177
			3, 2, 4	0.4181
5	1.166	0.4358	4, 1, 2	0.4363
2	1.050	0.5387	3, 0, 7	0.5367
			2, 1, 8	0.5380
			3, 3, 4	0.5384
2	1.041	0.5476	3, 2, 6	0.5483
4	0.9717	0.6284	4, 3, 2	0.6287
			5, 0, 2	0.6287

Reliability factor = 0.0010

Tetragonal cell constants a = 4.968 c = 9.551 A

Silver Hexafluorotantalate

Int.	d(A)	$\sin^2 \theta_{\text{obs}}$	h, k, l	$\sin^2 \theta_{\text{calc}}$
1	4.90	0.0247	1, 0, 0	0.0247
7	3.50	0.0483	1, 1, 0	0.0489
9	3.42	0.0506	1, 1, 0	0.0489
			1, 0, 2	0.0507
2	2.482	0.0964	2, 0, 0	0.0970
1	2.384	0.1043	2, 0, 1	0.1034
			0, 0, 4	0.1041
10	2.015	0.1461	2, 1, 2	0.1467
6	1.974	0.1521	1, 1, 4	0.1520
4	1.756	0.1925	2, 2, 0	0.1927
5	1.722	0.1999	2, 2, 1	0.1991
			2, 0, 4	0.1998
1	1.648	0.2184	3, 0, 0	0.2166
			2, 2, 2	0.2184
1	1.628	0.2234	3, 0, 1	0.2230
			2, 1, 4	0.2237
7	1.568	0.2410	3, 1, 0	0.2403
			3, 0, 2	0.2423
4	1.517	0.2573	1, 0, 6	0.2565
			2, 0, 5	0.2576
3	1.417	0.2948	2, 2, 4	0.2953
4	1.327	0.3368	3, 2, 2	0.3377
5	1.314	0.3430	3, 1, 4	0.3430
5	1.295	0.3533	2, 1, 6	0.3519
			2, 2, 5	0.3529
1	1.244	0.3833	4, 0, 0	0.3835
2	1.172	0.4316	3, 3, 0	0.4311
			4, 1, 2	0.4329
1	1.151	0.4480	3, 0, 6	0.4471
1	1.106	0.4852	4, 2, 1	0.4851
			4, 0, 4	0.4858
2	1.045	0.5432	3, 2, 6	0.5423
			4, 0, 5	0.5433
2	1.012	0.5794	4, 2, 4	0.5795
3	0.9758	0.6230	5, 0, 2	0.6227
2	0.9094	0.7173	5, 2, 2	0.7172
2	0.8470	0.8270	5, 0, 6	0.8275

Reliability factor = 0.0009

Tetragonal cell constants     $a = 4.993$      $c = 9.634 \text{ \AA}$

Potassium Hexafluorobismuthate(V)

Int.	d(A)	$\sin^2 \theta_{\text{obs}}$
5	5.21	0.0219
4	3.98	0.0376
5	3.65	0.0445
8	3.27	0.0556
1	2.984	0.0668
10	2.826	0.0744
5	2.558	0.0909
3	2.308	0.1116
3	2.238	0.1186
2	2.111	0.1333
1	2.069	0.1388
10	1.999	0.1487
1	1.824	0.1786
1	1.788	0.1859
10	1.720	0.2008
9	1.637	0.2218
1	1.539	0.2510
2	1.467	0.2761
5	1.417	0.2961
2	1.394	0.3060
3	1.382	0.3111
1	1.336	0.3331
3	1.267	0.3702
1	1.188	0.4208
3	1.157	0.4438
3	1.124	0.4700
1	1.0952	0.4955
5	1.0715	0.5176
2	1.0591	0.5298
2	1.0027	0.5911
3	0.9460	0.6641
1	0.9289	0.6887
2	0.9209	0.7007
1	0.7158	0.9112
4	0.8979	0.7571
4	0.8950	0.7419
2	0.8915	0.7477
1	0.8627	0.7985
2	0.8562	0.8108
2	0.8513	0.8592
4	0.8188	0.8864
5	0.7968	0.9600

weighted mean of  $\alpha_1$  and

$\alpha_2$  doublets

## Chapter 2

### The Vibrational Spectra of Complex Fluorides

#### 2.1 Introduction

The vibrational spectra of the volatile hexafluorides have been extensively studied and are now well understood. In all examples so far examined the observed spectrum is in complete agreement with an octahedral molecule having full  $O_h$  symmetry. The vibrational spectra of the salts of complex fluoro-acids containing hexafluoride anions have not been so fully investigated. PEACOCK and SHARP (1959) recorded the infra-red spectra of a large number of complex fluorides but in many cases only one of the fundamental frequencies of the hexafluoride anion occurred in the region available to them ( $4000 - 400 \text{ cm}^{-1}$ ). The present work was undertaken to extend the observed region down to  $200 \text{ cm}^{-1}$ , where the remaining fundamental frequencies were expected to occur.

#### 2.2 Neutral Hexafluorides

There are 15 vibrational degrees of freedom for a non-linear molecule  $XY_6$ , but some of the corresponding normal vibrations will be equivalent if the molecule has symmetry. The number of distinct vibrational modes expected for a particular symmetry is derived using the methods of group theory (HERZBERG, 1945). For an octahedral molecule  $XY_6$ , which belongs to point group  $O_h$ , there are six normal vibrations, having the group representation  $A_{1g} + E_g + F_{2g} + 2F_{1u} + F_{2u}$ . A corresponds to a non-degenerate vibration, E to doubly- and F to triply-degenerate vibrations. These six vibrations are usually designated

$\nu_1(a_{1g})$ ,  $\nu_2(e_g)$ ,  $\nu_3(f_{1u})$ ,  $\nu_4(f_{1u})$ ,  $\nu_5(f_{2g})$  and  $\nu_6(f_{2u})$ , using the convention of small letters for the species symbols of the fundamental vibrations.

Figure 2.1 shows one component each of the six normal vibrations.

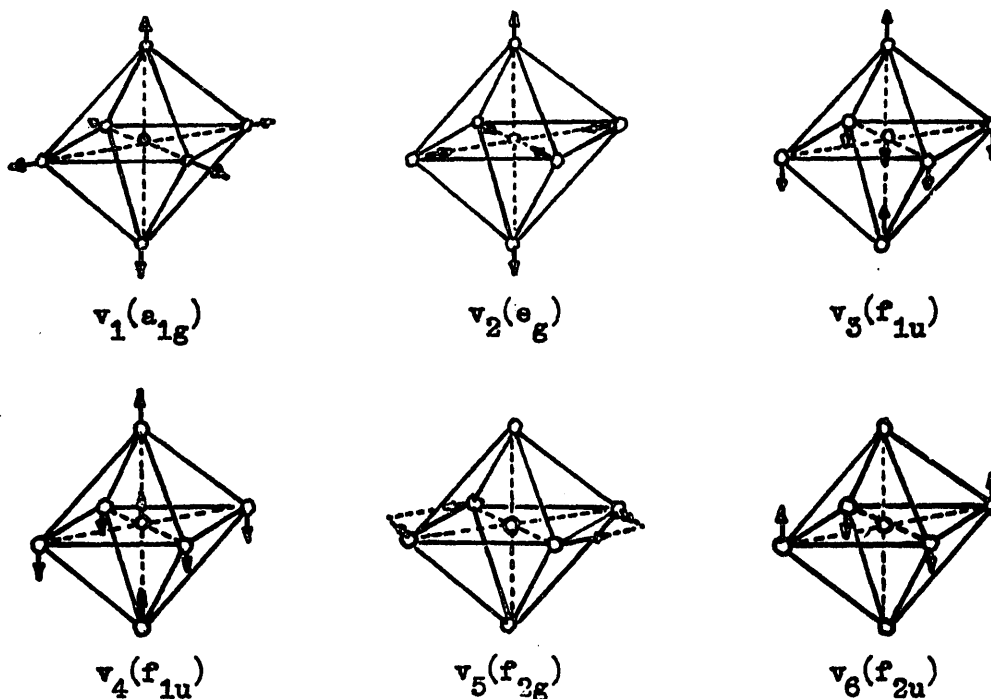


Figure 2.1

Normal vibrations of an octahedral molecule  $AB_6$

From the selection rules for infra-red and Raman activity it can be deduced that  $\nu_3$  and  $\nu_4$  are infra-red active,  $\nu_1$ ,  $\nu_2$  and  $\nu_5$  are Raman active and  $\nu_6$  is inactive. Certain combination frequencies of  $\nu_6$  with other fundamentals are infra-red active however and a value for  $\nu_6$  can usually be derived indirectly from these.

Some values of vibrational frequencies for hexafluorides are collected in Table 2.1. It is apparent that the two infra-red active frequencies  $\nu_3$  and  $\nu_4$  vary most with the different central atoms but not necessarily in the same order or extent as the other frequencies.

The frequency, or more accurately the force constant, of the fully symmetric vibration  $\nu_1$  is most dependent on the strength of the X - F bond. A surprising fact emerging from the  $\nu_1$  frequencies shown is that the second row transition metal M - F bonds must be weaker than their third row counterparts. This presumably reflects an increase in covalent character in going from second to third row metal (PEACOCK and SHARP, 1959).

The data presented in Table 2.1 was obtained from infra-red measurements, taken in the gas phase, and Raman effect studies in the liquid phase. Comparable conditions cannot be used for the ionic fluoro-acid salts in most cases because of their non-volatility and sensitivity to solvents, particularly water. Infra-red spectra can therefore only be taken in the solid phase, usually ground to a mull with paraffin to reduce light scattering. Unfortunately, in the solid state interactions may occur, which are not present in liquid or gas phases, tending to perturb the symmetry of the molecule or anion. Although in the free state a complex ion may have high symmetry, when bound in a lattice the presence of oppositely charged ions in fixed positions about the complex may cause it to distort from its true configuration; interactions between non-equivalent molecules in the same unit cell may cause similar perturbations. A further complication arises from the vibrations of the lattice as a whole; although these generally occur at much lower frequencies than the vibrations being considered here, they may couple with them having the effect of broadening the absorption bands of the complex ion. Infra-red studies of solids are therefore somewhat limited to the recognition of the

Table 2.1Vibrational frequencies ( $\text{cm}^{-1}$ ) of some hexafluorides

Compound	$\nu_1$	$\nu_2$	$\nu_3$	$\nu_4$	$\nu_5$	$\nu_6$
$\text{SF}_6^{\text{a}}$	775	644	940	615	524	363
$\text{SeF}_6^{\text{b}}$	708	662	780	437	405	260
$\text{TeF}_6^{\text{b}}$	701	674	752	327	313	197
$\text{MoF}_6^{\text{c}}$	741	643	741	264	306	190
$\text{WF}_6^{\text{b}}$	769	670	712	256	322	216
$\text{TaF}_6^{\text{c}}$	705	551	748	265	255	
$\text{ReF}_6^{\text{d}}$	755	596	715	257	246	193
$\text{RuF}_6^{\text{e}}$	675	573	735	275	262	
$\text{OsF}_6^{\text{f}}$	733	632	720	268	252	180 <sup>j</sup>
$\text{RhF}_6^{\text{e}}$	634	595	724	283	269	192
$\text{IrF}_6^{\text{g}}$	696	643	718	276	260	205
$\text{PtF}_6^{\text{f}}$	655	601	705	273	242	211
$\text{UF}_6^{\text{b}}$	668	532	626	189	202	144
$\text{NpF}_6^{\text{h}}$	648	528	624	200	206	164
$\text{PuF}_6^{\text{h}}$	625	522	617	205	211	176
$\text{XeF}_6^{\text{i}}$	579	644	610			

<sup>a</sup> LAGERMAN and JONES (1951). <sup>b</sup> GAUNT (1953). <sup>c</sup> CLAASSEN, SELIG and MALM (1962). <sup>d</sup> CLAASSEN, MALM and SELIG (1962). <sup>e</sup> WEINSTOCK, CLAASSEN and CHERNICK (1963). <sup>f</sup> WEINSTOCK, CLAASSEN and MALM (1960). <sup>g</sup> MATTHEW et al. (1955). <sup>h</sup> MALM, WEINSTOCK and CLAASSEN (1955). <sup>i</sup> WEAVER, WEINSTOCK and KNOP (1963). <sup>j</sup> WEINSTOCK and GOODMAN, unpublished reassignment.



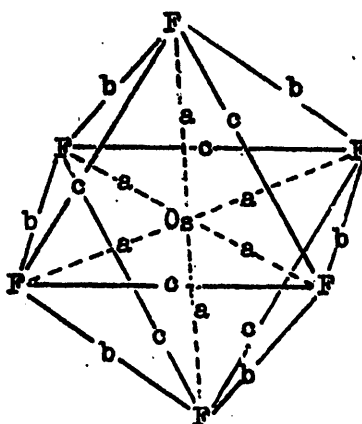
stronger fundamental vibrations, weaker combination frequencies and overtones are not usually observed.

Complex fluorides studied were chiefly restricted to those of the transition metals in an attempt to discover effects due to the presence of d-electrons.

### 2.3 ABF<sub>6</sub> Complex Fluorides

In Chapter 1 it has been shown that the salts of a large range of fluoro-acids of a given cation are isomorphous. This system therefore seemed suitable for a study of the vibrational frequencies of the hexafluoride anions known to be present in these compounds. The most convenient cation was thought to be caesium from the point of view of the higher stability of its salts and the minimisation of solid state interactions described above. Further, all caesium salts (except CsPF<sub>6</sub>) are isomorphous and the unit cell is known to contain only one molecule. A complete structure determination on KOsF<sub>6</sub>, a member of this isomorphous series, by HEPWORTH, JACK and WESTLAND (1956) showed that in the solid state the OsF<sub>6</sub><sup>-</sup> group has only D<sub>3d</sub> symmetry, caused by a contraction of the OsF<sub>6</sub> octahedron along a 3-fold axis. This contraction leaves all six Os - F bonds equal, but the twelve F - F distances are separated into two types, 6 at 2.66 and 6 at 2.48 Å (see Fig. 2.2). It is assumed that all isomorphous ABF<sub>6</sub> complexes show this distortion to a greater or lesser degree.

Using the methods of group theory as described by EYRING, WALTER and KIMBALL (1944), the fifteen possible vibrations of a molecule XY<sub>6</sub> with D<sub>3d</sub> symmetry were found to reduce to the representation  $2A_{1g} + A_{1u} + 2A_{2u} + 2E_g + 3E_u$  with ten fundamentals. Vibrations with



$$a = 1.82 \text{ \AA}$$

$$b = 2.48$$

$$c = 2.66$$

Figure 2.2

The distorted octahedron in  $\text{KOsF}_6$

(HEPWORTH, JACK and WESTLAND 1956)

symmetry  $A_{2u}$  and  $E_u$  are infra-red active,  $A_{1g}$ ,  $E_g$  are Raman active and  $A_{1u}$  is inactive. By considering the form of the octahedron vibrations (Figure 2.1) and the effect of the distortion present in  $\text{KOsF}_6$  the six octahedral normal vibrations are split thus:-

$$A_{1g} \rightarrow A_{1g}, E_g \rightarrow E_g, 2F_{1u} \rightarrow 2(A_{2u} + E_u), F_{2g} \rightarrow (A_{1g} + E_g), F_{2u} \rightarrow (A_{1u} + E_u).$$

The two infra-red active vibrations of the octahedron  $\nu_3$  and  $\nu_4$  are therefore both split into doublets, the extent of the splitting depending on the magnitude of the distortion. The inactive vibration  $\nu_6$  is also split into a doublet and one component of this becomes infra-red active.

The results of the present work are presented in Table 2.2, all frequencies are for caesium salts unless otherwise stated.

Table 2.2

Infra-red absorption maxima for complexes  $ABF_6^-$  (in  $\text{cm}^{-1}$ )

Anion	$\nu_3^a$	$\nu_3$	$\nu_4$	
$PF_6^-$	845	840	556	(559) <sup>a</sup>
$AsF_6^-$	700	658	403, 392	
$SbF_6^-$	660	656	282	(broad)
$VF_6^-$	715	605	315	
$NbF_6^-$	580	585, 619(sh)	256, 232	
$TaF_6^-$	580	560(broad)	240(broad)	
$MoF_6^-$	623	625, 595(sh)	260, 237	
$WF_6^-$	594	590	249, 230	
$ReF_6^-$	627	639, 629(sh)	235, 220	
$RuF_6^-$	640	649	296, 279	
$OsF_6^-$	616	629, 647(sh)	275, 255	
$IrF_6^-$	667	633	260, 248	

(sh) = shoulder

<sup>a</sup> PEACOCK and SHARP (1959) for potassium salts.

In nearly every case the spectrum consisted of two strong absorptions, each split into two peaks of comparable intensity. The lower frequency  $\nu_4$  pair were more clearly resolved, in most cases the  $\nu_3$  pair appeared as a single asymmetric peak with a shoulder. The  $CsReF_6$  and  $CsWF_6$  spectra also had extra bands of medium intensity at 295, 274  $\text{cm}^{-1}$ , and 338, 282  $\text{cm}^{-1}$  respectively, the cause of which could not be explained. The Raman spectrum of potassium hexafluorophosphate in the molten state has

been recorded by BUHLER and BUES (1961). They obtained frequencies of 735 for  $\nu_1$ , 563 for  $\nu_2$  and 462 for  $\nu_5$ .

#### 2.4 $A_2BF_6$ Complex Fluorides

The crystal structures of complex fluorides  $A_2BF_6$  are more varied than the corresponding  $ABF_6$  complexes (WELLS, 1962), but all are based on a close-packed structure of  $A^+$  cations and  $F^-$  ions. The  $SiF_6$  octahedron in  $K_2SiF_6$  is known to be regular in the solid state (MEYERS and COTTON, 1960). SIEBERT (1953) has examined the vibrational spectra of aqueous solutions of  $H_2SiF_6$  and  $Li_2SiF_6$  by the Raman effect and report  $\nu_1 = 726$ ,  $\nu_2 = 510 \text{ cm}^{-1}$ .

MELLOR and STEPHENSON (1951) found that there is a slight distortion of the  $PtF_6$  octahedron in  $K_2PtF_6$ . The distortion in  $K_2PtF_6$  is similar to that found by HEPWORTH, JACK and WESTLAND (1956) in  $KOsF_6$  but is very much smaller — the two different F - F distances are 2.66 and 2.63 Å. WOODWARD and WARE (1963) have recently studied the vibrational spectra of the  $PtF_6^{2-}$  ion by infra-red spectroscopy (caesium salts) and the Raman effect (aqueous solution of  $Na_2PtF_6$ ). They found that in the solid state the  $\nu_3$  absorption peak is slightly asymmetrical, but in solution the  $PtF_6^{2-}$  ion is a regular octahedron. ADAMS and GEBBIE (1963) report the spectrum of  $K_2OsF_6$  in the region  $400 - 40 \text{ cm}^{-1}$ , the  $\nu_4$  vibration is split with a peak at 262 and a shoulder at  $246 \text{ cm}^{-1}$ , in good agreement with the values obtained here (Table 2.3). They also find an absorption at  $118 \text{ cm}^{-1}$  which is assigned to a lattice mode.

In Table 2.3 are the infra-red absorption frequencies of caesium salts of complex fluoro-acids found in the present work, and the values obtained by PEACOCK and SHARP (1959) for  $\nu_3$  from potassium salts.

Table 2.3Infra-red absorption maxima for complexes  $A_2BF_6$ 

Anion	$\nu_3^a$	$\nu_3$	$\nu_4$
$SiF_6^{2-}$	726	727	474 (480) <sup>a</sup>
$ZrF_6^{2-}$	<400	-	-
$ReF_6^{2-}$	541	542	255, 250
$RuF_6^{2-}$	581	562 581(sh)	283, 256
$OsF_6^{2-}$	548	541 560(sh)	258, 234
$RhF_6^{2-}$	589	589	284, 258(w)
$IrF_6^{2-}$	568	556	268, 239
$PdF_6^{2-}$	602	600	289
$PtF_6^{2-}$	583	575, 566(sh); (571) <sup>b</sup>	272 (281) <sup>b</sup>

(sh) = shoulder, (w) = weak

<sup>a</sup> PEACOCK and SHARP (1959)<sup>b</sup> WOODWARD and WARE (1963)

Splitting of  $\nu_4$  into two clearly resolved peaks was observed in the case of Ru, Os, Rh and Ir with an associated asymmetry in  $\nu_3$ . An additional peak was found at  $314\text{ cm}^{-1}$  for  $Cs_2RhF_6$  which was considered to be due to an impurity rather than a further splitting of  $\nu_4$ , possibly the presence of  $Cs_3RhF_6$  (COX, SHARP and SHARPE, 1956). The spectrum of a sample of  $Cs_2ZrF_6$  did not have any clearly resolved peaks in the region  $700 - 200\text{ cm}^{-1}$ ; absorptions were found at  $3350$  and  $1640\text{ cm}^{-1}$  suggesting the presence of O - H groups; these absorptions persisted even after treatment with bromine trifluoride.

## 2.5 Discussion

It is now possible to discuss qualitatively trends in the vibrational frequencies of the  $\text{BF}_6^{n-}$  octahedron for both isoelectronic series and "isonuclear" series of complex fluoro-anions. Unfortunately only sufficient data exist for the comparison of  $\nu_3$  and  $\nu_4$  frequencies, but as pointed out previously, of the six octahedral vibrations the frequencies of  $\nu_3$  and  $\nu_4$  show the greatest range of magnitudes (c.f. Table 2.1). Some values of these frequencies for isoelectronic and isonuclear series (same central atom but varying charge) are collected in Tables 2.4 and 2.5; where splitting of frequencies occurred the average frequency is given.

In both types of series the largest changes in frequency occur with the  $\nu_3$  vibration, with increasing charge on the hexafluoride group the frequency falls; the reduction in frequency per unit charge is surprisingly constant at  $80 \pm 5 \text{ cm}^{-1}$ . The  $\nu_4$  vibration remains virtually constant however with only a slight tendency to fall with increasing charge. This difference in behaviour is understandable when the form of the vibrations is considered. The  $\nu_3$  mode is essentially a bond stretching mode, and consequently more sensitive to bond strength than  $\nu_4$ , which is a bond deformation mode (Figure 4.1). As the positive charge on the central atom is reduced its effective ionic radius must increase with a consequent reduction in covalent character in the atom-fluorine bond. The restoring force in a deformation reaction comes mainly from repulsions between atoms and, in the case of transition metals, non-bonding electrons. This effect is known to be smaller, the differences in  $\nu_4$  are comparable to

Table 2.4

$\nu_3$  and  $\nu_4$  Frequencies for isoelectronic series of fluoroanions

Complex( $d^4$ )	$\nu_3$	$\nu_4$	Complex( $d^5$ )	$\nu_3$	$\nu_4$	Complex( $d^8$ )	$\nu_3$	$\nu_4$
PtF <sub>6</sub>	705	273	IrF <sub>6</sub>	718	276	RhF <sub>6</sub>	724	283
IrF <sub>6</sub>	633	254	OsF <sub>6</sub> <sup>-</sup>	638	265	RuF <sub>6</sub> <sup>-</sup>	649	287
OsF <sub>6</sub> <sup>2-</sup>	552	246	ReF <sub>6</sub> <sup>2-</sup>	545	255	TcF <sub>6</sub> <sup>2-</sup>	574 <sup>a</sup>	

<sup>a</sup> SCHWOCHAU and HERR (1963)

Table 2.5

$\nu_3$  and  $\nu_4$  Frequencies for isonuclear series of complex fluorides

Complex	$\nu_3$	$\nu_4$	Complex	$\nu_3$	$\nu_4$	Complex	$\nu_3$	$\nu_4$
IrF <sub>6</sub>	718	276	OsF <sub>6</sub>	720	268	RuF <sub>6</sub>	735	275
IrF <sub>6</sub> <sup>-</sup>	633	254	OsF <sub>6</sub> <sup>-</sup>	638	265	RuF <sub>6</sub> <sup>-</sup>	649	287
IrF <sub>6</sub> <sup>2-</sup>	550	253	OsF <sub>6</sub> <sup>2-</sup>	552	246	RuF <sub>6</sub> <sup>2-</sup>	571	270

experimental error and no reliable generalisation can be made with the present data.

Although splitting of the  $\nu_3$  and  $\nu_4$  vibrations was observed in the solid state, as expected from the distortion from octahedral symmetry known to be present from X-ray studies (HEPWORTH, TACK and WESTLAND, 1956), the remaining infra-red allowed vibration arising from the octahedral  $\nu_6$  vibration was not detected. From Table 2.1, the frequency is expected to be slightly below 200 cm<sup>-1</sup>, which was below the limit of our instruments. It could be that this is responsible for the peak at 118 cm<sup>-1</sup> observed in K<sub>2</sub>OsF<sub>6</sub> by ADAMS and GEBBIE (1963), but as  $\nu_6$  is a

deformation mode it seems unlikely that the frequency would drop from  $180\text{cm}^{-1}$  in  $\text{OsF}_6$  to  $118\text{cm}^{-1}$  in  $\text{OsF}_6^{2-}$ . WOODWARD and WARE (1963) have suggested that  $\nu_6$  is  $143\text{cm}^{-1}$  in the octahedral  $\text{PtF}_6^{2-}$  ion.

Since this distortion from octahedral symmetry occurs chiefly in transition metal complex fluorides it could be that the presence of unfilled d-orbitals on the metal atom is influencing the structure of the complex. The Jahn-Teller theorem states that, for a non-linear molecule, an orbitally degenerate electron configuration is unstable with respect to nuclear displacements which would remove the degeneracy. The lifting of degeneracy in octahedral molecules has most frequently been connected with a molecular distortion involving a lengthening or shortening of the two axial bonds relative to the four planar ones. This effect would lower the point group symmetry of the  $\text{BF}_6$  ion from  $O_h$  to  $D_{4h}$ , and would give rise to the splitting of  $\nu_3$  and  $\nu_4$  vibrations observed in the present work. However both  $\text{OsF}_6^-$  and  $\text{ReF}_6^{2-}$  show splitting and yet both have the non-bonding electron configuration  $d^8$  which is not expected to show a distortion according to the Jahn-Teller theorem. In a study of transition metal hexafluorides, WEINSTOCK, CLAASSEN and MALM (1963) have come to the conclusion that, in these compounds, orbital degeneracy among non-bonding d electrons is removed not by a distortion in octahedral symmetry, but through some form of vibronic coupling between vibrational and electronic transitions in the molecule. The effect becomes apparent by an abnormal reduction in intensity of the Raman-active  $\nu_2$  vibration and broadening of all combinations bands involving this vibration.

In the light of these conclusions it seems incorrect to attribute



the splitting of the  $\nu_3$  and  $\nu_4$  vibrations to a Jahn-Teller effect. As was pointed out in Chapter 1, they are almost certainly due to a solid state interaction between the complex anion and cation. The distortion is therefore expected to be largely removed on melting or dissolution of the compound.

Mo, 26.8. Calc. for  $\text{CaMoF}_6$ : Mo 26.0%. Found: W 43.1.  
 SP.: W 42.6%. Found: Mo 26.7. Calc. for  $\text{CaMoF}_6$ : Mo 43.  
 Calcium hexafluorophosphate was prepared according to WYCK  
 dissolving phosphorus pentachloride in a solution of calcium  
 anhydrous hydrogen chloride.

#### Preparation of Potassium Hexafluorophosphate (IV)

This compound was prepared by the method of WYCK (1941) 2  
 dissolution of molten potassium hydrogen fluoride acid, according  
 hexafluorophosphate (IV). It was recrystallized from water as pale p  
 crystals.

#### Preparation of Calcium Hexafluorophosphate (IV)

## Experimental

Caesium fluoride was obtained from the American Potash and Chemical Company.

### Preparation of ABF<sub>6</sub> Complexes

Caesium salts of the ABF<sub>6</sub> complexes were prepared by analogous methods to those described in Chapter 1. Thus, fluorination of mixtures of caesium chloride and an appropriate starting material with bromine trifluoride was used for CsAsF<sub>6</sub>, CsSbF<sub>6</sub>, CsNbF<sub>6</sub>, CsTaF<sub>6</sub>, CsRuF<sub>6</sub>, CsOsF<sub>6</sub> and CsIrF<sub>6</sub>. Reduction of the metal hexafluoride with caesium iodide in sulphur dioxide was used to prepare CsMoF<sub>6</sub>, CsWF<sub>6</sub> and CsReF<sub>6</sub>. Found: Mo, 26.9. Calc. for CsMoF<sub>6</sub>: Mo 28.0%. Found: W 43.1. Calc. for CsWF<sub>6</sub>: W 42.69%. Found: Re 41.7. Calc. for CsReF<sub>6</sub>: Re 43.0%.

Caesium hexafluorophosphate was prepared according to WOYSKI (1950) by dissolving phosphorus pentachloride in a solution of caesium fluoride in anhydrous hydrogen fluoride.

### Preparation of Potassium Hexafluororhenate(IV)

This compound was prepared by the method of PEACOCK (1956) by the interaction of molten potassium hydrogen fluoride with ammonium hexalodorhenate(IV). It was recrystallised from water as pale pink crystals.

### Preparation of Caesium Hexafluororuthenate(IV)

Caesium hexafluororuthenate(V) was dissolved in a small quantity of water containing a molar proportion of caesium fluoride (HEPWORTH, PEACOCK and ROBINSON, 1954). The hexafluororuthenate(IV) was recrystallised from hot (70°C) water as a white powder.

Preparation of Caesium Hexafluoro-osmate(IV)

This was prepared by the action of water on caesium hexafluoro-osmate(V) as previously described (HEPWORTH, ROBINSON and WESTLAND, 1954). The compound was recrystallised from hot water as a white powder.

Preparation of Caesium Hexafluoro-iridate(IV)

This compound was prepared in a similar way to the hexafluoro-osmate(IV) above. However the product was a definite pink colour which persisted both in solution and after several recrystallisations.

Found: F 19.0 Calc. for  $Cs_2IrF_6$ : F 19.89%. Calc. for  $Cs_2IrF_6(OH)$ : F 16.64%.

The possibility of a partial hydrolysis to  $IrF_6OH^{2-}$  was suggested by HEPWORTH, ROBINSON and WESTLAND (1954) in strongly alkaline solution, and WEISE (1956) has suggested a similar hydrolysis in  $ReF_6^{2-}$  to account for the pink colour of some samples of  $K_2ReF_6$ . A mull of the pink  $Cs_2IrF_6$  showed no absorption in the region of  $3300cm^{-1}$  where the O - H bond normally absorbs strongly.

The presence of bromine from the decomposition of a trace of bromine trifluoride absorbed on the hexafluoro-iridate(V) does not seem likely since the addition of dilute hydrobromic acid to the pink solution did not cause any deepening of colour, but eventually caused the formation of a black precipitate of  $Ir_2O_3$  (HEPWORTH et al., 1954).

Preparation of Caesium Hexafluoro-rhodate(IV), -palladate(IV) and -platinate(IV)

These were prepared as previously described by the action of bromine trifluoride on equivalent mixtures of caesium chloride and the appropriate metal bromide ( $Cs_2RhF_6$ : COX, SHARP and SHARPE, 1956;  $Cs_2PdF_6$

and  $Cs_2PtF_6$ : SHARPE, 1953).

#### Attempted Preparation of Caesium Hexafluorozirconate(IV)

Hexafluorozirconates are reported to be prepared in solution from the alkali fluoride and zirconium fluoride (SHARPE, 1960).

Zirconium dioxide (1.2gms) was dissolved in Analar 40% hydrofluoric acid (50mls) and a concentrated solution of caesium fluoride (3.0gms) added. The solution was concentrated to a small volume when a white solid separated. After drying in vacuo over sodium hydroxide, an infra-red spectrum showed the presence of hydroxyl groups. The solid only partially redissolved in water with evidence of hydrolysis.

The solid was reacted with bromine trifluoride in an attempt to complete the fluorination, but although there was considerable evolution of gas, an infra-red spectrum of the product again showed the presence of hydroxyl groups.

#### Infra-red Spectra

Infra-red spectra were run as Nujol mulls, prepared in the dry-box, Nujol was dried by high vacuum distillation at 270°C approx., and was stored in contact with sodium wire. The mulls were supported between potassium bromide plates (5000 - 400  $cm^{-1}$ ) and thin polythene plates cut from polythene sheet, 0.6 mm. thick (for the region 550 - 200  $cm^{-1}$ ).

Infra-red spectra were recorded using Grubb Parsons S4 (NaCl optics) and DM 2 (CsI optics) spectrometers. The former machine was calibrated with a polystyrene film, and the latter against known bands of water vapour present in the atmosphere.

## Chapter 3

### The Electronic Spectra of Transition Metal Complex Hexafluorides

#### 3.1 Introduction

In the last ten years a considerable advance has been made towards understanding the spectra and magnetism of inorganic complexes. This has been accompanied by improvements in the approximations used for the description of the electronic energy levels in complexes of the transition metals. At first much attention was directed to the first row elements where certain simplifications can be applied to theories of electronic interactions, but recently extensions have been proposed to include the 4d and 5d series. The complex fluorides of these elements are among the few examples of compounds with straightforward stoichiometry and molecular symmetry, and should therefore provide useful examples where these theories may be applied. The magnetic properties of many complex fluorides have been studied, but there is very little literature concerning their visible and ultra-violet absorption spectra.

The first attempts to explain the absorption spectra of transition metal complexes were made using Crystal Field theory. The ligands were assumed to act as a perturbing electric field on the central metal ion orbitals. Using group theoretical methods, BETHE (1929) considered the effect of various field symmetries, arising from different spatial arrangements of ligands about the central atom, on the "field-free" atomic terms (DUNN, 1960). The extent of splitting of the atomic terms was calculated for increasing crystal field strengths ( $\Delta$ ) and the results

presented in the form of Orgel diagrams (ORGEL, 1952) for the weaker crystal fields, or Tanabe-Sugano diagrams (TANABE and SUGANO, 1954). In the latter diagrams the calculations have been extended to the "strong field" case where the crystal field energy has become greater than the d-electron spin-pairing energy. Since according to crystal field theory the effect of the ligands is purely electrostatic, such quantities as the interelectronic repulsion energy and spin-orbit coupling constants for the central atom configuration were assumed to remain the same as in the free ion. However it was realised from studies of the spectra of series of complexes having common central metal ions that this was not a valid assumption (OWEN, 1955). Ligand field theory was developed from the basic concepts of crystal field theory but allowing for a certain amount of orbital interaction, or covalent bond character, between the ligand and metal ion (DUNN, 1960).

In the Russell-Saunders coupling scheme, interelectronic repulsion energies for  $d^p$  electron configurations are conveniently expressed by the Racah parameters A, B and C. These parameters have been chosen so that repulsion energies for the terms of a given configuration are approximately dependent on B only, since here A is constant and  $C \approx 4B$ . It is found that when a metal ion forms a complex, the value of B is smaller than in the free-ion, implying reduced interelectronic repulsion, the amount by which it is reduced is dependent on the ligand. The nephelauxetic series gives a measure of the amount of covalent character in the metal-ligand bond (JØRGENSEN, 1962). It is expressed as the ratio of the reduced value of the Racah parameter B in the complexed metal ion to the value in the free ion.

For second and third row transition metals, magnetic coupling between electron spin and orbital momenta can no longer be considered negligible. In the isolated atom, the terms obtained by the Russell-Saunders scheme are  $(2S + 1)(2L + 1)$  - fold degenerate,  $S$  and  $L$  are the total spin and orbital quantum numbers for the configuration. Spin-orbit coupling lowers the degeneracy of the terms into sub-levels with different  $J$  quantum numbers;  $J$  has the values

$$J = (L + S), (L + S - 1), (L + S - 2), \dots, (L - S)$$

The distance between these levels is related to the spin-orbit coupling constant  $\zeta_{nl}$ .  $\zeta_{nd}$  increases from about  $500\text{cm}^{-1}$  in 3d elements to  $1500\text{cm}^{-1}$  for 4d and  $3500\text{cm}^{-1}$  for 5d elements. Again, the value of  $\zeta_{nd}$  for a metal ion in a complex is found to be smaller than the value in the free ion (OWEN, 1955).

MOFFITT, GOODMAN, FRED and WEINSTOCK (1959) measured the absorption spectra in the region 3 - 40 kK ( $1\text{kK} = 1000\text{cm}^{-1}$ ) for the hexafluorides of rhenium, osmium, iridium and platinum, which have non-bonding electron configurations  $5d^1$ ,  $5d^2$ ,  $5d^3$  and  $5d^4$  respectively. In the case of  $\text{ReF}_6$ , with estimated values of  $\Delta = 32.5 \text{ kK}$  and  $\zeta_{5d} = 3.4 \text{ kK}$  they find that Russell-Saunders coupling is still a more useful approximation than the other extreme of  $jj$ -coupling. Because of the magnitude of the octahedral ligand field, the non-bonding configuration can be considered as  $d_e^n$ . The effect of spin-orbit coupling in these degenerate and spherically symmetrical orbitals is analogous to the effect in  $p^{6-n}$  orbitals, and consequently interpretation of these transitions within the  $d_e$  orbitals can be simplified (GRIFFITHS, 1958).

The spectra of the hexafluorides could conveniently be separated into three types. A group of sharp, low intensity absorptions at the longest wavelengths were assigned to transitions occurring between the different J-levels of the ground state, split by spin-orbit coupling. Broad, intense absorptions between 30 - 40 kK were assigned to electronic transitions between terms split by the ligand field. Some additional bands were also observed which could be charge transfer transitions. JØRGENSEN (1960) considers that the bands between 30 - 40 kK are due to charge transfer, but EISENSTEIN has given a tentative assignment to all bands in  $\text{ReF}_6$  (1960) and  $\text{OsF}_6$  (1961) as metal d - d transitions.

Information concerning the energy levels in second and third row transition elements has come from magnetic studies on some of their halide complexes. By following the variation of the magnetic susceptibility with temperature, values of  $\zeta_{nd}$  and  $3B + C$  (Racah parameters) can be obtained using the theory of Kontani modified by Griffiths (EARNSHAW, FIGGIS, LEWIS and PEACOCK, 1961; FIGGIS, LEWIS and MABBS, 1961). They found that  $d^4$  complex fluorides are spin-paired.

### 3.2 Discussion of Results

The results obtained here for the visible and ultra-violet spectra of transition metal fluoride complexes were measured by the reflection method from the solids; in the diagrams the intensity of reflection is indicated on an arbitrary log scale. Where possible spectra were interpreted from Tanabe-Sugano diagrams as presented in DUNN (1960), but extrapolated to larger values of  $\Delta/B$ . Energy levels are designated by MULLIKEN's symbols (1933).

$d^4$  Configuration Ligand field theory predicts one band corresponding



to a transition between the ground state  ${}^2T_2$  and the  ${}^2E$  state with energy  $\Delta$ . Spin-orbit coupling splits the ground state into two levels with separation  $3/2 \zeta_{nd}$ . Since  $\zeta_{nd}$  for the second and third rows is of the order 1500 and 3000 K (FIGGIS and LEWIS, 1960), transitions between these levels would occur in the near infra-red. This region was not available in the present work. The peaks at 29 kK and 35 kK in  $\text{CsMoF}_6$  occur at too high an energy to be the  ${}^2E$  transition, other possibilities are charge transfer or an impurity. The peak at 32.4 kK in  $\text{CsWF}_6$  is comparable to the value of  $\Delta = 32.5$  kK found by MOFFITT et al. (1959) for  $\text{Re(VI)}$  in  $\text{ReF}_6$ . The broad absorption band at 18 kK varied in height from one sample to another and is probably due to a hydrolysis product, both  $\text{CsWF}_6$  and  $\text{CsMoF}_6$  are extremely moisture sensitive.

$d^2$  Configuration No clearly defined peaks could be recognised above the rather high background absorption, which is probably due to the presence of a small amount of a hydrolysis product.

$d^3$  Configuration The spectrum of  $\text{ReF}_6^{2-}$  has been recorded (DUNN and PEACOCK, 1962); peaks corresponding to transitions from the ground state  ${}^4A_2$  to  ${}^2E$  (11.4),  ${}^2T_2$  (10.8), and  ${}^4T_2$  (32 kK, shoulder) were recognised. These correspond to values of  $\Delta = 32$  kK and  $B = 490$  K. Similar results have been found here for  $\text{K}_2\text{ReF}_6$ ; also for  $\text{CsOsF}_6$  where  $\Delta = 33$  kK and  $B = 495$  K, and  $\text{CsRuF}_6$  where  $\Delta = 26$  kK and  $B = 480$  K.

The two peaks in  $\text{CsOsF}_6$  at 10.4 and 11.0 kK and the corresponding pair in  $\text{K}_2\text{ReF}_6$  have unusually high intensity for spin-forbidden transitions, but spin selection rules are known to be relaxed by spin-orbit coupling (JØRGENSEN, 1962 b). In the case of  $\text{IrF}_6$ , spin-orbit coupling splits the  $d^3$  sub-levels into four states (MOFFITT et al., 1959);

Table 3.1Energy states in  $d^3$  configuration (in kK)

Energy level	CsRuF <sub>6</sub>		K <sub>2</sub> ReF <sub>6</sub>		CsOsF <sub>6</sub>		IrF <sub>6</sub>	
	$\Delta=26, B=0.48$		$\Delta=32, B=0.5$		$\Delta=33, B=0.48$		$\Delta=36.5, B=0.41$	
	obs.	calc.	obs.	calc.	obs.	calc.	obs. <sup>a</sup>	calc.
<sup>2</sup> E		9.9	10.8	10.5	10.4	10.4	6.4 8.5	8.5
<sup>3</sup> T <sub>1</sub>	10.4	10.4	11.2	11.6	11.0	10.8	9.1	9.2
<sup>3</sup> T <sub>2</sub>	15.4	16.3	17.8	17.7	18.0	17.8	13.0 16.0	16.0
<sup>4</sup> T <sub>2</sub>	25.2	26.1	33.0	30.9	31.0	32.0	35.5	35.5
<sup>4</sup> T <sub>1</sub>	33.3	32.9	35.0	36.8	39.2	39.0	42.0	43.0

<sup>a</sup> MOFFITT, GOODMAN, FRED and WEINSTOCK (1959)

in CsOsF<sub>6</sub> the third transition is probably beyond the range of the present work. There is a certain ambiguity in the assignment of the observed peaks as shown in Table 3.1, satisfactory agreement can be obtained by simultaneously varying  $\Delta$  and B over a range of  $\pm 10\%$ .

$d^4$  Configuration Two clearly resolved peaks at 27 and 31 kK were obtained in the spectrum of Cs<sub>2</sub>RuF<sub>6</sub>. The former may correspond to transitions between the four closely spaced states <sup>3</sup>E, <sup>3</sup>T<sub>2</sub>, <sup>3</sup>A<sub>1</sub> and <sup>3</sup>A<sub>2</sub>. Transitions from the spin-paired ground state <sup>3</sup>T<sub>1</sub> are all spin allowed, and assuming values of  $\Delta = 26$  kK and  $B = 500\text{cm}^{-1}$  (values estimated from similar constants listed in JØRGENSEN, (1960 a), all should be in the range 25 - 27.5 kK. The stronger peak is possibly a charge transfer  $\pi \rightarrow d_e$  (JØRGENSEN 1960 a). The corresponding four d - d transitions in Cs<sub>2</sub>OsF<sub>6</sub> should appear between 27.5 - 31 kK, using estimated values of  $\Delta = 32$  kK and  $B = 460$  K. The spectra of both compounds have

shoulders in this region, but the charge transfer bands mask the structure of the peaks. Following JØRGENSEN (1962 a), the band at 32 kK is assigned to  $\pi \rightarrow d_g$ . A similar absorption at 32.5 kK was noted by HEPWORTH, ROBINSON and WESTLAND (1958), and TURNER and CLIFFORD (1958) in the spectrum of an aqueous solution of  $K_2OsF_6$ .

The weak absorptions at 20 kK correspond to a transition to  $^5E_g$ , which is expected at 19 kK from the estimated parameters above.

The faint peaks at 13 and 11 kK for  $Cs_2OsF_6$  and  $CsIrF_6$  are in a similar region to the inner -  $d_g$  transitions in  $PtF_6$  (MOFFITT et al., 1959).

$d^5$  Configuration It was not possible to assign all peaks with confidence for either  $CsRhF_6$  or  $Cs_2IrF_6$ . For the former compound, if  $\Delta = 21.5$  kK and  $B = 400$  K, calculated peaks would occur at  $^2T_2 \rightarrow ^4T_2$ , 12.4;  $^4T_2$  at 16.0;  $^2A_2$ ,  $^2T_1$  at 18.5;  $^2E$  at 20.6;  $^2A_1$  at 25.8; observed peaks were at 12.2, 16.1, 19 - 21 and 26.0 kK. The value of  $\Delta$  is rather lower than would be expected for a second row transition element.

The band at 19.0 kK in  $Cs_2IrF_6$  seems anomalous from its unusually high intensity. The compound was prepared according to HEPWORTH, ROBINSON and WESTLAND, (1954) who report pink or pale yellow products. The only product obtained here was pink, the same spectrum was obtained in aqueous solution and after several recrystallisations. The band corresponded closely with an absorption in  $IrBr_6^{2-}$  (JØRGENSEN, 1959), but the equally intense absorption at 15 kK was not present. Since strong absorptions caused by mixed valency effects do not usually persist in solution, the peak is assigned to a charge transfer transition. The lowering of energy of the transfer of an electron from a fluorine atom on to the iridium atom may be caused by the extra

stability of the resulting  $d_{\text{e}}^6$  configuration. The absorption spectrum of a solution of the free acid was measured in the region 40 - 28.5 kK by HEFWORTH, ROBINSON and WESTLAND (1958). They report absorptions at 47.0 and 31.6 kK the latter in fair agreement with the peak at 33 kK obtained here.

In view of the uncertainty in reason for the strong absorption at 19 kK, no attempt was made to assign the other bands.

$d^6$  Configuration The absorption spectrum of the  $\text{PtF}_6^{2-}$  ion has been reported by SCHLESINGER and TAPLEY (1924), WHEELER, PERROS and NAESER (1954) and assigned by JØRGENSEN (1962 a). Transitions from the ground state  $^1A_1$  to  $^3T_1$  (22.5),  $^3T_2$  (24.4),  $^1T_1$  (31.5) and  $^1T_2$  (36.4 kK) were identified. The reflectance spectrum obtained here for  $\text{Cs}_2\text{PtF}_6$  had corresponding peaks at 32.5 and 37 kK and a broad shoulder in the region 28 - 21 kK. Values of  $\Delta = 33$  kK and  $B = 380$  K were obtained by JØRGENSEN (1962 a).

The reflectance spectrum of  $\text{Cs}_2\text{PdF}_6$  had two clearly resolved peaks at 25 ( $^1T_1$ ) and 30 kK ( $^1T_2$ ) which correspond to values of  $\Delta = 26$  kK and  $B = 400$  K.

### 3.5 Conclusions

A summary of the available data for second and third row transition metal complex fluorides is given in Table 3.2.

Although the spectra of many compounds can be explained on the basis of ligand field theory, the number of variable parameters is of the same order as the number of independent observations at present available. The quantities in Table 3.2 cannot therefore be stated with sufficient precision for the investigation of trends.

Table 3.2

Ligand field parameters for some complex fluorides

Config.	Compound	$\Delta$	B	Config.	Compound	$\Delta$	B
5d <sup>1</sup>	CsWF <sub>6</sub>	32.4	-	4d <sup>4</sup>	Cs <sub>2</sub> RuF <sub>6</sub>	(26)	(500)
	ReF <sub>6</sub> <sup>a</sup>	32.5	-	5d <sup>4</sup>	Cs <sub>2</sub> OsF <sub>6</sub>	(32)	(460)
5d <sup>2</sup>	OsF <sub>6</sub> <sup>c</sup>	34.5	400		CsIrF <sub>6</sub>	(32)	(460)
4d <sup>3</sup>	CsRuF <sub>6</sub>	26	480		PtF <sub>6</sub> <sup>a</sup>	32.5	280
5d <sup>3</sup>	K <sub>2</sub> ReF <sub>6</sub>	32	500	4d <sup>5</sup>	Cs <sub>2</sub> RhF <sub>6</sub>	21.5	400
	CsOsF <sub>6</sub>	33	495	4d <sup>6</sup>	Cs <sub>2</sub> PdF <sub>6</sub>	26	400
	IrF <sub>6</sub>	36.5	410	5d <sup>6</sup>	K <sub>2</sub> PtF <sub>6</sub> <sup>b</sup>	33	380

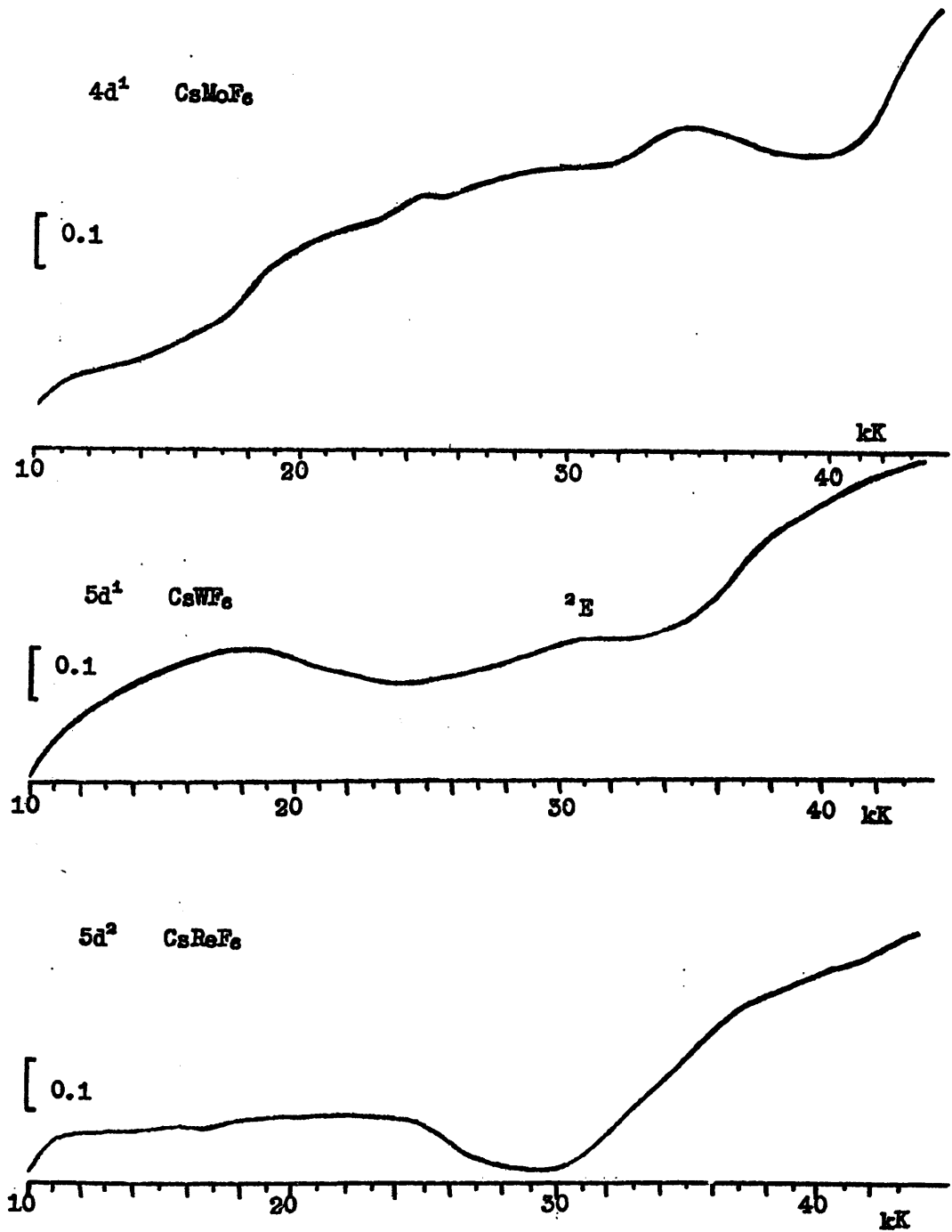
<sup>a</sup> MOFFITT et al., (1959)<sup>b</sup> JØRGENSEN (1962 a)<sup>c</sup> EISENSTEIN (1961)

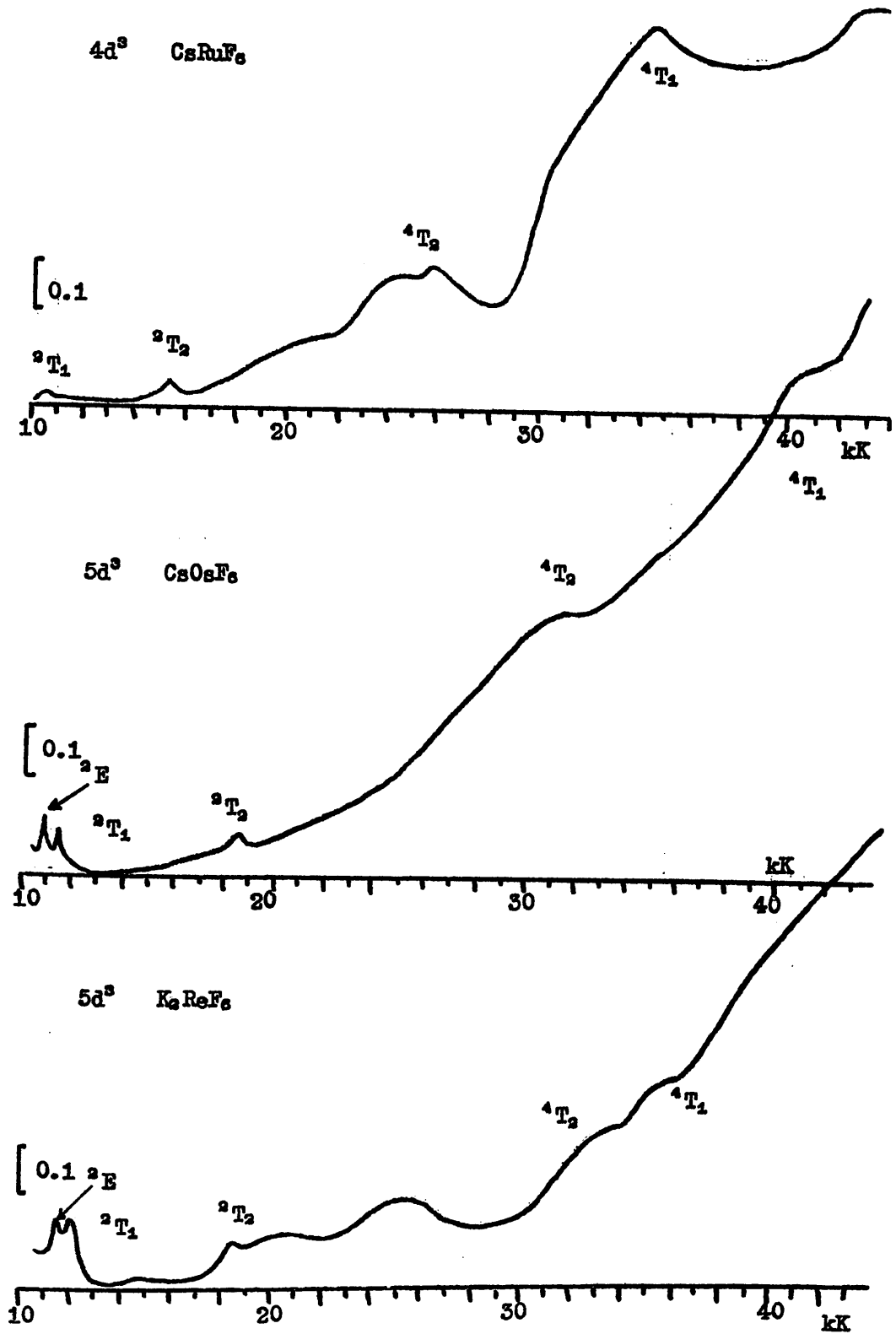
JØRGENSEN (1962) has compared the B parameters of a number of fluorides with the "free-ion" values for the metal ion concerned, and concludes there is an appreciable nephelauxetic effect even for the fluoride ion, which normally has the smallest effect of all ligands. Since a reduction in B may be interpreted as a reduction in inter-electronic repulsion in the metal atom, this in turn implies increased covalent bonding in the metal-fluorine bonds. However, because of the lack of direct evidence, many of these comparisons are based on highly empirical estimates of electron interaction and spin-orbit coupling constants.

Although the spectra obtained in the present work were complex, and in some cases could not be completely interpreted, nevertheless they do show that the absorptions occurring in this region are most likely due to metal d - d transitions. This is particularly interesting since in

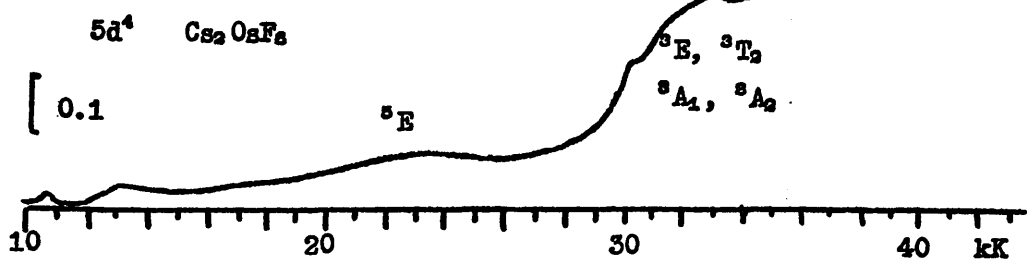
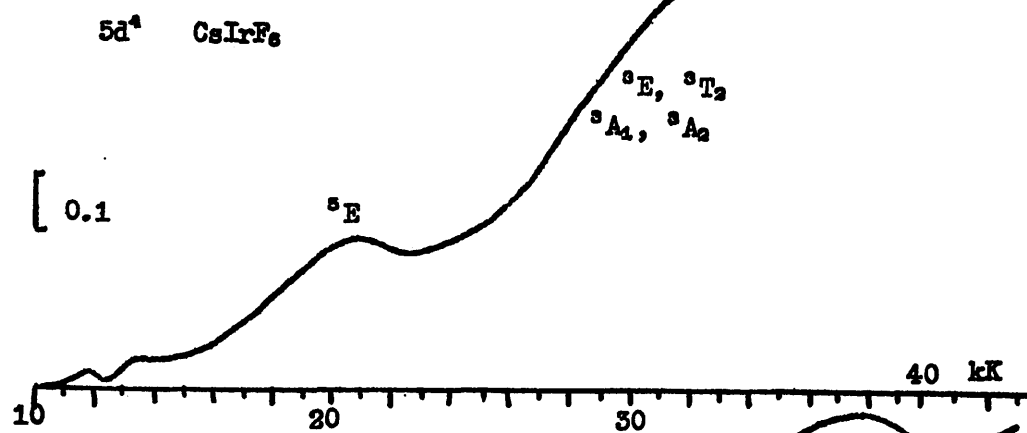
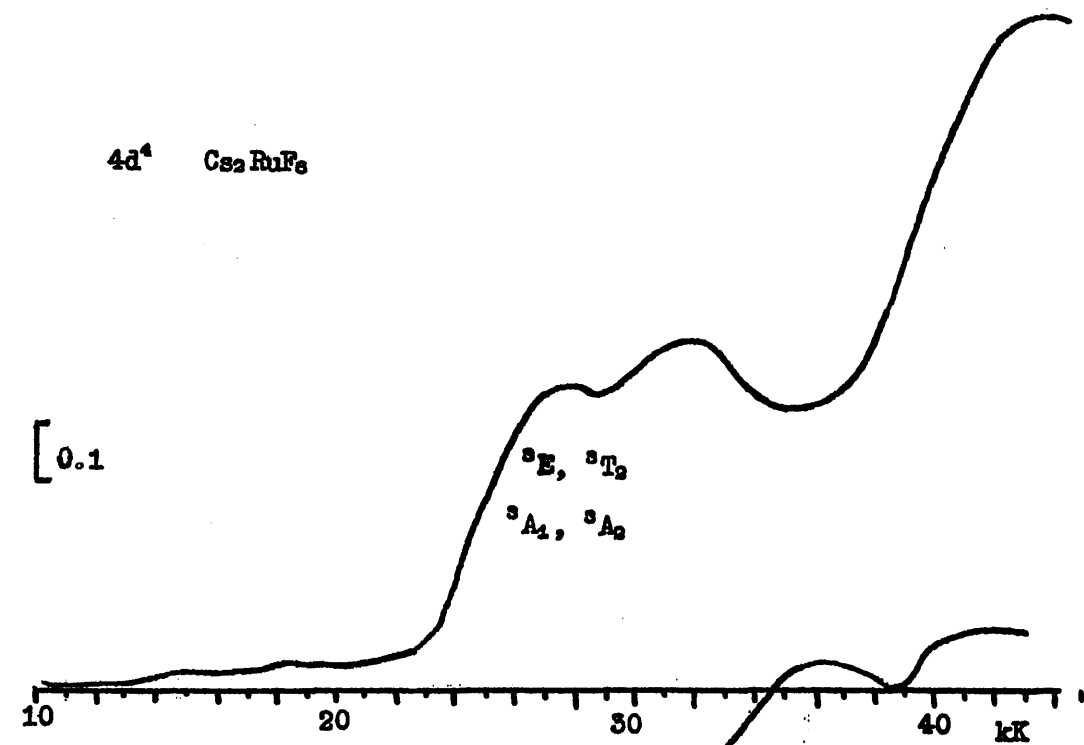
many complexes of these metals these weak absorptions are masked by strong charge transfer bands from the ligand (JØRGENSEN, 1960 a).

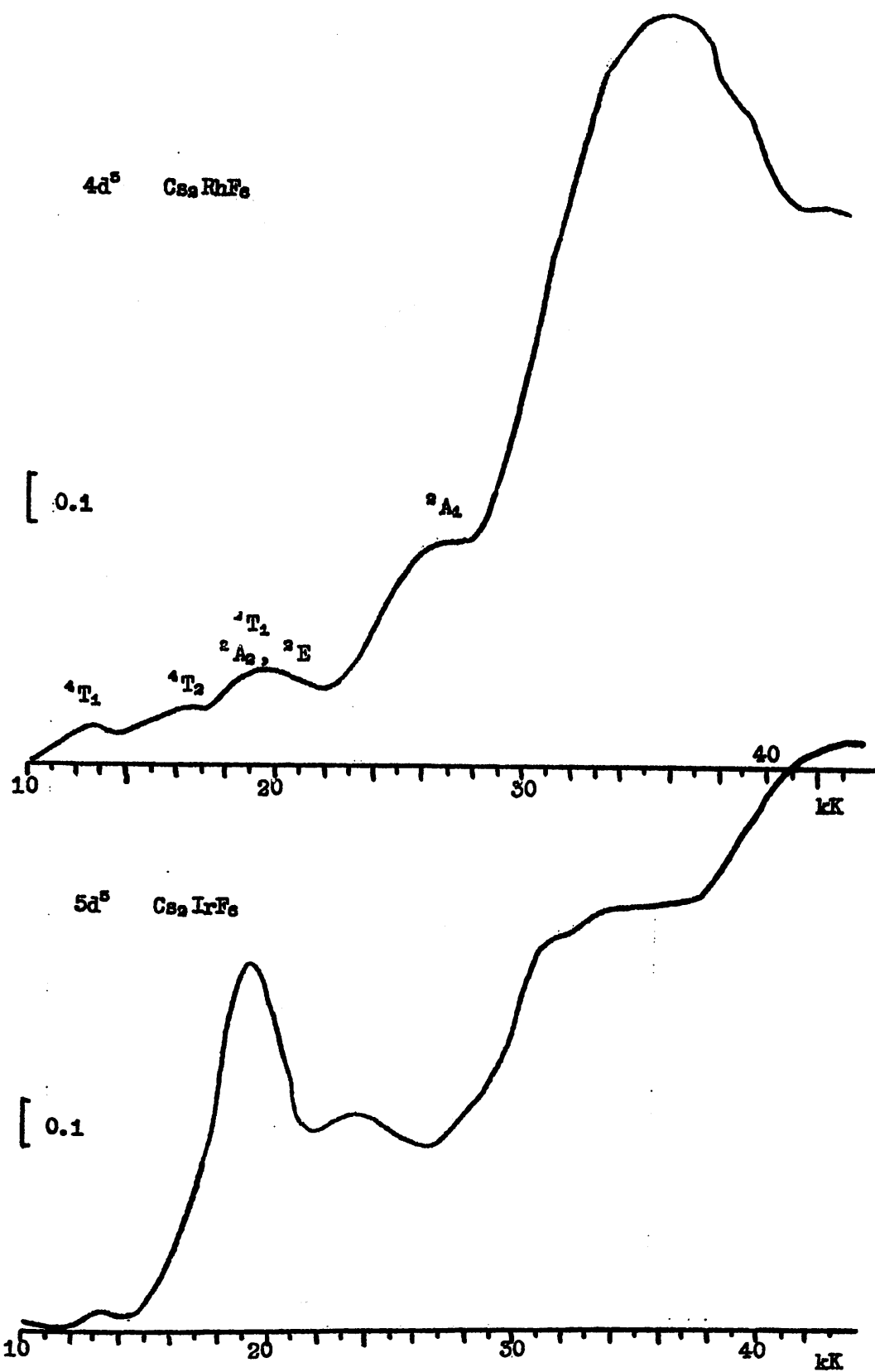
No mention has been made so far of the effect of octahedral distortions present in some of the complex fluorides (Chapter 1). In general the small extent of these distortions would merely have the effect of further broadening the absorption bands. Although the solubility of complex fluorides in anhydrous hydrofluoric acid has not been investigated in many cases, it is not unlikely that many will be soluble. Examination of their spectra in solution, where the distortions mentioned are not expected to arise, should provide important information on the energy levels in the heavier transition elements.

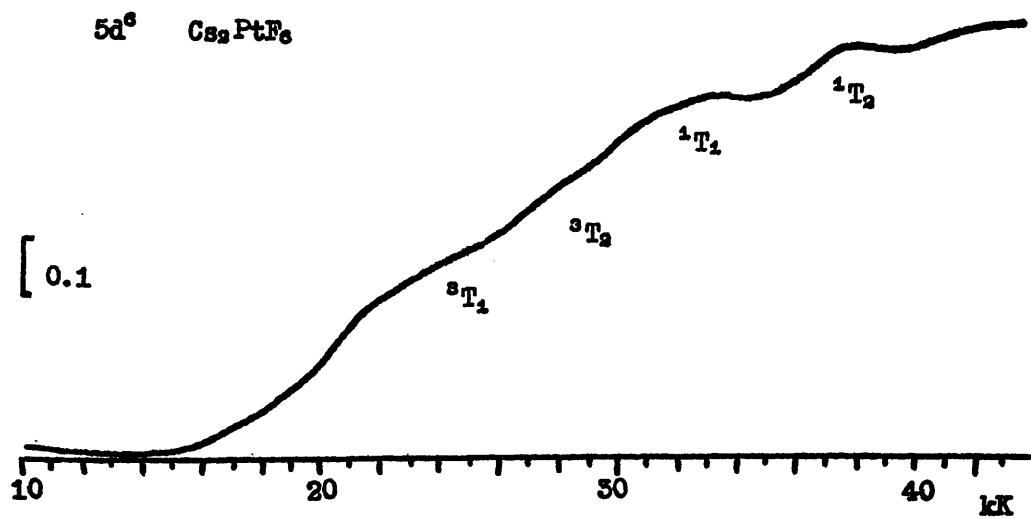
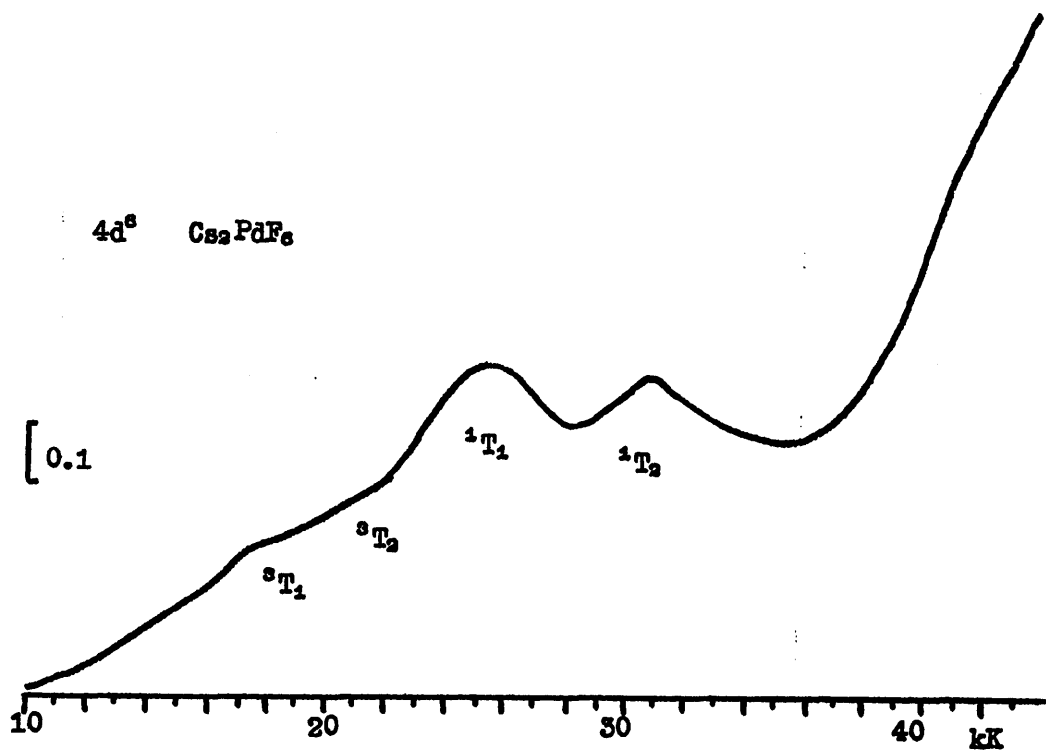
Diagrams of Reflection Spectra











## Experimental

### Preparation of Complex Fluorides

Samples used for examination of reflectance spectra were the same as prepared for infra-red measurements in Chapter 2. The method of preparation used is described in the Experimental section of Chapter 2.

### Measurement of Reflectance Spectra

As many of the complex fluorides were extremely sensitive to moisture a special procedure for specimen mounting was adopted. A thin layer of plasticine was placed on the rim of the holder of the reflectance attachment (Figure 3.7). The holder was then partly filled with spectroscopically pure calcium fluoride (vacuum dried at 200°C) in the dry-box.

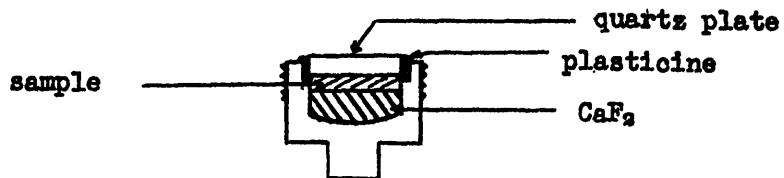


Figure 3.7

A layer of the finely ground material approximately 1 mm. thick was quickly spread on the calcium fluoride and the quartz plate bedded into the plasticine. When prepared in this manner the spectra of samples of  $\text{CsReF}_6$  did not appreciably alter over the period of one hour needed for the measurement. When the quartz plate was removed in moist air, the surface blackened in a few minutes. Most decomposition during the mounting procedure probably occurred when the sample was being handled in the open dry-box.

Reflection spectra were obtained using a Hilger Uvispek instrument

fitted with a standard H 740 Diffuse reflection unit. Readings were taken manually over the range 220  $m\mu$  to 1000  $m\mu$  at intervals of 5  $m\mu$  (220 - 400), 10  $m\mu$  (400 - 700) and 20  $m\mu$  (700 - 1000), with more frequent readings in the region of rapid changes in intensity. The machine was checked against zero and 100% reflection (magnesium oxide standard) between each reading.

carbonyls. The relative stability of the halides compared with the metal, than the copper carbonyl to decrease in stability to heat in the order  $Bi > Sb > As$ , whereas is true for the compounds  $Bi < Sb < As$ . As a general rule, carbonyl halides are volatile unless polymeric in nature. The halides are usually bridged via halogen atoms rather than metal atoms.

The number of known metal carbonyl fluorides is comparatively small. It was not until 1940 that the first examples of metal fluoride carbonyls were reported by SHAW. Previous attempts to characterize metal fluoride carbonyls had been made without success, resulting in the metal-

## Chapter 4

### Metal Carbonyl Fluorides

#### Introduction

Compounds containing both halogen and carbon monoxide bonded to a metal are known for many transition metals when the halogen is chlorine, bromine and iodine (CHATT, PAUSON and VENANZI, 1960). These carbonyl halides are of comparable stability to the straightforward metal carbonyls, but the oxidation state of the metal is often one or two compared with zero in the pure carbonyls; they also tend to occur with metals later in the transition metal series than the metals which form pure carbonyls. The relative stability of the iodides compared with the chlorides varies with the metal, thus the copper carbonyl halides  $\text{Cu}(\text{CO})\text{X}$  decrease in stability to heat in the order  $\text{Cl} > \text{Br} > \text{I}$ , whereas the reverse is true for the compounds  $\text{Fe}(\text{CO})_5\text{X}_2$ . As covalent molecules metal carbonyl halides are volatile unless polymeric; in such cases the metal atoms are usually bridged via halogen atoms rather than carbonyl groups.

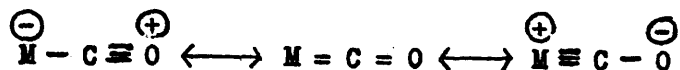
The number of known metal carbonyl fluorides is comparatively small however. It was not until 1960 that the first examples of such compounds were reported by SHARP. Previous attempts to obtain carbonyl fluorides had been made without success, reduction to the metal or lower fluorides was the most common result. SHARP (1960) found that the action of a stream of carbon monoxide on platinum tetrafluoride at  $100^\circ\text{C}$ , or better using a pressure of carbon monoxide at room temperature gave a compound which could be sublimed out of the reaction product at  $70^\circ$  under

vacuum as a pale yellow solid. The compound was considered to be  $\text{Pt}(\text{CO})_2\text{F}_2$  on the basis of infra-red measurements and analysis. A compound  $[\text{Rh}(\text{CO})_2\text{F}_3]_2$  was obtained in a similar way from rhodium tetrafluoride.

The high valency of the metals in these two complexes may be contrasted with that observed in other carbon-monoxide-containing molecules, and it must be concluded that fluorine behaves in a different way to the other halogens in these compounds. Accordingly the reaction between carbon monoxide and other metal fluorides was studied in an attempt to prepare further examples of metal carbonyl fluorides and perhaps provide an explanation for the unusually high metal valencies.

One of the most characteristic physical properties of carbonyl compounds is the intense infra-red absorption in the region  $2200\text{--}1800\text{cm}^{-1}$  due to the C-O stretching vibration. Apart from providing a simple method of recognition of a carbonyl compound, the actual value of the frequency has been used to obtain information about the nature of the bonding between the metal and carbon monoxide. The current theory of bonding in metal carbonyl complexes (ABEL, 1963) is based on the donation of the lone pair of electrons in carbon monoxide, which occupy an orbital directed along the C-O axis away from the oxygen atom, into a suitable empty metal orbital to form a  $\sigma$ -type bond between the carbon and metal atoms. The excess negative charge which would then be accumulated on the central metal can be dispersed in a  $\pi$ -type orbital formed by overlap between a filled metal d or dp-hybrid orbital and an empty antibonding p orbital of the carbon monoxide. Alternatively, using valence bond description resonance can occur between the canonical

forms.



The  $\pi$ -type bonding leads to a reduction in the order of the C-O bond. The C-O bond stretching vibration force constant is quite sensitive to changes in bond order, a lowering of bond order being associated with a reduced force constant. In metal carbonyl complexes a lowering of vibrational frequency compared to that in carbon monoxide itself is generally taken to infer the presence of M-C  $\pi$ -bonding. The extent of the  $\pi$ -bonding will depend on the electronegativity of the central metal, thus if the metal has a high electronegativity the need for relieving the negative charge donated by the carbonyl groups is much reduced compared to a metal with lower electronegativity. This will be reflected in the C-O stretching mode by an increase in frequency, approaching that in carbon monoxide itself, as the M-C bond order becomes closer to one. This effect is clearly demonstrated in the series of substituted carbonyl complexes  $[\text{C}_6\text{H}_5\text{M}(\text{CO})_3]^{n-}$  where M is V(-1), Cr(0), Mn(+1) and Fe(+2). The two C-O stretching frequencies for each compound are:- V 1748, 1645; Cr 1876, 1695; Mn 2035, 1953 and Fe 2120, 2070  $\text{cm}^{-1}$ . (DAVISON, GREEN and WILKINSON, 1961).

In the case of metal carbonyl halides, the electronegativity of a given metal in a molecule will vary with that of the halogen, but not necessarily in the same order as for the halogens because of the possibility of  $\pi$ -bonding. If empty metal d-orbitals and filled halogen p-orbitals have comparable energies,  $\pi$ -bonding could take place in the M-X bond. This would act on the C-O stretching frequency in the opposite sense to the inductive effect occurring in the M-X bond. For



the compounds shown in Table 4.1 however, the inductive effect seems to be more important.

Table 4.1

Carbonyl stretching frequencies in some metal carbonyl fluorides

Compound	Frequency in $\text{cm}^{-1}$	Reference
CO	2143	HERZBERG (1950)
$\text{Pt}(\text{CO})_2\text{F}_3$	2161, 2120	SHARP (1960)
$\text{Pt}(\text{CO})_2\text{F}_4$	2217, 2175, 1842	Present work
$[\text{Pt}(\text{CO})\text{Cl}_2]_2$	2152	IRVING and MAGNUSSON (1956)
$[\text{Pt}(\text{CO})\text{Br}_2]_2$	2150	"
$[\text{Pt}(\text{CO})\text{I}_2]_2$	2112	"
$[\text{Rh}(\text{CO})_2\text{F}_3]_2$	2103, 2086, 2035	SHARP (1960 a)
$[\text{Rh}(\text{CO})_2\text{Cl}]_2$	2104, 2088, 2033	YANG and GARLAND (1957)
$\text{Ru}(\text{CO})_{\text{x}}\text{F}_{\text{y}}$	2126, 2180	Present work
$[\text{Ru}(\text{CO})_2\text{I}_2]_n$	2050, 1995	IRVING (1956)

It will be noticed from Table 4.1 that some compounds have C-O stretching frequencies higher than that in carbon monoxide itself. One way of interpreting this is that the demand for electrons by the electronegative substituents has become so great that it has been transmitted to the carbon atom of the carbonyl group. The electronegativity difference between the carbon and oxygen is thereby reduced, which in turn causes a contraction of the  $\pi$  electron cloud and increases the force constant of the bond. The differences in frequency are small however, and too much reliance cannot be placed on comparisons made between vibrational frequencies measured in the gas phase (for CO)

and in carbon-tetrachloride solution (for most of the carbonyl halides).

#### Reaction of Carbon Monoxide with Group 1b Metal Fluorides

Solid cuprous chloride, bromide and iodide absorb carbon monoxide under high pressure, (100atm for 5 days) to give pure  $\text{CuCOCl}$ ,  $\text{CuCOBr}$  and a partial formation of a carbonyl iodide (WAGNER, 1951).

Cuprous fluoride has never been obtained pure, attempts to isolate it by quenching a melt of cupric fluoride which has lost fluorine produced only metallic copper and cupric fluoride (WARTENBERG, 1959). Carbon monoxide did not react with either cupric fluoride or equivalent mixtures of cupric fluoride and copper powder under any conditions tried (150 atm pressure,  $180^\circ\text{C}$  for three days). A solution of cuprous tetrafluoroborate (SHARP, 1960 b) in ether did not absorb carbon monoxide under pressure.

FRASER (1960) obtained evidence for the transient existence of a nitrosyl copper fluoride; a violet colour developed when nitric oxide was passed into a solution of cupric fluoride in tert-butanol. No equivalent reaction with carbon monoxide was found however.

Gold carbonyl chloride,  $\text{Au}(\text{CO})\text{Cl}$ , was first prepared by MANCHOT and GALL (1925) by the action of carbon monoxide on aurous chloride, it can also be obtained from gold trichloride (KHARASCH and ISBELL, 1950). Carbon monoxide reacts with gold trifluoride even at low temperatures, reduction to the metal taking place.

#### Reaction of Carbon Monoxide with Molybdenum Pentafluoride

Molybdenum pentafluoride is known to form adducts with sulphur tetrafluoride (KEMMITT, 1962) by the action of  $\text{SF}_4$  on molybdenum hexacarbonyl at  $165^\circ$ . The adduct was considered by Kemmitt to be a mixture

of  $\text{MoF}_5 \cdot \text{SF}_4$  and  $\text{MoF}_5 \cdot 2\text{SF}_4$ .

In an experiment to decide whether carbon monoxide would displace sulphur tetrafluoride, a pressure of carbon monoxide was applied to the  $\text{MoF}_5 \cdot \text{SF}_4$  complex. The product had infra-red absorptions at 2162 and  $2180\text{cm}^{-1}$ , similar in appearance to the spectrum of proposed molybdenum and tungsten carbonyl chlorides obtained by mixing solutions of the metal hexacarbonyls and chlorides (NUTTALL, 1962). The extreme sensitivity of the product and reactants prevented isolation and characterisation, but it seems that carbon monoxide can replace sulphur tetrafluoride with possible formation of an unstable carbonyl complex.

#### Reaction of Carbon Monoxide with Platinum Metal Fluorides

All transition metals of this group form carbonyl halide complexes (Cl, Br and I), for some metals several different compounds are known (CHATT, PAUSON and VENANZI, 1960).

Ruthenium. At  $200^\circ\text{C}$ , carbon monoxide is reported to reduce ruthenium pentafluoride to a reactive form of the trifluoride (PEACOCK, 1960). Under pressure reaction occurs at lower temperatures to give a product sufficiently soluble in carbon tetrachloride to give an infra-red spectrum showing absorptions in the carbonyl region. The spectrum varied from one reaction to another however, in particular depending on the method of preparation of the  $\text{RuF}_5$ . When fluorination of ruthenium metal or bromide by bromine trifluoride was used, a strong absorption at  $2120\text{cm}^{-1}$  was obtained with subsidiary peaks as in Figure 4.1. Ruthenium pentafluoride prepared by interaction of the elements needed a higher temperature before reaction would occur ( $90\text{--}100^\circ$ ) and spectra similar to Figure 4.2 were obtained. Obviously more than one species

of carbonyl compound was being formed, but unfortunately sufficient quantities for analysis and characterisation could not be obtained.

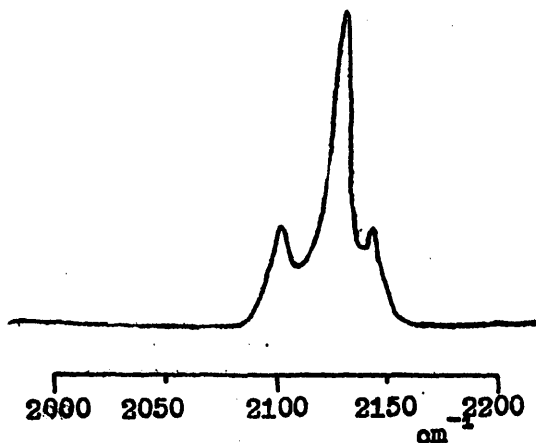


Fig. 4.1

I.R. spectrum of CO+RuF<sub>5</sub> (ex BrF<sub>3</sub>)  
(remainder of NaCl region clear).

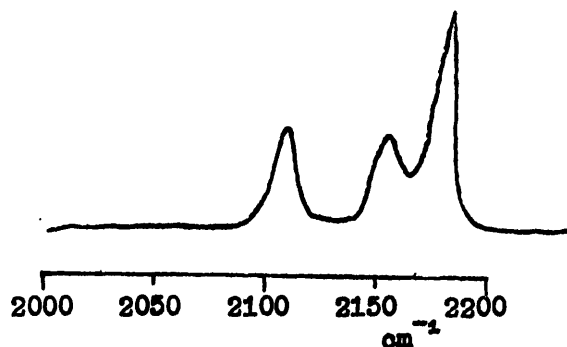


Fig. 4.2

I.R. spectrum of CO+RuF<sub>5</sub> (ex F<sub>2</sub>)  
(remainder of NaCl region clear).

The variation in reactivity between the differently prepared ruthenium pentafluoride samples can now partly be explained by the recent discovery by HOLLOWAY and PEACOCK (1963) of the oxyfluoride RuOF<sub>4</sub>. They find that the latter compound is formed during the fluorination of ruthenium metal by bromine trifluoride. The presence of this compound in the ruthenium pentafluoride, which would be difficult to detect analytically, could account for the variation in products obtained here. By comparing the reported properties of RuF<sub>5</sub> and RuOF<sub>4</sub> with samples prepared in the present work, it is tentatively suggested that RuF<sub>5</sub> reacts with CO under pressure at room temperature to give small quantities of a presumed carbonyl fluoride, whereas RuOF<sub>4</sub> reacts at a higher temperature to give a second type of carbonyl compound. From the position of the peaks it seems that the ruthenium atom is in a

high oxidation state, as found for platinum in  $\text{Pt}(\text{CO})_2\text{F}_6$ .

Osmium. At all temperatures tried, osmium hexafluoride was found to react with carbon monoxide, being completely reduced to the metal.

Rhodium. SHARP (1960) was able to isolate  $[\text{Rh}(\text{CO})_2\text{F}_2]_2$  from the reaction of carbon monoxide under pressure with rhodium tetrafluoride. From the absence of CO stretching frequencies in the bridging carbonyl region, the bridging was presumed to be through the F atoms.

Iridium. Iridium hexafluoride was reduced to the metal by carbon monoxide under pressure at all temperatures tried. This has also been found by WESTLAND and ROBINSON (1956).

Palladium. Palladium trifluoride did not absorb carbon monoxide below room temperature. As the temperature was raised successive reduction to the difluoride and finally the metal occurred. No evidence for the intermediate formation of a carbonyl was obtained.

Platinum. The compound  $\text{Pt}(\text{CO})_2\text{F}_6$  was obtained by the action of carbon monoxide on platinum tetrafluoride (SHARP, 1960). Its formulation was based on the presence of two sharp infra-red absorptions in the carbonyl region obtained in carbon tetrachloride solution and the absence of peaks elsewhere in the NaCl region of the spectrum. This immediately rules out structures such as  $\text{PtF}_4 \cdot 2\text{COF}_2$  and  $\text{Pt}(\text{OCF}_2)_2\text{F}_2$ , as C-F bonds have characteristically strong absorptions in the  $1250 - 1050 \text{ cm}^{-1}$  region.

A suggestion has been made by CHATT, (1961) that the compound is a hexafluoroplatinate (IV) of the cation  $[\text{O} \equiv \text{C} - \text{F}]^+$ . This previously unreported cation could be stabilised in highly oxidising environments

by resonance between the canonical structures.  $\text{O} \equiv \overset{\oplus}{\text{C}} - \text{F} \leftrightarrow \text{O} = \overset{\oplus}{\text{C}} = \overset{\ominus}{\text{F}}$

$\text{PtF}_6$  is known to be a powerful oxidising agent of the compounds  $\text{O}_2\text{PtF}_6$

and  $\text{XePt}^+\text{F}_6^-$ . (BARTLETT and LOHMANN, 1962; BARTLETT, 1962). The vibrational frequency of the C-F bond in such an ion could not easily be predicted and may be shifted up to about  $2100\text{cm}^{-1}$ , thus accounting for one of the two bands observed in this region.

However, carbon monoxide was evolved when carbon tetrachloride solutions of the platinum carbonyl fluoride and triphenylphosphine were mixed, with the formation of bis-(triphenyl phosphine) platinum dichloride and difluoride. This is a typical reaction of a carbonyl compound, whereas it would be difficult to explain the formation of CO from  $(\text{OCF})^+$  and triphenylphosphine. The fact that chlorine is found in the product suggests that  $\text{Pt}(\text{P}\phi_3)_2\text{F}_6$ , if this is the initial product in the reaction, is unstable and attacks the solvent. An X-ray powder photograph of  $\text{Pt}(\text{CO})_2\text{F}_6$  showed a complex pattern of lines indicating a unit cell with low symmetry; although not conclusive evidence, this points against the ionic structures as in general hexafluoroplatinates (IV) have relatively simple structures.

At low temperatures a compound thought to be an intermediate in the reaction of platinum tetrafluoride with carbon monoxide was prepared. Platinum analyses agree closely with the formula  $\text{Pt}(\text{CO})_2\text{F}_4$ . Although non-volatile itself, this compound appeared to disproportionate on warming into platinum metal and  $\text{Pt}(\text{CO})_2\text{F}_6$ , the reaction became violent above  $80^\circ\text{C}$ .  $\text{Pt}(\text{CO})_2\text{F}_4$  was insoluble in all solvents tried, but a hexachlorobutadiene mull had a broad infra-red absorption between  $2220 - 2170\text{ cm}^{-1}$  with a sharp maximum at  $2217\text{ cm}^{-1}$ , and a second band centred at  $1842\text{ cm}^{-1}$  in the bridging carbonyl region. It is most likely that platinum tetrafluoride is eight-coordinate in the solid

state (cf.  $\text{ThCl}_4$ , MOONEY, 1949), and as there is very little change in appearance when  $\text{PtF}_4$  absorbs carbon monoxide at low temperatures, it may be that two molecules of CO can be incorporated in the lattice without a radical change in structure. This lattice structure then breaks down on heating with disproportionation to Pt and  $\text{Pt}(\text{CO})_2\text{F}_2$ . Considerable energy must be released in this reaction as  $\text{CO}_2$ ,  $\text{COF}_2$  and  $\text{CF}_4$  have been identified as by-products from the reaction with  $\text{PtF}_4$  and CO at room temperature.

There is a compound  $\text{Pt}(\text{CO})_2\text{Cl}_2$  reported by PULLINGER (1891). Attempts to repeat this resulted in the preparation of a compound having similar properties to those described by Pullinger, but no evidence of any carbonyl group was obtained.

Although the results of these investigations have been disappointing, some evidence has been obtained indicating that further examples of metal carbonyl fluorides will eventually be obtained, once a suitable method for their preparation and isolation has been devised. In view of the great oxidising power of fluorine and the reducing properties of carbon monoxide, the conditions needed for their incorporation into the same molecule must be critical. Reaction of carbon monoxide under pressure is the most productive method to date, possibly with metal fluorides in lower valency states than tried in this work when these become more readily available. Methods involving reaction of fluorine or metal fluorides with metal carbonyls have so far been unrewarding (from the point of view of preparing carbonyl fluorides) (FEACOCK, 1957).

## Experimental

Carbon Monoxide was used direct from cylinders supplied by Imperial Chemical Industries Ltd. The 25 ml steel bomb used as reaction vessel was pressurised by connecting it directly to the cylinder.

Fluorinating Agents were as described for Chapter 1.

### Reaction of CO with $\text{CuF}_2$

Anhydrous copper fluoride, prepared by heating cupric chloride in a stream of hydrogen fluoride at  $400^\circ\text{C}$  was reacted with carbon monoxide at 150 atm pressure and  $180^\circ$  for 2 days. No reaction had occurred at the end of this time, as shown from an infra-red spectrum. Similar negative results were obtained with a 1:1 molar mixture of  $\text{CuF}_2$  and copper powder.

### Reaction of CO with Cuprous Fluoborate

Cuprous fluoborate was prepared in solution by shaking copper powder with silver fluoborate solution in ether (SHARP, 1960, b). No absorption of carbon monoxide had occurred after 24 hours contact of the solution with 100 atm of CO at room temperature, as shown by an infra-red spectrum of the solution.

### Reaction of CO with Gold Trifluoride

Gold trifluoride was prepared as previously described (SHARPE, 1949) by dissolving gold metal in bromine trifluoride and decomposing the adduct at  $180^\circ\text{C}$ . Reduction to the metal occurred even at low temperatures by the action of carbon monoxide under pressure.

### Reaction of CO with $\text{MoF}_5$ -sulphur Tetrafluoride Complex

A sample of the  $\text{MoF}_5$  -  $\text{SF}_4$  complex, prepared by Dr. R. A. W. Kemmitt, was reacted with carbon monoxide at 100 atms pressure and  $200^\circ\text{C}$  in a



steel bomb. An infra-red spectrum of a film of the product (which was a yellow-brown gum) pressed between rock salt plates showed two peaks at  $2162\text{cm}^{-1}$  and  $2180\text{cm}^{-1}$ . Weak absorptions also appeared at  $1750\text{cm}^{-1}$  and  $1055\text{cm}^{-1}$ .

Sublimation of the product under vacuum produced pale yellow crystals at about  $70^{\circ}\text{C}$ , which did not have the infra-red absorptions listed above and on analysis proved to be molybdenum pentafluoride. Found: Mo (as oxime) 49.2%. Calc. for  $\text{MoF}_5$ : Mo, 50.2%.

#### Preparation of Ruthenium Pentafluoride

##### 1. Bromine Trifluoride method. (HEPWORTH, PEACOCK and ROBINSON, 1954).

Ruthenium bromide, obtained by evaporating ruthenium chloride to dryness with hydrobromic acid and drying at  $100^{\circ}\text{C}$ , was fluorinated with bromine trifluoride in the presence of bromine to modify the reaction. Excess of  $\text{BrF}_3$  and bromine were removed under vacuum, finally heating at  $115^{\circ}$  for one hour. A dark green gum was obtained, which solidified on cooling when it could then be transferred quickly to the bomb in a dry-box. This preparation was very dependent on the form of the ruthenium bromide. If drying was continued for too long the product remained unattacked by bromine trifluoride, and if insufficiently dried dark red or black products were obtained by fluorination which would not react with carbon monoxide. Substitution of Ru metal for the bromide often gave a bright green or red liquid which would not solidify on cooling.

##### 2. Fluorine method. Ruthenium metal, pretreated with hydrogen at $400^{\circ}\text{C}$ , was heated in a stream of fluorine at $350^{\circ}\text{C}$ in a nickel reactor tube inclined so that the liquid product would run into the glass

receiving apparatus (HOLLOWAY, 1961). The product could be solidified by sublimation under high vacuum at 80° for 24 hours to give green crystals, which varied in depth of colour with volatility, the lighter material subliming further than the dark green material. Although all of this was used for reaction with carbon monoxide, it appears from HOLLOWAY and PEACOCK's (1963) work that this material must have contained some of the oxytetrafluoride  $\text{RuOF}_4$ .

#### Reaction of CO with Ruthenium Pentafluoride

The solid products from the two preparations above were reacted with carbon monoxide under pressure (80 - 100 atm.) in a steel bomb. The dark green material from the  $\text{RuBr}_3/\text{BrF}_3$  reaction reacted at room temperature giving a dark solid, out of which a trace of white material could be sublimed under vacuum at 100°C. This proved to be soluble in carbon tetrachloride and gave an infra-red spectrum similar to Fig. 4.1 with peaks at 2100(w), 2125(s) and  $2140\text{cm}^{-2}$ (w)., the rest of the NaCl region was blank. The white material could be removed from the solution by evaporation, but there was insufficient for analysis. This description represents the most rewarding of eight attempts, out of which three produced traces of the presumed carbonyl fluoride.

When the solid from the  $\text{Ru}/\text{F}_2$  reaction was pressurised with carbon monoxide, little reaction apparently occurred unless the bomb was heated to 100°C. In such cases, although no material could be sublimed at temperatures up to 150°C, a carbon tetrachloride extract of the contents of the bomb often showed an infra-red spectrum similar to Fig. 4.2. This reaction was repeated four times, but each time insufficient material could be extracted for analysis.

### Preparation of Osmium and Iridium Hexafluorides

Both compounds were prepared by the fluorination of osmium or iridium metal powders in a stream of fluorine gas at 350°C. The products were purified by trap to trap distillation under vacuum. They were then distilled under vacuum into the bomb, which was cooled in liquid nitrogen, via a copper connector fitted with a standard B14 brass socket and lubricated with a fluorube grease (supplied by Imperial Chemical Industries Ltd.). A pressure of 100 atms. of carbon monoxide was put into the bomb while still frozen in liquid nitrogen, the bomb was allowed to warm at room temperature. It was found from X-ray powder photographs that complete reduction to the metal occurred even at low temperatures (Tables 4.2 and 4.3).

### Reaction of CO with Palladium Trifluoride

Palladium trifluoride was prepared as previously described (SHARPE, 1950) by the fluorination of palladium bromide with bromine trifluoride. No reaction occurred with carbon monoxide under pressure (80 atm) below room temperature, at room temperature the brown  $\text{PdF}_3$  powder had become granular and an X-ray powder photograph showed the presence of  $\text{PdF}_3$ ; at 70°C no  $\text{PdF}_3$  remained and the X-ray powder photograph showed the presence of  $\text{PdF}_2$  and palladium metal (Table 4.4).

### Preparation of Platinum Dicarbonyl Octafluoride

Platinum tetrafluoride was prepared as described by SHARPE (1950) by the action of bromine trifluoride on platinum bromide. It was found that an increased yield of  $\text{Pt}(\text{CO})_2\text{F}_8$  could be obtained using the method of preparation described by SHARP (1960) if the bomb containing platinum tetrafluoride was cooled to  $\sim -80^\circ\text{C}$  before applying the pressure of

Table 4.2X-ray data for OsF<sub>8</sub>/CO

$d_{obs}$	$d_{lit}^a$
2.359	2.367
2.153	2.160
2.068	2.076
1.622	1.595
1.363	1.3668
1.228	1.2300
1.184	1.1840
1.153	1.1551
1.140	1.1416
1.077	1.0799
1.037	1.0383
1.015	1.0
0.982	0.9827
0.914	0.9145
0.912	
0.895	0.8949

Table 4.3X-ray data for IrF<sub>8</sub>/CO

$d_{obs}$	$d_{lit}^a$
2.217	2.25
1.93	1.9197
1.36	1.3575
1.16	1.1574
1.109	1.1082
0.961	0.9598
0.881	0.8808
0.858	0.8586
0.785	0.7838

Table 4.4X-ray data for PdF<sub>8</sub>/CO at 70°

$d_{obs}$	$d_{lit}^a$	
3.48	3.47	PdF <sub>8</sub>
2.79	2.77	PdF <sub>8</sub>
2.659		
2.478	2.46	PdF <sub>8</sub>
2.398		
2.256	2.246	Pd
1.939	1.945	Pd
1.851	1.846	PdF <sub>8</sub>
1.747	1.747	PdF <sub>8</sub>
1.691	1.689	PdF <sub>8</sub>
1.646		
1.563	1.561	PdF <sub>8</sub>
1.522	1.521	PdF <sub>8</sub>
1.480	1.480	PdF <sub>8</sub>
1.395	1.396	PdF <sub>8</sub>
1.371	1.376	Pd
1.271	1.272	PdF <sub>8</sub>
1.242	1.254	PdF <sub>8</sub>
1.216	1.218	PdF <sub>8</sub>
1.169	1.165	PdF <sub>8</sub>
1.149	1.148	PdF <sub>8</sub>
1.132	1.132	PdF <sub>8</sub>
1.121	1.123	Pd
1.007	1.007	PdF <sub>8</sub>
0.972	0.970	PdF <sub>8</sub>
0.9612	0.960	PdF <sub>8</sub>
0.951	0.950	PdF <sub>8</sub>

<sup>a</sup> X-ray Powder Data File, American  
Soc. for Testing Materials

carbon monoxide. Platinum dicarbonyl octafluoride was sublimed from the light grey reaction product at 80°C in vacuo as a white solid, slowly turning yellow in strong sunlight. When stored under vacuum in the dark, the compound crystallised as transparent, sparkling leaflets. An X-ray powder photograph of the crystalline material contained a complex pattern of lines, which no attempt was made to interpret, however the experiment did show that the compound was stable to X-rays for at least one hour. An infra-red spectrum in carbon tetrachloride solution had absorption peaks at 2181(s); 2139(s); 2096(w). (Sharp reports 2161, 2120cm<sup>-1</sup>).

Infra-red spectra of the gaseous products from the reaction of CO and PtF<sub>6</sub> showed the presence of CO<sub>2</sub>, COF<sub>2</sub> and CF<sub>4</sub>.

#### Reactions of Solvents with Pt(CO)<sub>2</sub>F<sub>6</sub>

SHARP (1960) reports that Pt(CO)<sub>2</sub>F<sub>6</sub> attacks solvents containing hydrogen atoms such as benzene, chloroform and acetone. The compound was found to dissolve quite readily in carbon disulphide solution, but infra-red spectra taken on the solution at 10 minute intervals showed the development of strong peaks at 1220cm<sup>-1</sup> (C-F), 790 and 760cm<sup>-1</sup> with simultaneous reduction in intensity of the bands at 2140cm<sup>-1</sup>, indicating attack of the solvent. A similar yellow solution was obtained with dry tetrahydrofuran, but evolution of gas also occurred. The infra-red spectrum of the solution in the carbonyl region showed only one intense absorption at 2100cm<sup>-1</sup>. A yellow gum remained after removal of solvent which slowly turned black on standing, platinum was also slowly deposited from the solution in tetrahydrofuran over a period of days.

### Reaction of $\text{Pt}(\text{CO})_2\text{F}_2$ with Triphenylphosphine

When solutions of  $\text{Pt}(\text{CO})_2\text{F}_2$  and recrystallised triphenylphosphine in carbon tetrachloride were mixed in the dry box, a stream of bubbles was evolved and after a period of minutes a fine white crystalline precipitate appeared.

Carbon monoxide was detected in the gas evolved from the reaction using the "P.S. Carbon Monoxide Detector" supplied by Siebe, Gorman and Co. Ltd. The gas was drawn through a tube containing pure silica gel impregnated with potassium palladosulphite, which changes colour from pale yellow to brown in the presence of carbon monoxide. All other gases and vapours are removed by a protective length of silica gel. Infra-red spectra of the pure gas at pressures up to 10mm. were completely blank (carbon monoxide does not usually give any absorption below 100mm), and the gas could not be condensed at these pressures in liquid nitrogen. Thus in the unlikely event of oxygen or hydrogen being released in the reaction as well, it was considered that the bubbles of gas were carbon monoxide.

An infra-red spectrum of a mull of the crystalline solid corresponded closely to that of either bis(triphenylphosphine) platinum difluoride or dichloride (McAVOY 1963). The presence of chlorine in the solid was confirmed by Beilstein's test. After washing the solid with benzene to remove difluorotriphenylphosphorane (SMITH, 1960), which was a further product of the reaction identified in this benzene solution by its characteristic spectrum (strong peak at  $750\text{cm}^{-1}$  due to P-F stretch), the solid was recrystallised from dichloromethane/ether mixtures.

Analyses varied from one preparation to another, but it was found

that the Pt:C:H ratio remained close to 1:36:30.

Found: Pt 21.57, C 48.36, H 3.42. Pt:C:H 0.94:36:30.5

Ratio for both  $\text{Pt}[\text{P}(\text{C}_6\text{H}_5)_3]_2\text{Cl}_2$  and  $\text{Pt}[\text{P}(\text{C}_6\text{H}_5)_3]_2\text{F}_2$  Pt:C:H 1:36:30

It is considered that the solid is a mixture of  $\text{Pt}(\text{P}\phi_3)_2\text{F}_2$  and  $\text{Pt}(\text{P}\phi_3)_2\text{Cl}_2$ . Separation of these two compounds would be very difficult even on a large scale.

#### Reaction of CO and $\text{PtF}_4$ at Low Temperatures

Before applying a pressure of carbon monoxide to platinum tetrafluoride, the bomb was first frozen down in liquid nitrogen. On one occasion when this was done the bomb leaked so that by the time it had warmed up to room temperature no pressure remained. The platinum tetrafluoride was apparently unchanged in appearance apart from a slight change of colour from light brown to yellow. However when heated under vacuum the compound suddenly exploded at about  $90^\circ$ , coating the vacuum line with a layer of platinum. A small quantity of  $\text{Pt}(\text{CO})_2\text{F}_2$  had sublimed before this happened. The formation of the yellow compound could be repeated by releasing the CO pressure from the bomb below  $0^\circ\text{C}$ . An infra-red spectrum (as a hexachlorobutadiene mull, Nujol was fluorinated) had a broad absorption band between  $2220 - 2170\text{cm}^{-1}$  with a maximum at 2117, and a faint band at  $1842\text{cm}^{-1}$ . Platinum analyses corresponded to a formula  $\text{Pt}(\text{CO})_2\text{F}_4$ . Found: Pt 57.8, 58.7. Calc. for  $\text{Pt}(\text{CO})_2\text{F}_4$ : Pt 59.6%.

#### Attempted Preparation of $\text{Pt}(\text{CO})_2\text{Cl}_2$

Alternating streams of carbon monoxide and chlorine gas were passed over platinum powder at  $250^\circ\text{C}$  as described by PULLINGER (1891). Volatile carbonyl chlorides sublimed into the cooler parts of the tube

leaving an involatile yellow solid, which was found to be  $\text{Pt}(\text{CO})_2\text{Cl}_2$  by Pullinger. However an infra-red spectrum of this solid proved to be completely clear over the  $\text{NaCl}$  region, and a platinum analysis corresponding to a mixture of  $\text{PtCl}_2$  and Pt.

Found: Pt 83.6%, Calc. for  $\text{PtCl}_2:\text{Pt}$ , 73.5%. Calc. for  $\text{PtCl}_2 + \text{Pt}:\text{Pt}$  84.6%

Pt was analysed by evaporating to dryness with concentrated sulphuric acid followed by reduction in hydrogen.

Since the recent developments in high speed computing using electronic devices, and the increasing availability of relatively cheap electronic calculators, largely based on vacuum tube technology, which can perform a number of hours of complete with mechanical machines can be replaced in a few minutes or even seconds. This machine is now being used for the analysis of results with a number of other applications.

#### The Electronic Digital Computer

The fundamental difference between the use of an electronic digital computer and a simple calculating machine lies in the use of a program. This program is a statement in general terms of the way to be taken in the calculation of the results from a



## Chapter 5

### Computer Programmes for X-ray Powder Photography

#### 5.1. Introduction

One of the main reasons why the maximum information is not always obtained from a good powder photograph of a pure crystalline phase is the large amount of tedious computation involved. The use of a semi-automatic mechanical calculating machine does save considerable labour, but there would have to be a very pressing need for a full least-squares refinement of unit cell parameters involving an extrapolation function, even with the aid of such a machine.

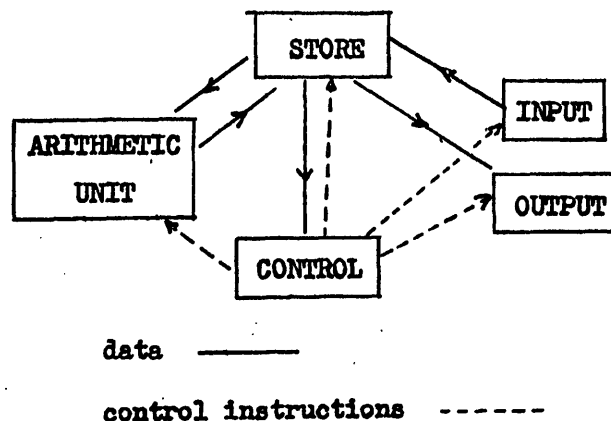
With the recent developments in high speed computing using electronic circuits, and the increasing availability of relatively cheap computers, this problem has largely been overcome. Calculations which would have taken several hours to complete with mechanical machines can now be performed in a few minutes or even seconds, thus enabling a more thorough mathematical analysis of results with a minimum of effort.

#### 5.2 The Electronic Digital Computer

The fundamental difference between the use of an electronic digital computer and a simple calculating machine lies in the so-called computer programme. This programme is a statement in general terms of every step to be taken in the calculation of the results from a given set of data; when followed logically step by step the programme enables the computer to carry out a complete calculation without any intervention by the operator.

As the electronic computer works at a very high speed, e.g. Sirius

can perform 4000 operations a second, it would be extremely inefficient for the operator to supply the computer with numbers at each stage of the calculation. Besides an Arithmetic Unit therefore, a computer must have some form of storage within the machine where numbers needed by the programme can be held until required. The computer is also provided with a Control Unit, this methodically follows each instruction in the programme of calculations, at the same time coordinating the various functions of the computer. Finally some means of external communication must be provided whereby data can be put into the computer at the start of a calculation and the results obtained at the end. This is generally referred to as Input and Output respectively. Transfer of information within the computer can be represented in the form of a block diagram.



A description of these various components for the Ferranti Sirius computer used in this work, follows.

### 5.5 The Sirius Computer

1) Input/Output. Programmes and data are presented to the computer on 5-hole paper tape using the Ferranti Pegasus code. They are prepared and "read" using a conventional teleprinter. The tapes

are read into the computer by a photo-electric reader having a maximum speed of 300 characters per second; output is also on 5-hole tape using a punch at a maximum speed of 60 characters per second. There is also a keyboard which can be used for the manual input of numbers or to select a particular course in a programme.

2) Store. The store has a total capacity of 4000 locations which are referred to by numerical "addresses" running from 0 to 3999 inclusive; each location can hold ten decimal digits. The contents of a location, usually referred to as a word, can either represent a number or a computer instruction since programme and data are held in different parts of the same store. The 4000 word store consists of 80 nickel delay lines holding 50 words each. The digits of a word are represented in the machine by voltage pulses, each decimal digit is coded by four binary digits (bits) in the 5,4,2,1 system, the presence of a pulse corresponding to binary 1 and no pulse to zero; the full 10 decimal digit word therefore contains 40 bits. The computer works at 500 kc/s, each 40-bit word takes 80 microseconds to pass through the machine, and a complete cycle of each 50 word delay line occurs once every 4 milliseconds. A particular word is therefore only available once every 4 milliseconds.

There are also nine one word delay lines, called accumulators 1 to 9 inclusive, which are always available without any access time. These are actually part of the arithmetic unit, numbers are first transferred from main storage to an accumulator where the actual arithmetical operation is carried out.

3) Arithmetic Unit. Sirius is a serial machine - the 40 word-bits pass through the unit in sequence. Possible operations involving

numbers held in the accumulators are addition, subtraction, multiplication and division of two numbers, multiplication and division of one number by 10 (shifting) and collation (selecting digits from specified positions in a number).

4) Control. The major function of this unit is to follow the set of instructions which forms the programme. The store address of the first order is supplied to control at the start of a calculation, this is always held in accumulator 1. The actual order is transferred from store to the control register where it is interpreted, during which time the address in accumulator 1 is normally advanced by one ready for the next instruction. As the various parts of the computer perform their respective functions they are kept in synchronisation by signals from control until the order is completed. Instructions involving transfer from store to accumulator, and input/output orders particularly require such synchronisation.

Another characteristic feature of an electronic computer is that the programmed series of orders may be interrupted and rejoined at a point further on in the sequence, or the computer may be made to repeat a set of instructions. An order causing such a break in the sequence is usually referred to as a jump instruction, and has the effect of resetting the contents of accumulator 1, - the control address. Jump instructions can be made conditional, e.g. a jump is made to a new specified order only if an accumulator is storing zero, otherwise the next order is obeyed in the usual manner. This enables a series of instructions to be followed a specified number of times, the instructions within this "loop" then need only be included once

in the programme.

#### 5.4 The Programme

The programme is simply a series of instructions, in a code which can be interpreted by the computer, representing how the problem is to be solved; it is usually intended to operate on a set of data. The programme is written in the most general form, any parameters are left to be specified for the particular set of data being processed, e.g. to obtain  $\sin^2\theta$  values from line measurements taken from an X-ray powder photograph, parameters such as camera constant, X-ray wavelength, are left to be specified with the data for each photograph. The first step in writing a programme is to break the problem down into a flow diagram, taking care to account for every possible situation that could arise. To obtain the maximum efficiency from the computer, this should then be converted into the basic machine order format of the particular computer. However it is possible to make the computer do a lot of the coding itself, in particular using a coding programme available for Sirius known as Autocode. This enables the programme to be written in a form using conventional mathematical symbols more easily understood than the machine code, which is necessarily purely numerical. When the programme in Autocode form is to be presented to the computer, the Autocode coding programme (itself in basic machine code of course) is first stored in the machine; then under the control of this Coding programme, the operator's programme is automatically converted on input into basic machine orders. This can either be stored directly in the machine or punched out by the computer to be used as input at some later time. In this way many of the initial

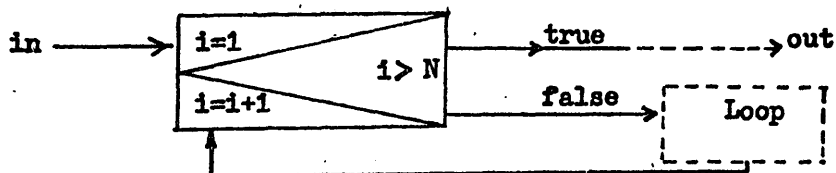
mistakes in a programme can be found and corrected, and much of the labour involved in writing a programme reduced.

### 5.5 Flow Diagrams

There are many conventions used for the presentation of flow diagrams, the form of diagram used here is taken from GALLER (book). The shapes of the boxes in the diagram are used to represent the role of their contents in the programme. Rectangular boxes contain actual calculations. A statement such as  $SSQ_i = a + b$  means that  $a$  and  $b$  are summed and the result is stored in the location  $SSQ_i$ ;  $SSQ_i$  is a name given (for the purposes of the diagram) to the  $i$ 'th member of a block of consecutive locations  $SSQ_m$  to  $SSQ_n$  where  $m \leq i \leq n$ , and  $m, n$  are given. Names without subscripts e.g. LL, represent single locations.

Diamond shaped boxes contain the test for a conditional jump. The condition in the box will either be true or false, and one of the two paths labelled accordingly will be taken.

For a loop of instructions which is to be repeated several times, the box shown is used. When the loop is entered, the initial condition



is set (shown as  $i = 1$ ). The termination condition is examined and the appropriate path taken. Every time the loop of instructions is obeyed the box is re-entered through the modification section and the termination condition re-examined, passing on to the next instruction when this is finally satisfied.

Short ancillary programmes, or sub-routines, which are used by the main programme to perform some minor task such as forming the sine of an angle, are given a name in capital letters and enclosed in a double-box. Any values that are obtained by the sub-routine are enclosed in parentheses. The routine labelled SORT arranges a collection of numbers into increasing order of magnitude.

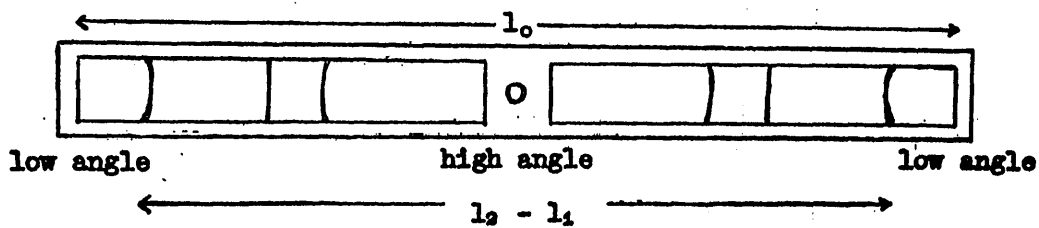
Finally to assist in layout, flow paths that end in  $\rightarrow \textcircled{2}$ , are continued from the correspondingly numbered circle elsewhere in the diagram i.e.  $\textcircled{2} \rightarrow$ .

The programmes written in this work for use in X-ray powder photography will now be presented a) as a written description of what each programme will do; and b) in the form of a flow diagram. Actual copies of the programme as presented to the computer are not readily interpreted.

### Programme 1: Data from Photographs

Values of  $\theta$ ,  $\sin^2\theta$ , d-spacing and  $\sin\theta/\lambda$  are calculated from line position measurements taken from Debye powder photographs, obtained using a Van Arkel type camera<sup>x</sup>. It is possible to suppress the printing of  $\sin\theta/\lambda$  if this is not required, and also to use the programme to produce  $\sin^2\theta$  only in a form suitable for use in the following programmes.

#### 1. Method



The programme calculates the data by reading in measurements for each line one at a time. If  $\phi$  is the camera constant,  $\lambda$  the X-ray wavelength,  $l_0$  the distance between the knife edges,  $l_1$  and  $l_2$  the left and right hand line readings resp. ( $l_2 > l_1$ ), then

$$\theta = \left[ \pi - (l_2 - l_1) \times \phi / l_0 \right] \times 57.295773 \text{ degrees}$$

$$d = \lambda / 2\sin\theta$$

#### 2. Data Required

The programme requires the following data, in order:

- 1) Camera constant: one quarter of the angular distance in radians between the knife edges of the camera (i.e. about 1.5).

<sup>x</sup> Bradley - Jay can be used with small programme alterations.



ii) X-ray wavelength: to be used in calculating d-spacings.

If some of the lines have been resolved into  $\alpha_1$ , and  $\alpha_2$  components, they must be treated as separate sets of data.

iii) Knife edge readings: smaller reading first.

iv) Line data: an integral estimate of the line intensity, followed by two line position readings are needed for each line.

The intensity can be any integer from 0 to 9999. The line position readings must have the smaller one first for each line, and it is necessary to measure from low to high angle systematically if the output is to be used in the following programmes.

v) End of data: the last line measurement must be followed by the warning character L, and the last set of data by Z.

### 3. Operation of Programme and Output

The results are printed out in tabular form under the following headings:

LINE	lines are numbered in order
INT.	copied directly from the input tape
DIFF.	distance between lines of diffraction cone, to 3 dec. places
THETA	Bragg angle to 3 dec. places in degrees
SIN TH.SQ.	$\sin^2 \theta$ to 5 dec. places
D-VAL.	d-spacing to 4 decimal places in the same units as $\lambda$
SIN TH/L	$\sin \theta / \lambda$ to 3 dec. places

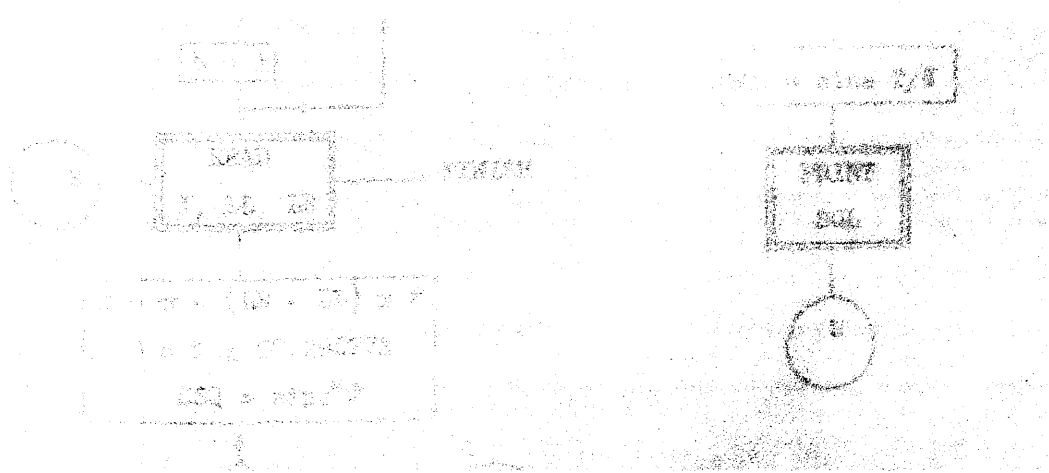
The most significant digit ( $D_0$ ) of the keyboard may be set to have the following effect:

$D_0$	Effect
0	All data is punched out
2	$\sin^6/\lambda$ is suppressed
5	All printing except $\sin^2\theta$ is suppressed
9	Computer stops and proceeds on resetting keyboard and pressing CONTINUE

In the case of  $D_0 = 5$ , the  $\sin^2\theta$  values are preceded by 6 ins. of blank tape, and followed by L and three erases.

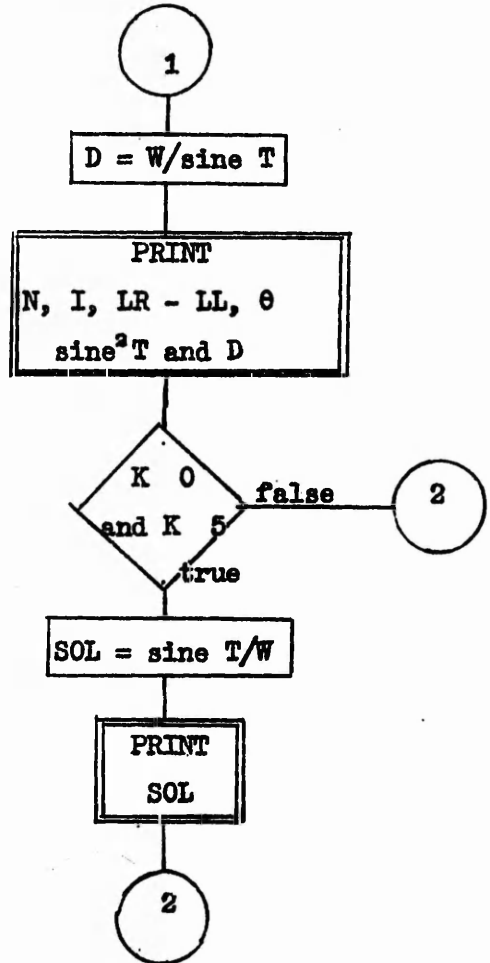
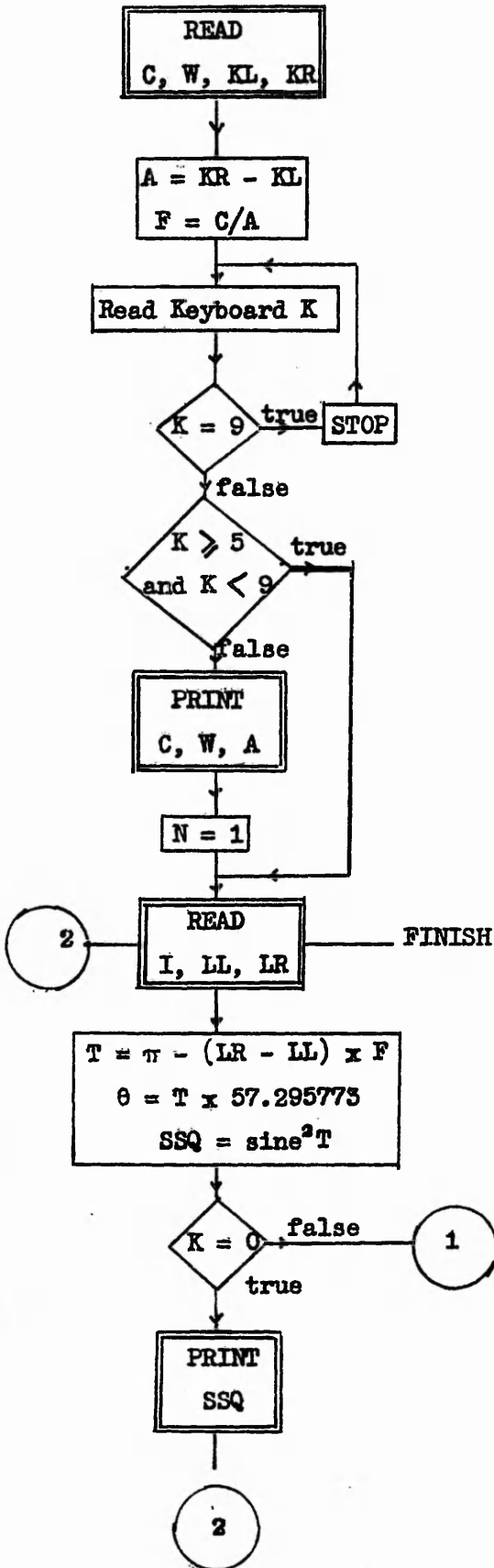
#### 4. Time

About 30 lines a minute, or 100 lines a minute for  $\sin^2\theta$  only.



Flow Diagram for Programme 1

C = Camera constant  
 KL, KR = L.H. and R.H. knife edge readings  
 W = X-ray wavelength  
 I = Intensity  
 LL, LR = L.H. and R.H. line readings



## Programme 2. Sorting Differences of $\sin^2 \theta$

From a series of  $\sin^2 \theta$  values in ascending order, all possible positive differences between any pair of  $\sin^2 \theta$  values are calculated and sorted into blocks of a given numerical interval. Blocks containing more than a specified number of  $\sin^2 \theta$  differences are selected for printing.

This is essentially the procedure given by LIPSON (1949) for indexing powder photographs of compounds with structures of orthorhombic or higher symmetry.

### 1. Method

Differences  $\sin^2 \theta_p - \sin^2 \theta_q$  ( $D_{pq}$ ), where  $0 < p < n$ , and  $0 \leq q < n$ , are calculated from a series of  $n$  values of  $\sin^2 \theta$ , rejecting those values outside the limits  $D_{\max} > D_{pq} \gg D_{\min}$ . The  $D_{pq}$  values are then sorted into ascending order. Using a chosen interval  $h$ , which represents the estimated experimental error in the value of  $\sin^2 \theta$ , the number of differences  $D_{pq}$  within consecutive blocks of numbers,  $h$  wide, are counted, starting with the block  $(D_{\min} + h) \gg D_{pq} > D_{\min}$  and finishing with  $D_{\max} \gg D_{pq} > (D_{\max} - h)$ . If there are more  $D_{pq}$  values in a given block than a specified Minimum Number for Printing, then the number of values within the block is recorded together with the upper limit of the block. Any block containing less than the minimum number is rejected.

### 2. Data Required

From now onwards, "differences of  $\sin^2 \theta$ " is abbreviated to D-S<sub>2</sub>. The programme requires the following data, in this order.

i) Maximum D-S<sub>2</sub>: which is to be considered by the programme. It is not the maximum value of  $\sin^2\theta$  in the data. A suitable value to be used is 0.2, as recurring differences greater than this are usually fairly high multiples of the constants A, B or C.

ii) Minimum D-S<sub>2</sub>: to be considered, again it is not the minimum  $\sin^2\theta$  value in the data. Normally zero would be used, but irrelevant small differences may be eliminated in this way, thus saving time and storage space.

It is important that i) and ii) are in the correct order otherwise the machine enters an infinite loop.

iii) Interval: the width 'h' of the numerical blocks within which it is desired to group all the D-S<sub>2</sub> values. It can be the estimated experimental error in the original values of  $\sin^2\theta$ , usually between 0.0005 and 0.001.

iv) Minimum Number for Printing: this must be an integer, and is used to eliminate the background D-S<sub>2</sub> values. It is difficult to give an idea of size as it depends on the total number of  $\sin^2\theta$  values as well as their frequency. A rough value may be derived from Table 5.1, but if insufficient data is obtained it is a simple matter to repeat with a smaller number. Too small a number will result in the production of a large amount of irrelevant data.

v) Sin<sup>2</sup>θ Values: must be in ascending order and separated from each other by Spaces or CR/LF's. A set of  $\sin^2\theta$  values is terminated by the warning character L and the end of the data by Z.

vi) Output from Programme 1: obtained when run with D<sub>0</sub> = 5, may be used as input for this programme. The tape is complete except

Table 5.1

choice of Min. No. for Printing  
( $h = 0.001$ )

max. $\sin^2 \theta$	min. no. for print- ing (N)	add 1 to N if no. $\sin^2 \theta$ more than:
0.1	1	10
0.5	2	30
0.6	3	50
0.9	4	80
1.0	5	-

Table 5.2

capacity of programme

n	b(max) a = 0
54	54
60	34
70	25
100	16

for i) - iv) above and the final Z, which are added separately.

### 3. Output of Data

The parameters i) - iv) in section 2 above are recorded, followed by the list of "blocks" and their contents under the headings RANGE (UPPER LIMIT) and NUMBER. The upper limit only of each block is recorded.

### 4. Capacity of Programme

The number of  $\sin^2 \theta$  values that can be scanned depends on the total number of values read in, and on the sizes of MAX D-S<sub>2</sub> and MIN D-S<sub>2</sub>. It is possible to calculate the approximate number of D-S<sub>2</sub> values that will be obtained.

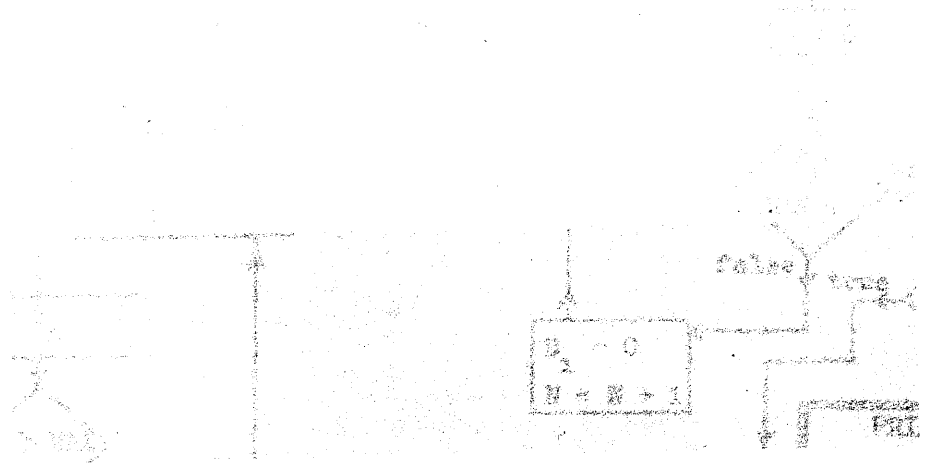
Suppose  $n \sin^2 \theta$  values are read in, and there are  $a \sin^2 \theta$  values less than MIN D-S<sub>2</sub> and  $b$  values such that  $\text{MIN D-S}_2 \leq b < \text{MAX D-S}_2$ . Then the approx. no. of D-S<sub>2</sub> values which will be in the range is given by

$$\text{no. of D-S}_2 \text{ values} = \frac{b}{2} [2(n - a) - b + 1]$$

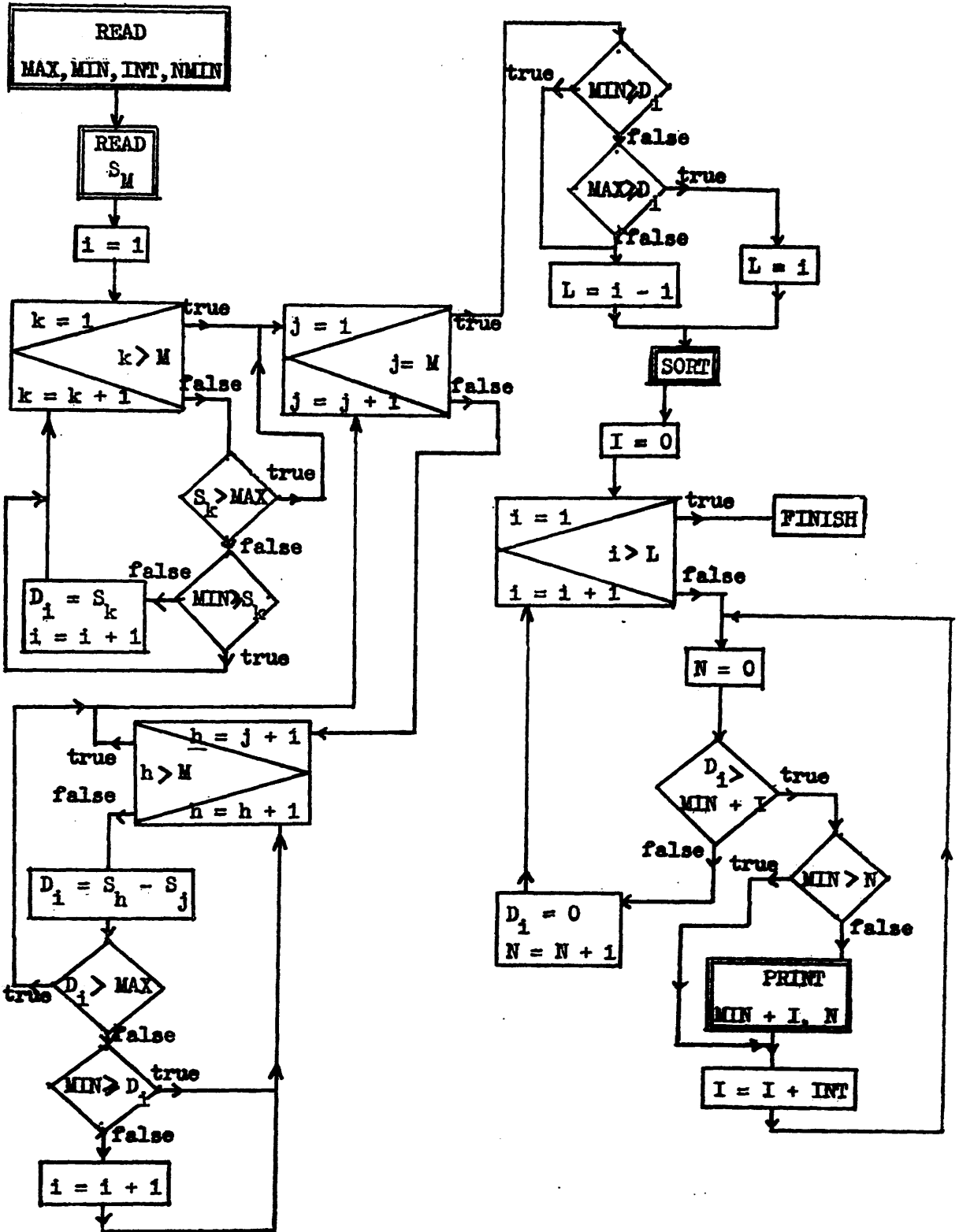
The maximum number of values that can be handled in the store is 1480. The maximum values of  $b$  for some values of  $n$  are given in Table 1.2 (for  $a = 0$ ). Obviously  $b$  is greater if  $a > 0$ . If more than 1480 values are generated in the computer, but less than 2960, the machine will come to a 1480009900 wait. On pressing CONTINUE, calculation will proceed ignoring those differences after the first 1480 -- they are not in numerical order at this stage so the results will not be completely reliable. If more than 2,960 differences are generated, the machine will stop with a parity failure.

#### 5. Time

Not greater than 5 minutes for full capacity.



Flow Diagram for Programme 2





Programme 5: Check Indexing

This programme is intended to assist in the indexing of X-ray powder photographs. A list of  $\sin^2 \theta$  values and corresponding  $h, k, l$  in ascending order can be produced for any symmetry from orthorhombic to cubic, and for any lattice constants. The programme may also be used to check the indexing of a set of observed  $\sin^2 \theta$  values. With a slight modification any space group extinction conditions may be imposed.

1. Method

The programme calculates all  $\sin^2 \theta$  values, within a given range, for the lattice constants supplied according to the specified symmetry. The actual constants required A, B and C are related to the cell dimensions as shown in Table 5.3

Table 5.3

	Cubic	Rhombohedral <sup>*</sup>	Hexagonal	Tetragonal	Orthorhombic
A	$\lambda^2/4a^2$	$\lambda^2/3a^2$	$\lambda^2/3a^2$	$\lambda^2/4a^2$	$\lambda^2/4a^2$
B	-	-	-	-	$\lambda^2/4b^2$
C	-	$\lambda^2/4c^2$	$\lambda^2/4c^2$	$\lambda^2/4c^2$	$\lambda^2/4c^2$

\* The related hexagonal cell (3 times rhomb. cell) is used for indexing.

If a series of observed  $\sin^2 \theta$  measurements (in ascending order) is to be checked for correct indexing, these values are compared with the calculated values and where agreement closer than a specified limit is obtained, the observed and calculated  $\sin^2 \theta$  values are printed out

together with the corresponding h, k and l. The number of observed lines not indexed is counted, and the R-factor = 
$$\frac{\sqrt{\sum (\sin^2 \theta_{\text{obs}} - \sin^2 \theta_{\text{calc}})^2}}{n - 1}$$
 calculated.

## 2. Data Required

The observed  $\sin^2 \theta$  values, if required, are supplied in ascending order on tape, with a title as usual. The output from Programme 1, run with the keyboard  $D_0 = 5$  is suitable. All other data is read from the keyboard.

## 3. Output of Data

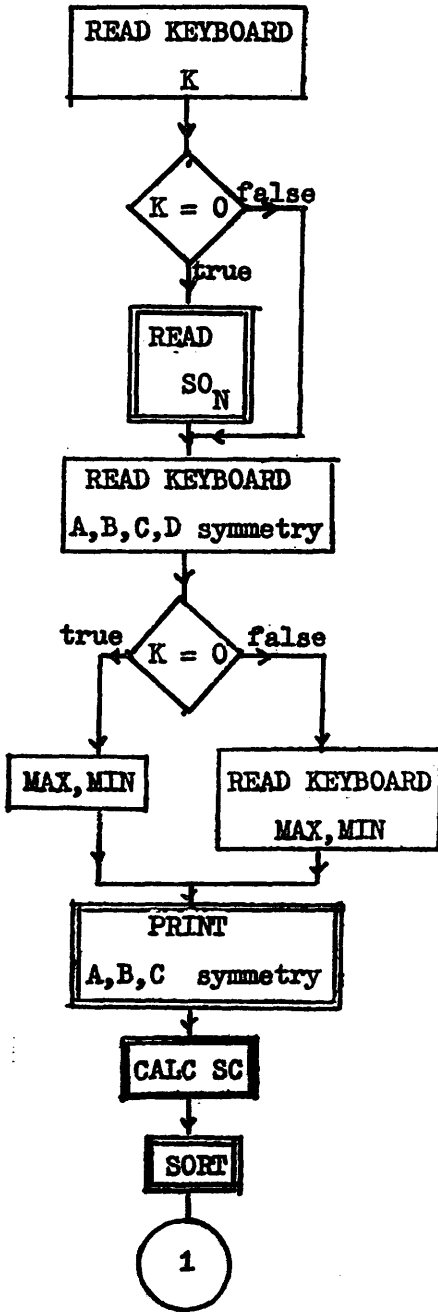
The cell symmetry and the A, B and C supplied are recorded. When a series of observed  $\sin^2 \theta$  values has been indexed, the indexed values are printed out together with the h,k,l and  $\sin^2 \theta_{\text{calc}}$  values found under the headings OBS. H,K,L and CALC. The R-value for the indexed lines and the number of unindexed lines are printed followed by a list of the actual  $\sin^2 \theta_{\text{obs}}$  not indexed.

When only  $\sin^2 \theta_{\text{calc}}$  values are required, they are presented in increasing order of magnitude together with the corresponding h,k,l.

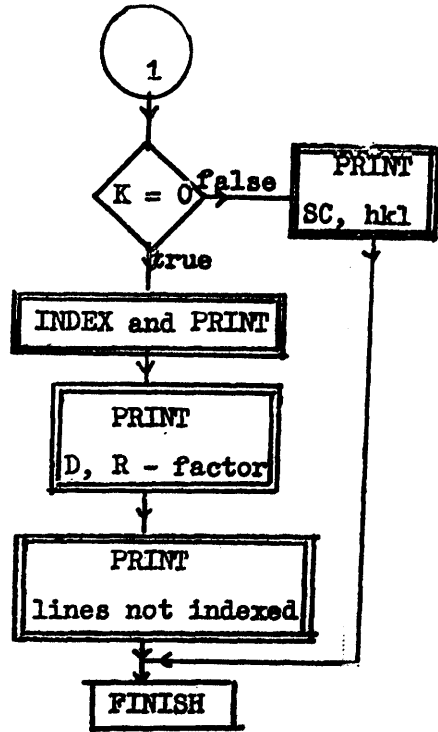
## 4. Time

Apart from the time needed to set up the keyboard, calculation of  $\sin^2 \theta_{\text{calc}}$  and indexing takes from one to two minutes depending on the range of  $\sin^2 \theta$  and the lattice constants.

Flow Diagram for Programme 3



A, B, C    Approximate constants  
 D    Maximum difference between  
       obs. and calc values  
 SO<sub>N</sub>    N observed sin<sup>2</sup>θ values  
 CALC SC    and    INDEX and PRINT  
               routines are described below



Programme 4: Unit Cell Least Squares Refinement

This programme refines the unit cell constants of a crystalline substance by the method of least squares; given approximate cell constants and the values of  $\sin^2\theta$  obtained from a powder photograph of that substance. An attempt is made to correct for systematic errors in  $\theta$  using the Nelson-Riley function. It is possible to substitute other functions from a separate "library" tape.

Cubic, tetragonal, rhombohedral, hexagonal and orthorhombic unit cells can be handled. With the library tape it is possible to adapt the programme to deal with single crystal rotation photographs.

It is possible to return the constants obtained from one refinement to the start for further refinement cycles until the best possible values are obtained.

1. Method

From the cell constants supplied all possible values of  $\sin^2\theta$  are calculated within the range of the supplied  $\sin^2\theta_{\text{obs}}$ . These calculated  $\sin^2\theta$  values are then systematically compared with the observed values and where agreement better than a specified limit is found, the values of h,k,l for that line are stored together with the corresponding  $\sin^2\theta_{\text{obs}}$ .

Correction for systematic errors in  $\theta$  is made by assuming that the relative error in the corresponding d-value is proportional to some function of  $\theta$ ; the Nelson-Riley function  $\frac{1}{2} \cos^2\theta \left[ \frac{1}{\sin\theta} + \frac{1}{\theta} \right]$  is provided as standard. For example, in the orthorhombic case the equation connecting A, B and C with  $\sin^2\theta$  becomes

$$Ah^2 + Bk^2 + Cl^2 + D \sin^2 \theta \cdot \frac{1}{2} \cos^2 \theta \left[ \frac{1}{\sin \theta} + \frac{1}{\theta} \right] = \sin^2 \theta$$

where  $\theta$  is the observed Bragg angle, A, B, C, h, k, l have conventional meaning and D is the drift constant for the particular photograph.

(See Appendix for derivation of formulae). The best values of A, B, C using all the  $\sin^2 \theta$  data are obtained by the method of least squares, the matrix form of the normal equations is shown in Table 5.4, with the individual meanings of the parameters for each symmetry in Table 5.5.

Table 5.4

Matrix elements of least squares normal equations

$$\begin{pmatrix} \sum \alpha^2 & \sum \alpha\beta & \sum \alpha\gamma & \sum \alpha\delta \\ \sum \alpha\beta & \sum \beta^2 & \sum \beta\gamma & \sum \beta\delta \\ \sum \alpha\gamma & \sum \beta\gamma & \sum \gamma^2 & \sum \gamma\delta \\ \sum \alpha\delta & \sum \beta\delta & \sum \gamma\delta & \sum \delta^2 \end{pmatrix} \begin{pmatrix} A \\ B \\ C \\ D \end{pmatrix} = \begin{pmatrix} \sum \alpha \sin^2 \theta_{\text{obs}} \\ \sum \beta \sin^2 \theta_{\text{obs}} \\ \sum \gamma \sin^2 \theta_{\text{obs}} \\ \sum \delta \sin^2 \theta_{\text{obs}} \end{pmatrix}$$

Table 5.5

Meaning of symbols in Table 5.4

Unit cell	A	B	C	$\alpha$	$\beta$	$\gamma$
Orthorhombic	$\lambda^2/4a^2$	$\lambda^2/4b^2$	$\lambda^2/4c^2$	$h^2$	$k^2$	$l^2$
Hexagonal Rhombohedral	$\lambda^2/3a^2$	-	$\lambda^2/4c^2$	$(h^2+hk+k^2)$	-	$l^2$
Tetragonal	$\lambda^2/4a^2$	-	$\lambda^2/4c^2$	$(h^2+k^2)$	-	$l^2$
Cubic	$\lambda^2/4a^2$	-	-	$(h^2+k^2+l^2)$	-	-

$$D = 10 \times \frac{\cos^2 \theta}{2} \left[ \frac{1}{\theta} + \frac{1}{\sin \theta} \right]$$

These refined values for the constants may then be fed in at the start of the programme and the whole process repeated. However if the new values of A, B and C are so close to the previous values used for the calculation of  $\sin^2\theta$  that the indexing of every  $\sin^2\theta_{\text{obs}}$  is unchanged, then further refinement cycles will not change A, B and C. This is because different values for A, B and C will only be obtained if the coefficients in the normal equations (Table 5.4) are changed. This set of A, B and C is the best that can be obtained from the available data, and so when this point has been reached recycling of the A, B and C parameters ceases and the next stage in the calculation is automatically entered.

B and  $\beta$  are not used for the tetragonal and trigonal cases, and B, C,  $\beta$  and  $\gamma$  are not used for cubic unit cells. Rhombohedral unit cells are treated by using the related larger hexagonal unit cell; the values of h, k and l for a given line are then governed by the formula  $-h + k + l = 3n$  (n an integer), all other combinations of h,k,l are rejected by the programme for this symmetry.

The same  $\sin^2\theta_{\text{obs}}$  may be indexed by more than one combination of h, k and l provided the agreement is close enough, similarly more than one  $\sin^2\theta_{\text{obs}}$  may agree with the same  $\sin^2\theta_{\text{calc}}$ , thus giving complete coverage for even very closely spaced lines.

The unit cell sides are calculated from the final A, B and C values, and in the relevant case, rhombohedral constants are calculated as well. A reliability factor is calculated using the formula

$$R = \sqrt{\frac{\sum_n (\sin^2\theta_{\text{obs}} - \sin^2\theta_{\text{calc}})^2}{(n - 1)}}$$

where n is the number of  $\sin^2\theta_{\text{calc}}$  values accepted.

The number of lines not indexed is also presented.

## 2. Data Required

The following must be supplied on the data tape, in order.

i) Symmetry of Unit Cell: this is written out immediately after a title and a directive to enter the programme. Only the first letter is recognised, which must therefore be O, T, H, R or C, anything following is merely copied onto the output tape.

ii) Approximate Constants A, B and C: as in Table 5.5. B is ignored for tetragonal and trigonal, and B and C for cubic cells, however a number must be punched, e.g. zero or A.

iii) Max D(OBS - CALC): this is the maximum difference between  $\sin^2\theta_{\text{obs}}$  and  $\sin^2\theta_{\text{calc}}$  that can be tolerated for indexing. The size will depend on the estimated experimental error and accuracy of A, B and C, it may range between 0.001 to 0.005. Too large a value will result in unnecessary duplication of indexing.

iv) X-ray Wavelength: this is used in calculating the final cell sides. Values of  $\text{MAX D(OBS - CALC)} = 0.002$  and  $\text{X-RAY WAVELENGTH} = 1.5418$  (CuK $\alpha$ ) are provided in the programme, they may be changed when not suitable.

v) Sin<sup>2</sup> $\theta$  Values: in ascending order as for Programme 2, terminated by an L, and the final set terminated by L and Z. Output from Programme 1 may be used with the appropriate leader tape and final Z in any of the ways suggested previously.

## 3. Operation of Programme

After the data has been read in, D<sub>9</sub>(Least Significant Digit) of the keyboard may be used to affect the course of the calculations.

i) Keyboard Zero: calculation proceeds as in Method until

the first refined values of A, B and C are obtained. The corresponding  $\sin^2\theta$  values are recalculated and the indexed lines are printed out as described in Section 4 below, followed by cell parameters etc.

ii) D<sub>0</sub> = 5-9: computer eventually comes to a 9900009900 wait after punching out the refined values of A, B and C obtained at the end of the current cycle. The keyboard may then be altered to i) or iii) depending on the values of A, B and C, and on CONTINUE calculation will proceed.

iii) D<sub>0</sub> = 1-4: similar to i) except that the first refined values of A, B and C are recycled to give second refined values, and so on until the keyboard is altered. However the degree of refinement is limited, since improved values will only be obtained if the new A, B and C cause a different set of indices for the indexing. When the ultimate values of A, B and C have been obtained the indexed lines will be printed out as in Section 4 below.

The number of the cycle the programme is in can be followed using the DISPLAY button. Thus if it is required to operate two cycles only the programme is started with D<sub>0</sub> of the keyboard 1 - 4, and left until 1 appears in Display. The keyboard should then be cleared and when 2 appears punching out of indexed lines will occur.

#### 4. Output of Data

The symmetry of the unit cell, copied from the data tape follows the title, then the MAX D(OBS - CALC) and X-RAY WAVELENGTH used. The values of A, B and C obtained after each cycle are printed out under the headings

CYCLE; the number of the cycle, zero represents the initial values.



A,B,C; where appropriate, to 6 decimal places.

L,N,I; number of lines not indexed by the corresponding set of A, B and C.

When the refinement of A, B and C is completed the indexed lines are printed out in a table with the headings,

OBS ;  $\sin^2 \theta$  observed printed to 5 decimal places.

H,K,L; the conventional h, k and l indices. In the case of rhombohedral unit cells, these are the indices of the related hexagonal cell, h and k are in the correct order to satisfy the condition  $-h + k + l = 3n$ .

CALC ;  $\sin^2 \theta$  calculated to 5 decimal places.

At the end of the table the following results are printed,

R - value; the reliability factor (see Section 1). This is in floating point form, i.e. the second number is the power of 10 which the first number must be multiplied by. The number in brackets is the number of lines not indexed using the final set of A, B and C values. It is a more powerful check on the correct indexing than the R-value since the latter is controlled to some extent by the  $\text{MAX } D(\text{OBS} - \text{CALC})$ .

CELL CONSTANTS(A); the cell parameters according to Table 5.5.

RHOMBOHEDRAL " ; only in the case of a rhombohedral unit cell.

The true rhombohedral parameters  $a_R$  and  $R$  are related to the hexagonal parameters  $a_H$  and  $c_H$  by

$$a_R^2 = \frac{1}{3} a_H^2 + \frac{1}{9} c_H^2 \quad \sin \frac{1}{2} \alpha_R = \frac{3}{2(3 + c_H^2/a_H^2)^{1/2}}$$

### 5. Capacity of Programme

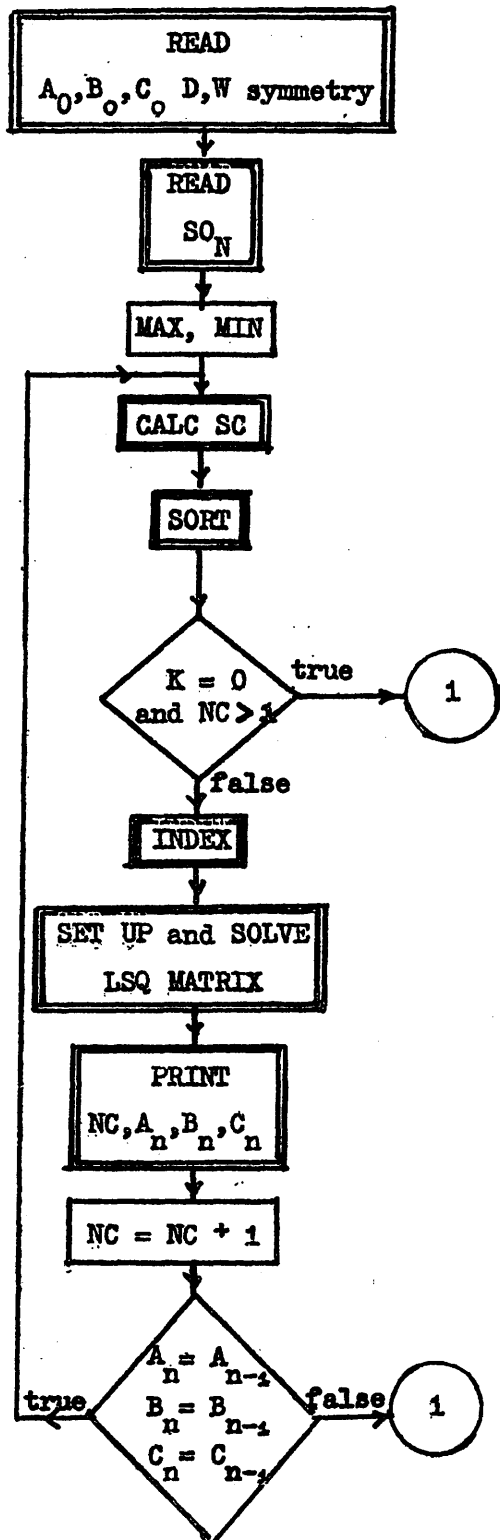
There is sufficient storage for 110  $\sin^2\theta_{\text{obs}}$  values and 970  $\sin^2\theta_{\text{calc}}$ . However there are limitations set on the minimum values of A, B and C by the method of coding the  $\sin^2\theta$  values and their appropriate values of h,k,l within a single computer word. The result is that for the h,k,l of any one line, one integer must not be greater than 19, and either of the other two not greater than 9.

Warning is given if this condition is exceeded, also if more than 970  $\sin^2\theta(\text{calc})$  are generated.

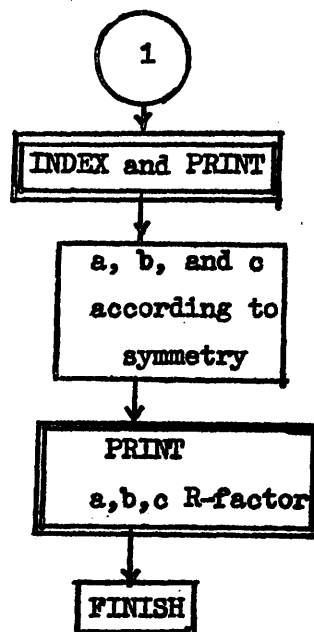
### 6. Time

The time taken depends on too many variables for an exact estimate to be made, but an average photograph containing 30 lines takes about  $2\frac{1}{2}$  minutes for one refinement, each extra cycle takes about  $1\frac{1}{2}$  minutes. A photograph of an orthorhombic substance with 50 lines took a total of 16 minutes for an analysis which included 3 refinement cycles.

Flow Diagram for Programme 4

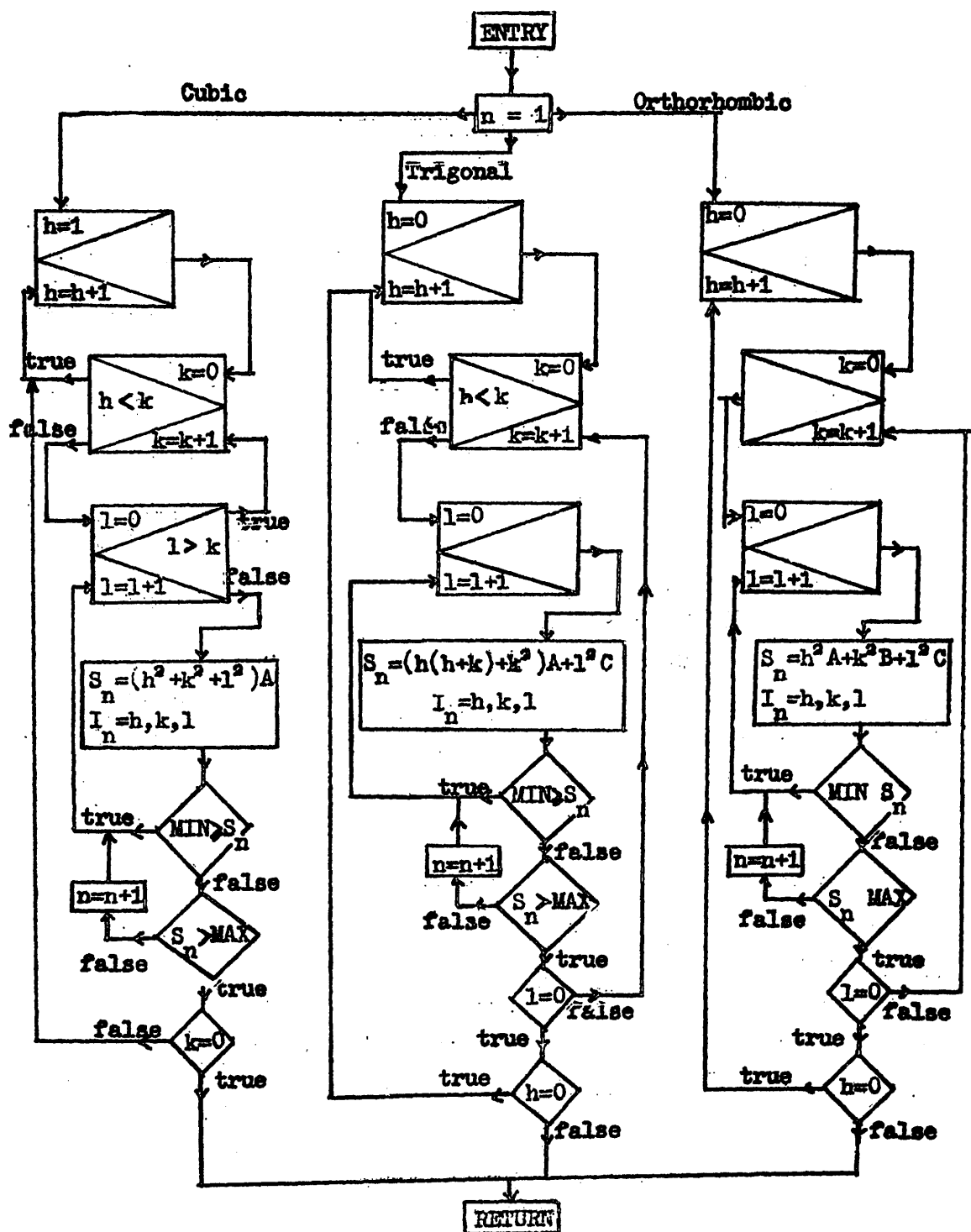


$A_0, B_0, C_0$  Approximate constants  
 D Max. difference between  
 obs. and calc. values  
 $S_{0N}$  N observed  $\sin^2 \theta$  values  
**CALC SC**, **INDEX** and **PRINT**, **INDEX**  
 and **SET UP** and **SOLVE LSQ MATRIX**  
 sub-routines are described below

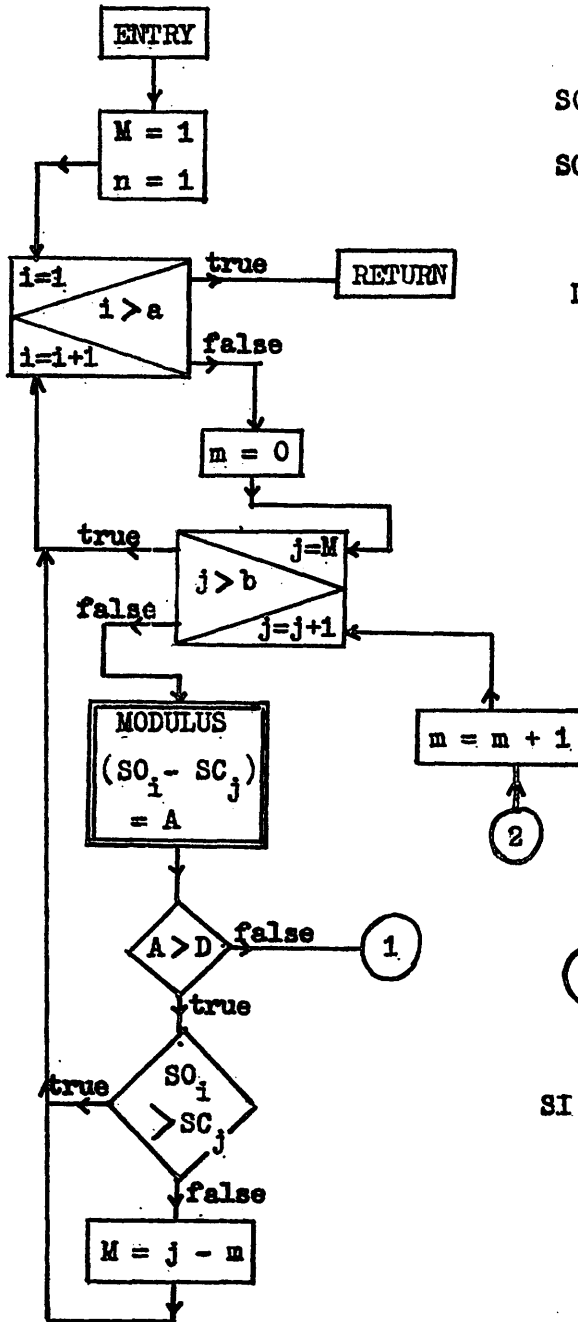


CALC SC Sub-routine

Calculates  $\sin^2 \theta$  from given parameters A, B and C



INDEX Sub-routines



Required:

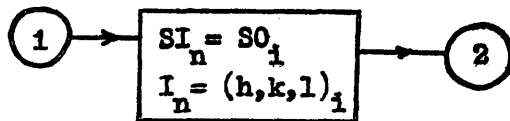
$SO_a = a$  values of  $\sin^2 \theta_{obs}$

$SC_b = b$  values of  $\sin^2 \theta_{calc}$  and

corresponding  $h, k, l$

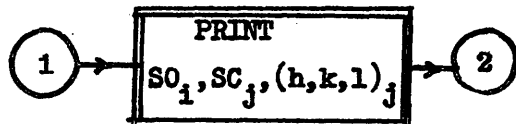
$D =$  Maximum difference for indexing

INDEX

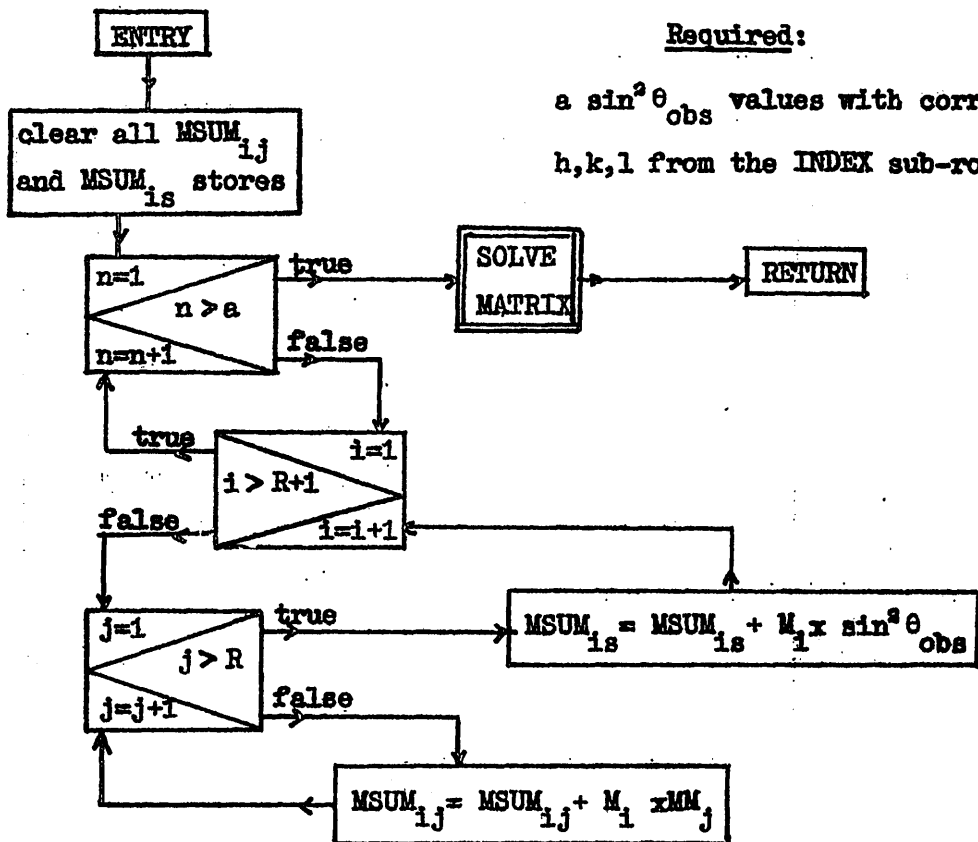


$SI =$  indexed  $\sin^2 \theta_{obs}$  with corresponding corresponding  $h, k, l$  (I)

INDEX and PRINT



SET UP and SOLVE LSQ MATRIX Sub-routine



Required:

a  $\sin^2 \theta_{\text{obs}}$  values with corresponding  $h, k, l$  from the INDEX sub-routine

	Orthorh.	Tetrag.	Trigonal	Cubic
$M_1$	$h^2$	$h^2 + k^2$	$h^2 + hk + k^2$	$h^2 + k^2 + l^2$
$M_2$	$k^2$	$l^2$	$l^2$	$\sin^2 \theta \cdot f(\theta)$
$M_3$	$l^2$	$\sin^2 \theta \cdot f(\theta)$	$\sin^2 \theta \cdot f(\theta)$	-
$M_4$	$\sin^2 \theta \cdot f(\theta)$	-	-	-
R	4	3	3	2

### 5.7 Use of Programmes

Assuming that a good photograph of an unknown pure crystalline phase is available, and it is desired to identify the unit cell of the crystal lattice and obtain accurate cell dimensions, the following procedure is suggested involving the use of the computer programmes described above.

Having accurately measured the positions of all visible lines and the two knife-edge shadows on the photograph, and estimated an intensity for each line, Programme 1 can be used to convert this information into Bragg angle  $\theta$ , lattice spacing  $d$ , and other useful functions of  $\theta$ . As the value of  $\sin^2\theta$  for each line is used in the ensuing calculations, Programme 1 can also be used to produce a tape containing a list of  $\sin^2\theta$  values only, suitable for use in any of the following programmes.

The list of  $\sin^2\theta$  values representing the lines in the photograph is then checked for the presence of a cubic phase; i.e. all values are multiples of some lowest common factor (A). If this is found to be so, then the problem is solved and an accurate value for A can be obtained from Programme 4. However if the unit cell does not have cubic symmetry, it is best to examine the  $\sin^2\theta$  values using the method of LIPSON(1949), (D'EYE and WATT,1960). This consists of forming the difference between every pair of  $\sin^2\theta$  values and noting those differences which occur most frequently. For the orthorhombic, trigonal and tetragonal symmetries, these differences are often simply related to the lattice constants. This task is made simple by Programme 2 which selects these commonly occurring differences. Usually two or more possible unit cells may fit the first few lines quite closely, and the

choice between them may only be settled by considering all  $\sin^2\theta$  values. Programme 3 can be used to calculate a list of all possible  $\sin^2\theta$  for any unit cell, and also to index the set of observed  $\sin^2\theta$  values against any unit cell, noting those lines which are not indexed for the particular cell chosen.

If at this stage a satisfactory choice of unit cell cannot be made, it is probable that the compound has a symmetry lower than orthorhombic. For such cases the powder method is not really sufficiently unambiguous to decide the lattice structure.

When rough values for the unit cell have been obtained, Programme 4 can be used to obtain the most accurate cell dimensions which will best fit the available data.

Using this type of plan it would be possible to programme a computer to perform the whole sequence of operations without any human intervention. Although with the limited storage capacity and speed of Sirius, complete automation of the problem would probably take longer and be less reliable than the combination of machine and mind outlined above, the much larger and faster computers now in use could certainly improve on this; HAENDLER (1963) has devised programmes based on the general method of De WOLFF (1957) for indexing triclinic substances. In fact the larger computers are capable of supervising a complete single crystal structure analysis, but this stage must await development of a suitable computer programme.



Least Squares Refinement of Powder Photographs

The semi-vertical angle  $2\theta$  of the cone of diffraction of monochromatic X-rays from a randomly oriented crystalline powder is given by the Bragg law

$$\lambda = 2d\sin\theta \dots \dots \dots (1)$$

where  $\lambda$  is X-ray wavelength and  $d$  the spacing of the lattice planes giving rise to the diffraction. The spacing of the lattice planes related to the unit cell dimensions and the symmetry of the unit cell. Thus by measuring the diffraction cone angles for various lattice planes it is theoretically possible to deduce the unit cell parameters. However, in the calculation from cone angles to cell constants, two types of error are introduced and must be allowed for.

The first is Random Error, caused by slight experimental errors in the measurement of line positions on the photographic film. Random errors may be reduced by duplication of results. As six parameters, at the most, are calculated from as many as 20 to 30 independent measurements, proper mathematical analysis of these can reduce random errors extensively even on data from a single film.

Systematic errors arise from such causes as wrong alignment of the camera or film, and absorption of X-rays by the finite size of specimen used. In general these errors vary with  $\theta$ , and several functions of  $\theta$  have been proposed in an attempt to allow for them. One of the most commonly used is the so-called Nelson - Riley function,  $\frac{1}{2}\cos^2\theta\left[\frac{1}{\theta} + \frac{1}{\sin\theta}\right]$ . Attention has been paid to the design of cameras to reduce errors; 9 or 19 cm diameter cameras using the Van Arkel film mounting method, or

Guinier focussing cameras appear to be the most favoured. (HENRY, LIPSON and WOOSTER, 1951).

The following method, involving the least squares method to reduce random error and a suitable function of  $\theta$  for systematic errors, has been used in the computer programme described here. (The Nelson - Riley function is used in the standard version). The derivation below has been largely taken from COHEN (1955, 1956).

Let  $\Delta\theta$  be the small error in  $\theta$  which must be added to the experimentally determined value of  $\theta$ ,  $\theta_e$ , for the Bragg law to hold (first assuming no random error) i.e.

$$\lambda = 2d\sin(\theta_e + \Delta\theta) \dots\dots\dots(2)$$

Squaring, and expanding  $\sin^2(\theta_e + \Delta\theta)$  by the Taylor theorem we have

$$\frac{\lambda^2}{4d^2} = \sin^2(\theta_e + \Delta\theta) = \sin^2\theta_e + \Delta\theta \cdot \sin 2\theta_e \dots\dots\dots(3)$$

ignoring higher powers of the small angle  $\Delta\theta$ .

Now the relative error in the d-spacing derived from  $\theta$  is found to be approximately proportional to the Nelson - Riley function, written  $f(\theta)$ , over a large range of  $\theta$ .

$$\text{i.e.} \quad \frac{\Delta d}{d} = k f(\theta) \dots\dots\dots(4)$$

Differentiating the Bragg equation (1) and rearranging we have

$$\frac{\Delta d}{d} = \frac{-\cos\theta}{\sin\theta} \Delta\theta \dots\dots\dots(5)$$

Combining (3), (4) and (5) by eliminating  $\Delta\theta$  and  $\Delta d$

$$\frac{\lambda^2}{4d^2} = \sin^2\theta_e - 2\sin^2\theta_e k \cdot f(\theta) \dots\dots\dots(6)$$

Consider now the orthorhombic case where the d-spacing  $d_{hkl}$  is given by

$$\frac{1}{d_{hkl}^2} = \left[ \frac{h^2}{a^2} + \frac{k^2}{b^2} + \frac{l^2}{c^2} \right] \dots\dots\dots(7)$$

Substituting (7) in (6) and writing  $A = \frac{\lambda^2}{4a^2}$ ,  $B = \frac{\lambda^2}{4b^2}$ ,  $C = \frac{\lambda^2}{4c^2}$

$$Ah^2 + Bk^2 + Cl^2 = \sin^2 \theta_e - 2k \cdot \sin^2 \theta_e f(\theta) \dots\dots\dots(8)$$

for all  $\theta$ .

However, associated with each  $\theta_i$  measurement there is a small random error  $\epsilon_i$ .

Let  $h^2 = \alpha$ ,  $k^2 = \beta$ ,  $l^2 = \gamma$ ,  $\sin^2 \theta_e f(\theta) = \delta$ ;  $2k = D$ , the "drift" constant then

$$\alpha_i A + \beta_i B + \gamma_i C + \delta_i D - \sin^2 \theta_i = \epsilon_i \dots\dots\dots(9)$$

The least squares method states that the most accurate values of A,B,C,D are those which make the sum of the squares of the errors a minimum. Equation (9) is summed over all i

$$\sum_i (\alpha_i A_0 + \beta_i B_0 + \gamma_i C_0 + \delta_i D_0 - \sin^2 \theta_i) = \sum_i \epsilon_i \dots\dots\dots(10)$$

Squaring, and for  $\sum \epsilon_i^2$  to be a minimum, the partial derivatives must all vanish.

$$\frac{d}{dA_0} \sum_i \epsilon_i^2 = \sum_i \alpha_i (\alpha_i A_0 + \beta_i B_0 + \gamma_i C_0 + \delta_i D_0 - \sin^2 \theta_i) = 0$$

$$\frac{d}{dB_0} \sum_i \epsilon_i^2 = \sum_i \beta_i (\alpha_i A_0 + \beta_i B_0 + \gamma_i C_0 + \delta_i D_0 - \sin^2 \theta_i) = 0$$

$$\text{etc. for } \frac{d}{dC_0} \text{ and } \frac{d}{dD_0} \dots\dots\dots(11)$$

Therefore the following "normal equations" are obtained

$$\left[ \sum \alpha_i^2 \right] A_0 + \left[ \sum \alpha_i \beta_i \right] B_0 + \left[ \sum \alpha_i \gamma_i \right] C_0 + \left[ \sum \alpha_i \delta_i \right] D_0 = \sum \alpha_i \sin^2 \theta_i$$

$$\left[ \sum \alpha_i \beta_i \right] A_0 + \left[ \sum \beta_i^2 \right] B_0 + \left[ \sum \beta_i \gamma_i \right] C_0 + \left[ \sum \beta_i \delta_i \right] D_0 = \sum \beta_i \sin^2 \theta_i$$

$$\left[ \sum \alpha_i \gamma_i \right] A_0 + \left[ \sum \beta_i \gamma_i \right] B_0 + \left[ \sum \gamma_i^2 \right] C_0 + \left[ \sum \gamma_i \delta_i \right] D_0 = \sum \gamma_i \sin^2 \theta_i$$

$$\left[ \sum \alpha_i \delta_i \right] A_0 + \left[ \sum \beta_i \delta_i \right] B_0 + \left[ \sum \gamma_i \delta_i \right] C_0 + \left[ \sum \delta_i^2 \right] D_0 = \sum \delta_i \sin^2 \theta_i$$

.....(12)

Similar equations are obtained for the other symmetries.

REFERENCES

- ABEL (1963), *Quart.Rev.*, 17, 133
- ADAMS and GEBBIE (1963), *Spectrochim. Acta*, 19, 925
- ANDERSON, BAK and HILLEBERT (1953), *Acta Chem.Scand.*, 7, 236
- BARTLETT (1962), *Proc.Chem.Soc.*, 218
- BARTLETT and LOHMANN (1962), *Proc.Chem.Soc.*, 115
- BETHE (1929), *Ann.Phys.Lpg.*, (5), 3, 133
- BODE (1951), *Z.anorg.Chem.*, 267, 62
- BODE and CLAUSEN (1951), *Z.anorg.Chem.*, 265, 229
- BODE and DOHREN (1957), *Naturwiss.*, 44, 179
- BODE and DOHREN (1958), *Acta Cryst.*, 11, 80
- BODE and TEUFER (1952,a), *Z.anorg.Chem.*, 268, 20
- BODE and TEUFER (1952,b), *Z.anorg.Chem.*, 268, 129
- BODE and VOSS (1951), *Z.anorg.Chem.*, 264, 144
- BOSTON and SHARP (1960), *J.Chem.Soc.*, 907
- BUHLER and BUES (1961), *Z.anorg.Chem.*, 308, 62
- BURNS (1962), *Acta Cryst.*, 15, 1098
- CHATT (1961), private communication to D.W.A.Sharp
- CHATT, PAUSON and VENANZI (1960), *Organometallic Chemistry*, ACS Monograph  
No.147, edited by H.Zeiss. p.468
- CLAASSEN, MALM and SELIG (1962), *J.Chem.Phys.*, 36, 2890
- CLAASSEN, SELIG and MALM (1962), *J.Chem.Phys.*, 36, 2888
- CLARK and EMELEUS (1957), *J.Chem.Soc.*, 2119
- COHEN (1935), *Rev.Sci.Inst.*, 6, 68
- COX (1956), *J.Chem.Soc.*, 876
- COX, SHARP and SHARPE (1956), *J.Chem.Soc.*, 1242

- DAVISON, GREEN and WILKINSON (1961), J., 3172
- D'EYE and WAIT (1960), X-ray Powder Photography, Butterworth
- DUNN (1960), Modern Coordination Chemistry, ed, Lewis and Wilkins,  
Interscience, p. 248
- DUNN and PEACOCK (1962), private communication to JØRGENSEN, in Absorption  
Spectra and Chemical Bonding in Complexes
- EARNSHAW, FIGGIS, LEWIS and PEACOCK (1961), J.Chem.Soc., 3132
- EDWARDS and PEACOCK (1961), J.Chem.Soc., 4254
- EISENSTEIN (1960), J.Chem.Phys., 33, 1530
- EISENSTEIN (1961), *ibid.*, 34, 310
- EMBLEUS and GUTMANN (1949), J.Chem.Soc., 2979
- EMBLEUS and WOOLF (1950), J.Chem.Soc., 165
- EYRING, WALTER and KIMBALL (1944), Quantum Chemistry, Wiley
- FIGGIS and LEWIS (1960), Modern Coordination Chemistry, Interscience p.428
- FIGGIS, LEWIS and MABBS (1961), J.Chem.Soc., 3138
- FISCHER and RUDZITIS (1959), J.Amer.Chem.Soc., 81, 6375
- FRASER (1960), Nature, 188, 738-9
- GALLER (1962), The Language of Computers, McGraw - Hill
- GAUNI (1953), Trans.Far.Soc., 49, 1122
- GRIFFITHS (1958), Trans.Far.Soc., 54, 1009
- GUTMANN and JACK (1951), Acta Cryst., 4, 246
- HAENDLER (1963), private communication
- HARGREAVES and PEACOCK (1957), J.Chem.Soc., 4212
- HARGREAVES and PEACOCK (1958), J.Chem.Soc., 3776
- HENRY, LIPSON and WOOSTER (1951), The Interpretation of X-ray Diffraction  
Photographs, MacMillan
- HEPWORTH, JACK and WESTLAND (1956), J.Inorg.Nucl.Chem., 2, 79

- HEFWORTH, PEACOCK and ROBINSON (1954), J.Chem.Soc., 1197
- HEFWORTH, ROBINSON and WESTLAND (1954), J.Chem.Soc., 4269
- HEFWORTH, ROBINSON and WESTLAND (1958), J.Chem.Soc., 611
- HERZBERG (1945), Spectra of Polatomic Molecules. Van Nostrand. Infra-red and Raman
- HERZBERG (1950), Molecular Spectra and Molecular Structure, Vol.I Van Nostrand. p. 123
- HOARD and VINCENT (1940), J.Amer.Chem.Soc., 62, 3126
- HOLLOWAY (1961), private communication
- HOLLOWAY and PEACOCK (1963), J.Chem.Soc., 527
- IRVING and MAGNUSSEN (1956), J., 1860
- JACK (1959), personal communication to D.W.A.Sharp
- JØRGENSEN (1959), Mol.Phys., 2, 309
- JØRGENSEN (1960), ibid., 3, 201
- JØRGENSEN (1962), Progress in Inorg.Chem., 4, 73
- JØRGENSEN (1962,a), Absorption and Chemical Bonding in Complexes, Pergamon
- JØRGENSEN (1962,b), Orbitals in Atoms and Molecules, Academic Press p.142
- KEMMITT (1962), Ph.D.Thesis, London
- KEMMITT and SHARP (1961), J.Chem.Soc., 2496
- KHARASCH and ISBELL (1930), J.Amer.Chem.Soc., 52, 2919
- KLEMM (1954), Angew.Chem., 66, 468
- LAGEMAN and JONES (1951), J.Chem.Phys., 19, 534
- LIPSON (1949), Acta Cryst., 2, 43
- MAVOY (1963), private communication
- MALM, WEINSTOCK and CLAASSEN (1955), J.Chem.Phys., 23, 2192
- MANCHOT and GALL (1925), Ber., 58, 2175

- MATTHEW, HAWKINS, CARPENTER and SABOL (1955), *J.Chem.Phys.*, 23, 985
- MELLOR and STEPHENSON (1951), *Australian J. of Sc.Research*, A4, 406
- MEYERS and COTTON (1960), *J.Amer.Chem.Soc.*, 82, 5027
- MOFFITT, GOODMAN, FRIED and WEINSTOCK (1959), *Mol.Phys.*, 2, 109
- MOONEY (1949), *Acta Cryst.*, 2, 189
- MOSS (1962), Ph.D.Thesis, London
- MULLIKEN (1953), *Phys.Rev.*, 45, 279
- NUTTALL (1962), Ph.D.Thesis, London
- ORGEL (1952), *J.Chem.Soc.*, 4756
- OWEN (1955), *Proc.Roy.Soc., A* 227, 183
- PEACOCK (1957), *J.Chem.Soc.*, 467
- PEACOCK (1957 a), *Proc.Chem.Soc.*, 59
- PEACOCK (1960), *Progress in Inorg.Chem.* edited by Cotton, Vol 2, p. 193
- PEACOCK (1960), *Progress in Inorg.Chem.*, Vol. 2 p. 243
- PEACOCK and SHARP (1959), *J.Chem.Soc.*, 2762
- PULLINGER (1891), *J.*, 59, 598
- ROOF (1955), *Acta Cryst.* 3, 739
- SCHLESINGER and TAPLEY (1924), *J.Amer.Chem.Soc.*, 46, 276
- SCHREWELIUS (1938), *Z.anorg.Chem.*, 258, 241
- SCHREWELIUS (1942), *Ark.Kemi, Mineral.Geo.*, B16, 1
- SCHWOCHAU and HERR (1963), *Angew.Chem.*, 75, 95
- SHARP (1960), *Proc.Chem.Soc.*, 317
- SHARP (1960 a), private communication
- SHARP (1960 b), *Adv. in Fluorine Chem.*, 1, Fluoroboric Acids and their Derivatives p.87
- SHARP and SHARPE (1956), *J.Chem.Soc.*, 1855



- SHARPE (1949), J., 2901
- SHARPE (1950), J., 3444
- SHARPE (1960), Adv. in Fluorine Chem., 1, 29
- SIEBERT (1953), Z.anorg.Chem., 274, 34
- SMITH (1960), J.Amer.Chem.Soc., 82, 6176
- TANABE and SUGANO (1954), J.Phys.Soc. Japan, 9, 753, 766
- TEUFER (1956), Acta Cryst., 9, 559
- TURNER and CLIFFORD (1958), Nature, 182, 1369
- WADDINGTON (1958), J.Chem.Soc., 4340
- WAGNER (1931), Z.anorg.Chem., 196, 364
- WARTENBERG (1939), Z.anorg.Chem., 241, 381
- WEAVER, WEINSTOCK and KNOP (1963), J.Amer.Chem.Soc., 85, 111
- WEINSTOCK, CLAASSEN and CHERNICK (1963), J.Chem.Phys., 38, 1470
- WEINSTOCK, CLAASSEN and MALM (1960), J.Chem.Phys., 32, 181
- WEISE and KLEMM (1955), Z.anorg.Chem., 279, 74
- WELLS (1962), Structural Inorganic Chemistry, 3rd Edition, Clarendon Press.
- WESTLAND and ROBINSON (1956), J., 4481
- WHEELER, PERROS and NAESER (1955), J.Amer.Chem.Soc., 77, 3488
- WOODWARD and WARE (1963), Spectrochim.Acta, 19
- De WOLFF (1957), Acta Cryst., 10, 590
- WOOLF and EMELEUS (1949), J.Chem.Soc., 2865
- YANG and GARLAND (1957), J.Phys.Chem., 61, 1504